QUANTIFICATION OF THE INFLUENCES OF SUBSURFACE UNCERTAINTIES ON SEISMIC BEHAVIOR OF SHALLOW FOUNDATIONS

A Thesis
Submitted to the Graduate Faculty
of the
North Dakota State University
of Agriculture and Applied Science

By

Mohammad Feroz Ahmed Kayser

In Partial Fulfillment of the Requirements
for the Degree of
MASTER OF SCIENCE

Major Department:
Civil Engineering

July 2011

Fargo, North Dakota

North Dakota State University

Graduate School

Title

Quantification of the Influences of Subsurface Uncertainties on Seismic Behavior of Shallow Foundations.

By

Mohammad Feroz Ahmed Kayser

The Supervisory Committee certifies that this ***disquisition*** complies with North Dakota State University's regulations and meets the accepted standards for the degree of

Master of Science

ABSTRACT

Kayser, Mohammad Feroz Ahmed, M.S., Department of Civil Engineering, College of Engineering and Architecture, North Dakota State University, July 2011. Quantification of the Influences of Subsurface Uncertainties on Seismic Behavior of Shallow Foundations. Major Professor: Dr. Sivapalan Gajan.

The properties of geomaterials are uncertain. These uncertainties not only affect the dynamic behavior of the geomaterials, but also significantly influence the complex nonlinear dynamics between the soil, foundation, and the structure (dynamic soil-foundation-structure interaction – SFSI). However, current civil engineering approach in incorporating the effects of SFSI on the seismic behavior of structures is still largely deterministic without considering uncertain geomaterial properties.

The objectives of this research are to characterize the uncertainties in soil properties in a probabilistic framework and to quantify their effects on dynamic soil-foundation system behavior during seismic loading. The research methodology includes systematic propagation of uncertainties in soil properties through soil-foundation interface to the dynamic behavior of the structure during seismic loading. A recently developed Contact Interface Model (CIM), to model the soil-foundation system behavior during seismic loading, has been used in numerical simulations. To study the sensitivity of the response of the soil-foundation system to the random input parameters, probabilistic analyses have been carried out using Tornado Diagram analysis, Spider Plot analysis, First Order Second Moment (FOSM) analysis, and small scale Monte-Carlo simulations.

Results obtained from the probabilistic numerical simulations indicate that ultimate moment capacity of the soil-foundation system during seismic loading is more sensitive to the uncertainty in the applied vertical load on the foundation than the uncertainties in soil

properties. Since the uncertainty in applied vertical load is considerably smaller than the uncertainties in soil properties, the ultimate moment capacity of shallow foundation is predictable with reasonable accuracy. Energy dissipation beneath the foundation mainly depends on the applied vertical load and initial vertical stiffness of the foundation, while initial vertical stiffness of the foundation and rebounding ratio were found to contribute the most to the settlement of the foundation. The rotation of the foundation is more sensitive to the shaking intensity than uncertainties in soil properties.

ACKNOWLEDGEMENTS

I am grateful to my advisor Dr. Sivapalan Gajan for his guidance and unwavering support. Needless to say, the thesis would not be in the present form without his help, involvement and commitment. I would not have enjoyed this research program without his attention and direction, as well as the freedom I received from him.

It is also my pleasure to thank Dr. Dinesh Katti, Dr. Jimmy Kim, and Dr. Jerry Gao for their time and contributions as members of my graduate committee. I would like to thank the Civil Engineering Department at North Dakota State University for giving me the opportunity to complete this master's program; also many thanks to all the other staff in this school who gave me a lot of help during my study.

I take this opportunity to express a deep sense of gratitude to my mother, who inspired and supported me to become what I am today. I also had the affection of my brothers and sisters all along. Their touching care and love provided me the necessary strength to withstand the pressures of my research program. Their contributions to this work, though invisible, are invaluable to me.

Last but not least I would like to thank all my friends and well wishers who helped me in one way or the other.

TABLE OF CONTENTS

LIST OF TABLES

Table | Page

LIST OF FIGURES

CHAPTER 1. INTRODUCTION

1.1. Motivation

Subsurface properties can be significantly influenced by the geological history of a site. To design a shallow foundation considering soil uncertainty, it is very crucial to get the geological history of the construction site before starting the design. According to Tomlinson and Boorman (1995), adequate information of geology of an area with exact position to the major geologic formations constituting the site, the likelihood of subsidence from mineral extraction, and general topography is critical in foundation design. The history and use of a geological site, including knowledge on any defects of current or previous buildings attributable to foundation conditions, is also very significant in design.

It is well known that the properties of geomaterials are uncertain. Uncertain geomaterial properties could significantly influence the complex nonlinear dynamics between soil, foundation, and structure (Soil-Foundation-Structure Interaction - SFSI) during earthquake loading. The uncertainties in geomaterial properties can be (a) spatial uncertainties (natural variability), (b) testing uncertainties (uncertainties associated with Standard Penetration Test, SPT/ Cone Penetration Test, CPT), and (c) transformational uncertainties (the uncertainties in the correlations that are used to obtain the soil properties from SPT/CPT test results).

In general, at a geotechnical site, the soil profile information is known with some certainty at the borehole locations, and the engineers use deterministic interpolation methods to estimate the soil properties in between boreholes. However, due to the uncertainties in geomaterial properties, questions arise on the accuracy of interpolated parameters and subsequently the designed behaviors of the structures they support.

Probabilistic approach to data analysis, would reduce this difficulty by considering all possible values of soil parameters and assigning a probability of occurrence to each. In addition, engineers can quantify their confidence in knowledge about the subsurface at any site, and with subsequent probabilistic simulations, can quantify their confidence in the designed behavior of foundations and structures.

Current earthquake engineering approach, in incorporating the effects of nonlinear dynamic SFSI in design, is still largely deterministic. Engineers responsible for designing geotechnical and structural components always want to be safe in their design. Therefore, in designs, engineers impose an empirical factor of safety, which most often leads to overdesigned systems. In recent years, uncertainties in soil parameters and the effect of these uncertainties on the different demand and capacity issues have become very popular and demanding. In the recent past, several researchers have performed studies to explore the effect of uncertain soil properties on the response of geotechnical systems. A couple of past research studies have incorporated the uncertainties in soil properties in dynamic soil-foundation interaction analysis, especially for shallow foundations; however, all of them are site specific studies. In present study, the effects of uncertain soil properties on nonlinear dynamic behavior of shallow foundation supported by various types of soils have been investigated under various intensities of earthquake loading.

1.2. Objectives of the Research

- To characterize the uncertainties in soil properties, in general, in a probabilistic framework (for sandy soils and clayey soils)

- To quantify the effects of uncertainties in soil properties on dynamic soil-shallow foundation system behavior (especially, moment-rotation-settlement behavior and energy dissipation characteristics) during seismic loading

1.3. Scope of the Research

In this study, soil properties (mainly shear strength and shear stiffness) have been categorized in a probabilistic framework for cohesionless soils and cohesive soils. The uncertainties in soil properties (probabilistic distribution of soil properties) have been systematically propagated through soil-foundation interface to the dynamic behavior of the structure (an elastic shear wall) during seismic loading. OpenSees (Open System for Earthquake Engineering Simulations) finite element framework has been used for numerical simulations of the nonlinear dynamic behavior of soil-foundation-structure system. A recently developed Contact Interface Model (CIM), to model the soil-foundation system behavior during seismic loading, and an elastic beam-column element, to simulate the behavior of shear wall structure, have been used in numerical simulations. Probabilistic sensitivity analyses have been carried out using Tornado Diagram analysis, Spider Plot analysis, First Order Second Moment (FOSM) analysis, and small scale Monte-Carlo simulations. The findings of this research quantify the effect of uncertainties in soil properties on soil-foundation system behavior (cyclic moment-rotation-settlement behavior and energy dissipation characteristics) during seismic loading.

1.4. Outline of Thesis

This thesis includes seven chapters with detailed descriptions. The organizations of these chapters have been described below:

- Chapter 1: Introduction: Addresses the motivation and general background of the study and provides the scope of this research and organization of the thesis.
- Chapter 2: Literature Review: Describes a detailed review of the state-of-the-art knowledge regarding combined cyclic loading on shallow foundation, uncertainties in soil properties, and their application in foundation engineering.
- Chapter 3: Soil Uncertainty and Statistical Parameters: Presents details about different types and sources of uncertainties in soil properties and describes how different statistical soil parameters have been selected.
- Chapter 4: Numerical Modeling using OpenSees and Contact Interface Model (CIM): Briefly describes the OpenSees finite element framework. Provides the framework of footing-soil CIM and the methodology of calculating these input parameters for CIM.
- Chapter 5: Probabilistic Numerical Simulations: Describes details of different probabilistic methods that are incorporated in this study with example results. Also presents the tables with detailed description of number of simulations and input matrices for the different probabilistic methods used.
- Chapter 6: Results and Discussions: Presents a detailed description of results and discussion. The effects of uncertainties on soil properties on the seismic behavior of soil-shallow foundation systems are discussed.
- Chapter 7: Summary and Conclusions: Briefly summarizes the research and highlights key findings of this study. Suggestions for future research are also discussed.

CHAPTER 2. LITERATURE REVIEW

2.1. Introduction

This chapter presents the literature review of past research, related to present study, conducted by other researchers. The purpose of this chapter is to present a state-of-the art review of the current progress of relevant research and information related to the scope of this research work. The literature review includes uncertainties in soil properties and their probabilistic distributions, application of uncertainties in soil properties in the design of geotechnical systems, and the numerical models available to simulate the soil-foundation system behavior during seismic loading.

2.2. Uncertainties in Soil Properties

Early studies on the uncertainties in soil properties have been performed by Lumb (1966). In his study, four different types of soils were used (Marine clay, alluvial sandy clay, residual silty sand, and residual clayey silt) and normal distribution was selected for undrained shear strength and friction angle of soils. In a later study, Lacasse and Nadim (1996) and Wolff et al. (1996) recommended different probability density functions for different soil strength parameters. For friction angle, φ, normal distribution was suggested and for undrained shear strength (C_u) of clay, a lognormal distribution was suggested. Fenton and Griffiths (2005) assumed lognormal distribution for undrained shear strength as it evades the generation of negative values. Massih et al. (2008), in their bearing capacity reliability analysis study, compared the results by considering both normal distribution and beta distribution for undrained shear strength. Fenton and Griffiths (2005) assumed a lognormal distribution for elastic modulus of soil, while Jimenez and Sitar (2009) used

lognormal, beta and gamma distribution for Young's modulus of soil. Recently, Sett et al. (2010) used normal distribution for both young's modulus and shear modulus.

Phoon and Kulhawy (1999a) developed a method to estimate the probable range of variability in the overall estimation of soil properties assuming soil properties as complex characteristics from different sources. Coefficient of variation (COV) of inherent variability, scale of fluctuation, and COV of measurement error were evaluated in detail, along with the general soil type and the approximate range of mean value for which the COVs are applicable (Phoon and Kulhawy, 1999a). COV was selected to support the probable range of variability inherent in the estimation of soil properties. Measurement error was calculated from field measurements using a simple additive probabilistic model or was determined directly from comparative laboratory test results. The relative contribution of inherent soil variability, measurement error and transformation uncertainty to the overall variability in the design parameter was found to be dependent on the site conditions, degree of equipment and procedural control during testing, and quality of the transformation model.

In a companion paper describing the evaluation of transformation uncertainty, Phoon and Kulhawy (1999b) evaluated the uncertainties in the design soil properties reasonably by combining the appropriate component uncertainties using a second moment probabilistic approach. Transformation model was evaluated using regression analyses. A first-order estimate of standard deviation of transformation uncertainty was obtained by noting that about two thirds of the data typically fall within ± one standard deviation of the transformation model. This study concluded with specific guidelines on the typical coefficients of variation (COVs) for some common design soil properties as a function of

the type of test and the type of correlation used. This study demonstrated that transformation uncertainty is a significant and independent source of geotechnical variability. Jones et al. (2002) presented the sources and types of uncertainties in soil properties and discussed the probabilistic treatment of geotechnical data using geostatistics. The theory of regionalized variables, including concepts of autocorrelation, variograms, and stationarity were presented, along with tabulated values of parameters describing spatial variability.

2.3. Application of Soil Uncertainty in Geotechnical Earthquake Engineering

Baynes (2005) analyzed the effects of soil uncertainties and the input parameters of a pressure-dependent soil constitutive model on seismic behavior of soils. Three statistical analyses were carried out in this study: Tornado diagram, First-order-second-moment, and Monte Carlo simulations. Statistical analysis of structural engineering demand parameters (EDPs) of a single-degree-of-freedom non-linear structure subjected to ground motions was evaluated. This study discussed the effect of uncertainty in site response analysis, and both the Tornado diagram analysis and the Monte Carlo analysis indicated that uncertainty in the input bedrock was dominant in contributing to the uncertainty in the EDPs.

Na et al. (2008) studied a probabilistic approach based on an appropriate treatment of uncertainty of soil properties to identify and rank the sources of uncertainty according to their relative influence on the performance of a port structure. In this study the propagation of basic uncertainties were investigated using the Tornado diagram analysis and the First-order-second-moment (FOSM) method. In this study it has been found that the uncertainties in the friction angle and the shear modulus of reclaimed soil contributed most to the variance of the output, residual horizontal displacement (RHD). Moreover COV of

response due to ground motion variability was found to be comparable to the maximum COV of response due to uncertainty in material properties alone. In another study, Na et al. (2009) analyzed the effect of spatial variation of soil property on residual horizontal responses (RHD) of quay wall considering three different ground motions and coefficients of variations (COV) of material properties. Monte Carlo simulation was used in this research to evaluate the probability distribution of RHD of the quay wall. In this study spatial variation of shear modulus of backfill soil has been considered as the most important uncertain parameters and it was found that larger variation of shear modulus of backfill soil may lead to larger mean and larger dispersion of quay wall RHD response.

Considering soil stiffness and strength parameters as uncertain Raychowdhury (2009) conducted uncertainty analyses to demonstrate the effect of uncertainty in soil parameters on seismic response of structures. Time history analyses were carried out considering different ground motions to demonstrate the variability of structural response. FOSM analysis and Monte Carlo simulations were carried out to obtain relative variance contributions of the uncertain parameters. In this study friction angle was defined as the most important parameter in structural response variability and the variability due to soil parameter uncertainty was found to be dominant over ground motion uncertainty. In another study, a first-order sensitivity analysis was performed by Raychowdhury and Hutchinson (2010) to assess the effect of the BNWF (Beam on Nonlinear Winkler Foundation) model input parameters on its capability to capture foundation behavior during cyclic loading. It was found that the normalized moment demand on the foundation is mostly dependent on the friction angle and spring spacing of the model, while it is fairly insensitive to the modulus of elasticity, the stiffness ratio, and Poisson's ratio.

Sett et al. (2010) used the Fokker–Planck–Kolmogorov Equation (FPKE) approach to find the effect of soil uncertainty over simulated modulus reduction (G/G_{max}) and damping behavior of soils. Probabilistic soil parameters (elastic shear modulus (G_{max}) and undrained shear strength (c_u)) needed for the simulations were obtained using transformation from commonly used in-situ measured properties. Sett et al. (2010) concluded that, though the deterministic solutions fail to predict the realistic soil behavior, probabilistic results, even with the simplest elastic–perfectly plastic soil model, are comparable to the experimental observations reported in this study.

2.4. Combined Cyclic (V-H-M) Loading on Shallow Foundation

Cremer et al. (2001) developed a dynamic macro element model to study dynamic soil-structure interaction (SSI) on cohesive soil. The macro-element duplicated the cyclic behavior of the foundation, considering the effects of non-linearity occurring in the near field. A plasticity model with yielding of the soil beneath the foundation and an uplift model to introduce contact non-linearity considered by the uplift of the foundation were coupled to study the dynamic soil structure interaction. This study concluded that macro-element is a handy and proficient tool for the accurate evaluation of the effect of dynamic soil-structure interaction.

Skirted footings under combined loadings have been numerically investigated by Kellezi et al. (2007) for clay soil with constant and increasing undrained shear strength with depth. The analyses take into account the operational loads for the considered jack-up and were focused on the variation in (V-H) and (V-M) planes. The Mohr Coulomb elastic-plastic constitutive soil model was applied assuming drained conditions for sand and undrained conditions for clay. Differences between the yield capacities calculated from

different methods were discussed and design yield envelope was proposed. The results for coarser mesh were used to compare with the 3D FE analyses where the mesh cannot be very fine. This study found that 2D FE analyses give conservative capacities compared to the 3D ones. Depending on the developed failure mechanism, application of the 3D FE modeling was recommended for the final design.

Paolucci et al. (2007) studied response of shallow foundations, resting on dry sand and excited by accelerograms of different levels of amplitude, by performing shaking table experiments and numerical simulations using a macro-element model. Uniform soil conditions was assured in various experiments to make the results a prospect for better understanding of the dynamic nonlinear soil–structure interaction (SSI) problem and for the calibration of numerical approaches. This study depicted that after a proper improvement of the numerical method (by introducing a simple stiffness degradation rule), it is possible to capture overturning moment and rotation of the experimental response with an acceptable agreement.

Zhang and Tang (2007) developed macroscopic foundation models that can describe the nonlinear behavior and energy dissipation mechanism of shallow foundations. They studied dynamic response of shallow foundations on linear and nonlinear soil medium using finite element method. Finite element method was used to conduct dynamic analyses of strip foundation under harmonic displacement excitation in vertical and horizontal directions. The dynamic stiffness was evaluated and effects of foundation width, input motion amplitude and frequency, and development of soil nonlinearity were quantified by hysteretic damping ratio. Zhang and Tang (2007) found that the radiation damping decreases monotonically with the increase of hysteric damping ratio. At the end

they concluded that the numerical results from FEM compared well with the theoretical solution for elastic soil with proper choices of appropriate domain scale, mesh size and boundary conditions.

Grange et al. (2008) studied dynamic SSI for circular foundation by developing a macro element model taking into account the plasticity of the soil and the uplift of the foundation. The performance of a circular shallow foundation resting on an infinite space of soil, under combined loading was evaluated in this study. After developing the macro-element model, numerical simulations were performed and results compared with experimental tests and similar trend was found for the approaches.

Gajan and Kutter (2009) introduced contact interface microelement model (CIM) to study the rocking nature of shallow foundation under combined cyclic loading. The contact interface model was developed to study the nonlinear relationship between cyclic loads and displacements at the footing–soil interface. A single microelement was considered for the rigid footing and the soil under the footing. Applying combined loading which is responsible for the soil yielding and footing uplift, the contact interface model considers the coupling between forces, moment, and displacements. The results obtained from CIM simulations were compared with centrifuge model test results where combined loading was applied for shear wall structures resting on shallow foundations. This study concluded that the results obtained from numerical simulations and experiments illustrate similar trend for moment and shear capacities, energy dissipation and displacements.

Raychowdhury and Hutchinson (2009) developed a macro-element model using beam on nonlinear Winkler foundation (BNWF) approach to simulate the combined cyclic loading behavior of shallow foundations supported by both sandy soils and clayey soils.

The two-dimensional BNWF model was developed by closely spaced mesh with independent nonlinear spring elements placed vertically along the length of the footing and horizontally at the ends of the footing. Raychowdhury and Hutchinson (2009) concluded that the developed model can obtain experimentally observed behavior for a wide range of shallow footings, soil types, vertical factors of safety and loading histories.

CHAPTER 3. SOIL UNCERTAINTY AND STATISTICAL PARAMETERS

3.1. Introduction

Uncertainties in soil properties could significantly influence the nonlinear dynamic soil-foundation system behavior. To this end, the first objective of this research is to characterize the uncertainties in soil properties, in general, in a probabilistic framework (for sandy soils and clayey soils). This chapter describes the types and sources of uncertainties in soil properties and the statistical parameters that are used to quantify the uncertainties in soil properties. This chapter also provides the values of the statistical soil properties used in this research.

3.2. Soil Uncertainty Types and Sources

In many earlier studies geotechnical engineering field was explored assuming soil as a uniform source of uncertainty. Due to randomness in soil's depositional process, soil itself is a variable. To characterize soil properties, different field test procedures, such as cone penetration tests (CPT) or standard penetration tests (SPT), and laboratory experiments, such as triaxial and index tests were performed. In most of the earlier studies, soil uncertainty was described considering three sources of geotechnical uncertainty (Phoon and Kulhawy [1999a]). They are (a) inherent variability, (b) measurement error, and (c) transformation uncertainty (Fig. 3.1). The inherent soil variability mainly occurs from natural geologic processes of in situ soil formation. Apparatus, testing process, and random testing are responsible for measurement errors. These two sources of uncertainty together were described as data scatter (Phoon and Kulhawy [1999a]). This can be decreased by performing more tests. However, due to limitation of resources, it is not possible to perform huge amount of tests. The last source of uncertainty arises due to the

use of empirical models for the transformation of field or laboratory measurements into design soil properties. All of these uncertainties contribute to the whole uncertainty of the design of soil property estimation and these uncertainties depend on the site conditions, degree of equipment and technical control, and accuracy of the correlation model.

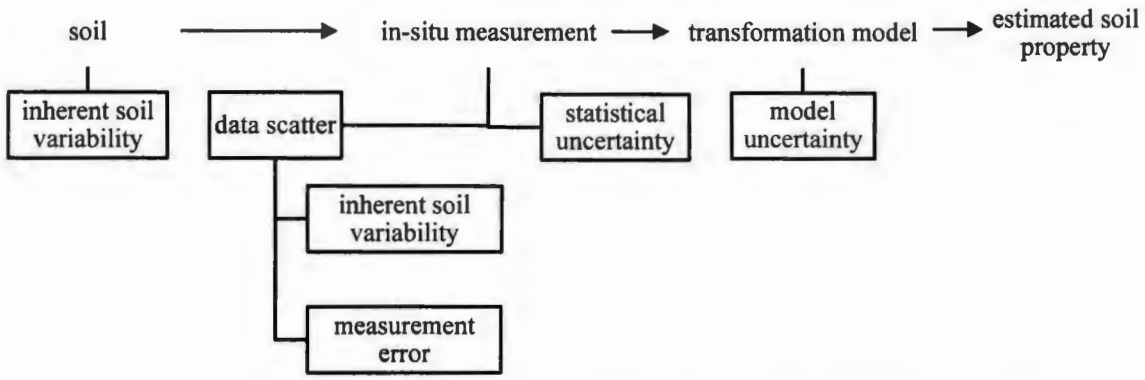

Fig. 3.1. Uncertainty in soil property estimates (Phoon and Kulhawy, 1999a)

As shown in Fig. 3.2, the uncertainties in geomaterial properties can be broadly divided into two categories: aleatory uncertainties and epistemic uncertainties (Lacasse and Nadim [1996]). Aleatory uncertainty is the natural variability of soil, which is inherent and cannot be reduced by taking additional care and additional testing. Epistemic uncertainty arises due to deficient amount of information and error in the transformation procedures and modeling methods. The uncertainty ensuing from testing and sampling procedures, uncertainty in modeling method and the uncertainty as a result of limited availability of data are the main cause of epistemic uncertainty. Therefore, the epistemic uncertainty can be avoided by performing more tests and taking procedural quality control.

Soil properties vary due to various geologic, depositions of high-energy environments, weathering and physical-chemical reasons. Spatial variation of soil

properties occurs both in vertical and horizontal direction. In addition, basic soil properties

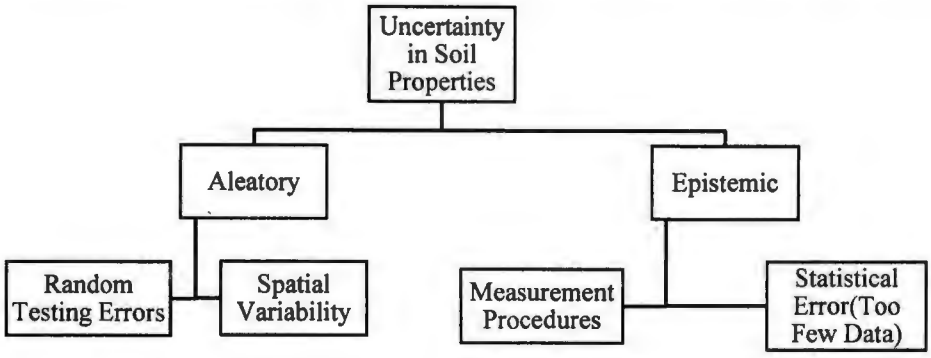

Fig. 3.2. Categories of uncertainty in soil properties (Jones et al., 2002)

vary highly due to effective confining pressure. As effective confining pressure increases with depth, soil properties are anticipated to show predictable trend with depth. In general, the value of a soil property can be characterized as (Phoon and Kulhawy [1999b]) (Fig 3.3)

$$\xi(z) = t(z) + w(z) + e(z) \qquad (3.1)$$

where ξ is the in-situ parameter value at depth z, t(z) is a function defining the trend in terms of depth, w(z) is the variation from the trend at a depth z and e(z) is measurement error at depth z.

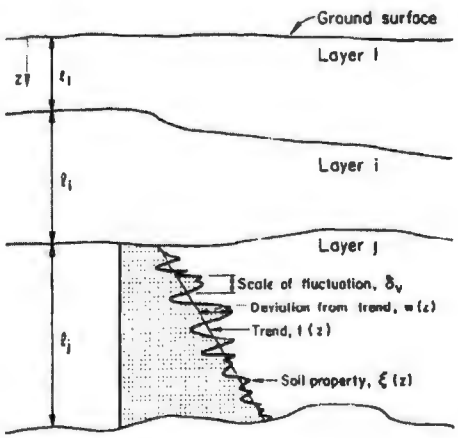

Fig. 3.3. Inherent soil variability (Phoon and Kulhawy, 1999a)

The trend function of a soil property can be obtained from the deterministic value, which is the mean of the soil property, and the deviation from the trend can be related to the standard deviation of the soil variability.

3.3. Statistical Parameters

In most of the probabilistic geotechnical engineering studies, the shear strength and stiffness parameters of soil, such as, friction angle (Φ), undrained shear strength (C_u), Young's modulus (E), shear modulus (G), and Poisson's ratio (ν), were assumed as prime random variables. The uncertain soil properties are characterized using mean (μ), standard deviation (σ), coefficient of variation (COV) and spatial correlation length (δ).

In the uncertainty study the major parameters those characterize the variability of the random variables are the variable's mean and standard deviation and/or variance. The mean and variance are also known as the first and second central moments of a random variable. Definitions of different statistical parameters are described in the following with the equation to calculate that statistical parameter:

Mean (μ_x): The mean of a variable implies the central trend of the function. The mean, μ_x, of some non-grouped data values $x_1, x_2 \ldots, x_n$ can be expressed by (Spiegel and Stephens 2007)

$$\mu_x = \frac{\sum_{i=1}^{n} x_i}{n} \qquad (3.2)$$

Standard deviation (σ): The standard deviation and variance of a distribution are measurements of the deviation from the mean. The variance, σ^2, of a data set is described by (Spiegel and Stephens 2007)

$$\sigma^2 = \frac{\sum_{i=1}^{n}(x_i - \mu_x)^2}{n-1} \qquad (3.3)$$

The standard deviation, σ, is simply the square root of the variance.

Coefficient of variation (COV): The coefficient of variation (COV) which is a very valuable parameter in probabilistic study, and can be defined as the ratio of the standard deviation to the mean (Phoon and Kulhawy, 1999a)

$$COV = \frac{\sigma}{\mu_x} \qquad (3.4)$$

Spatial correlation length: Spatial correlation length can be defined as the distance in which the desired soil property at two points is considered as independent. In other words, spatial correlation length is the distance within which a soil property shows relatively strong correlation (Vanmarcke [1977]). As this study has been performed for shallow soil foundations, spatial correlation length was not considered in this study.

Probability density function (PDF): The possibility of occurrence of a particular value at a given point for a continuous random variable is generally described by probability density functions (PDF). Probability distribution for a random variable can be generated by performing good number of analysis and sorting data by frequency of occurrence of values. The probability of a random variable to situate within a particular area is obtained by the integral of the variable's density over the limit of the region.

The basic properties for a probability distribution function $f_X(x)$ of a continuous random variable, X are (Griffiths and Fenton, 2007)

$$f_x(x) \geq 0 \qquad (3.5)$$

$$\int_{-\infty}^{\infty} f_x(x)\,dx = 1 \qquad (3.6)$$

The normal distribution function (Fig. 3.4) is applicable for any random variable between $-\infty$ and $+\infty$. The distribution can be expressed as (Griffiths and Fenton, 2007)

$$f_x(x) = \frac{1}{\sigma_x\sqrt{2\pi}} \exp\left[-\frac{1}{2}\left(\frac{x-\mu_x}{\sigma_x}\right)^2\right], \quad -\infty < x < +\infty \qquad (3.7)$$

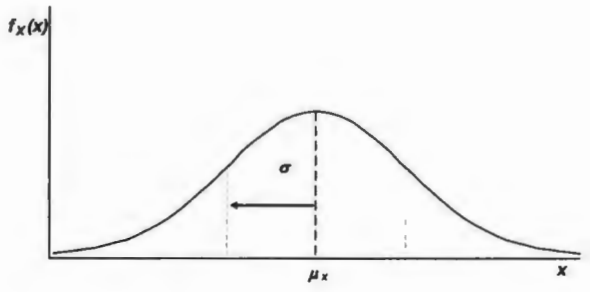

Fig. 3.4. Normal distribution PDF

Cumulative density function (CDF): The cumulative density function (CDF) is a special way of depicting a probability distribution and can be expressed as (Griffiths and Fenton, 2007)

$$F_X(x) = P[X \le x] = \int_{-\infty}^{x} f_X(x)\,dx \qquad (3.8)$$

$$\text{or } P[a \le X \le b] = \int_{a}^{b} f_X(x)\,dx \qquad (3.9)$$

where a and b are the values between which the random variable, X will probably fall. In this study to verify the probability distribution function of output, from the Monte Carlo simulation different points were incorporated to the plot.

Coefficient of correlations: In most geotechnical modeling a correlation factor is used to correlate the random variables. When two random variables are independent then correlation coefficient is considered as zero. In this study, the CIM initial vertical stiffness

(Kv), initial horizontal stiffness (Kh) and ultimate vertical load (Vult) were assumed to have strong correlation among them as these parameters were calculated using soil strength and stiffness parameters. For the other CIM input parameters coefficient of correlation was assumed as zero. More details about the specific input parameters of CIM are described in Chapter 4. The equation used to calculate correlation coefficient is (Spiegel and Stephens 2007)

$$r = \frac{\sum xy}{\sqrt{\sum x^2 \times y^2}} \tag{3.10}$$

where x = random value - mean value of first sample and y = random value- mean value of second sample.

3.4. Uncertain Soil Properties from the Literature

In Contact Interface Model (CIM), the numerical model used in this study, the major soil parameters considered to calculate the input parameters are friction angle of soil, undrained shear strength and shear modulus of soil. This study has been performed for both dry sandy soils and saturated clay type soils. Sand was considered as cohesionless soil and clay was considered as purely cohesive soil. From the available literatures, COV of friction angle, undrained shear strength and shear modulus are tabulated in table 3.1, table 3.2 and table 3.3 respectively.

3.5. Uncertain Soil Properties Used in this Study

To study the sensitivity of the seismic foundation response, uncertain soil parameters values were selected from the available literatures. Both sandy and clayey soils were divided into three categories each based on their strength and stiffness: dense sand, medium dense sand, loose sand, stiff clay, medium stiff clay, and soft clay. Uncertain

Table 3.1. COV of friction angle

Soil type	COV (%)	Source
Gravel	6	Harr (1977)
Sand	7-11	Harr (1977)
Sand	4-10	Wolff et al. (1996)
Sand	2-5	Lacasse and Nadim (1996)
Sand	5-15	Phoon and Kulhawy (1999a)
Clay	5-15	Phoon and Kulhawy (1999a)
Silty Sand	10	Raychowdhury (2009)
Clay	11	Srivastava and Babu (2009)
Clay	29	Most and Knabe (2010)

Table 3.2. COV of undrained shear strength

Soil type	COV (%)	Source
Marine Clay	18	Lumb (1966)
London Clay	16	Lumb (1966)
Clay	20 - 50	Meyerhof (1995)
Clay	5-35	Lacasse and Nadim (1996)
Clayey Silt	10-30	Lacasse and Nadim (1996)
River Clay	40	Wolff et al. (1996)
Clay	10-45	Phoon and Kulhawy (1999a)
Clay	13 - 40	Duncan (2000)
Clay	39	Srivastava and Babu (2009)

Table 3.3. COV of shear modulus

Soil type	COV (%)	Source
Off shore soil	20 - 50	Meyerhof (1995)
Sand	20 - 70	Phoon and Kulhawy (1999a)
Clay	30 - 90	Phoon and Kulhawy (1999a)
Clay	34	Srivastava and Babu (2009)
Silty Sand	10	Raychowdhury (2009)

friction angle and shear modulus values were used for foundation resting on sandy soils and uncertain undrained shear strength and shear modulus values were used for foundations resting on clayey soils. Table 3.4 presents the mean and COV of friction angle, undrained shear strength, and shear modulus used in this study for each category. The equations that were used to calculate the shear modulus values are given in table 3.5. As can be seen from

table 3.5, shear modulus of clay was calculated from undrained shear strength and shear modulus of sand was calculated from an equivalent standard penetration number N_{60}. The following equation was used to convert the friction angle of sand to N_{60}.

$$N_{60} = (12.2 + 20.3\,\frac{\sigma'_{v0}}{P_a})(tan\varphi)^{\frac{1}{0.34}} \qquad (3.11)$$

Table 3.4. Soil properties used in CIM sensitivity analysis

	Soil Type	Friction angle Mean (°), COV	Undrained Shear Strength Mean (KPA), COV	Shear Modulus Mean (MPA), COV
	Dense	40, 10 %	--	88.7, 30 %
Sand	Medium Dense	32, 10 %	--	49.2, 30 %
	Loose	25, 10 %	--	27.4, 30 %
	Stiff	--	150, 33 %	73.5, 33 %
Clay	Medium Stiff	--	75, 33 % and 50%	37.5, 33 % and 50 %
	Soft	--	37.5, 33 %	19.1, 33 %

Table 3.5. Equations used to calculate shear modulus

	Sand	Clay
Method-1	$G_{max} = 325N_{60}^{0.68}$ (3.12)	$G_{max} = 516C_U^{1.012}$ (3.13)
Method-2	$G_{max} = 1000K_{2,max}(\sigma'_m)^{1/2}$ (3.14)	$G_{max} = 487C_U^{0.928}$ (3.15)
Reference	(Kramer 1996)	(Hara et al. 1974)
N_{60} is standard penetration number, C_U is the undrained shear strength of clay, $K_{2,max}$ is constant depends on the density of soil (Kramer, 1996) and σ'_m is mean effective stress of the soil in lb/ft^2		

Mean and COV of friction angle for different types of sandy soils were selected from Phoon and Kulhawy (1999a) and mean and COV of undrained shear strength of different clayey soils were obtained from Kulhawy and Phoon (2002). As the uncertainty in the undrained shear strength of clay soil could be high, two different COV values were used for the undrained shear strength of medium stiff clay. More details about the specific input parameters of CIM are described in Chapter 4.

CHAPTER 4. NUMERICAL MODELING USING OPENSEES AND CONTACT INTERFACE MODEL (CIM)

4.1. Introduction

This chapter describes the numerical modeling of a shear wall-shallow foundation-soil system when it is subjected to seismic loading. OpenSees (Open System for Earthquake Engineering Simulations) finite element platform is briefly described first. Structural constitutive model, used to model the behavior of shear wall, and the constitutive model for the footing-soil system contact interface model (CIM) are briefly described. Finally, material parameters selection and interpretation of an example numerical simulation results are presented.

4.2. OpenSees

The OpenSees finite element framework is used for numerical modeling of shaking table experiments (OpenSees, 2010). OpenSees was developed by Pacific Earthquake Engineering Research Center (PEER, 2010). It is capable of performing static and dynamic finite element simulations for structural and geotechnical applications. OpenSees includes different material models (constitutive models) and elements that are capable of performing linear and nonlinear finite element simulations. The object-oriented nature of OpenSees allows one to choose different materials, elements, and solution algorithms that are most suitable to simulate a particular analysis (Gajan and Saravanathiiban, 2011).

The four major components in OpenSees are model builder, domain, analysis and recorder (Fig. 4.1). Model builder is used to build the input file, which describes the loading, structural components, material properties and other required components for

running the simulation. Model builder builds the numerical model in domain and the analysis object performs the numerical analysis in the domain. The recorder object records the desired outputs at the end of each loading step.

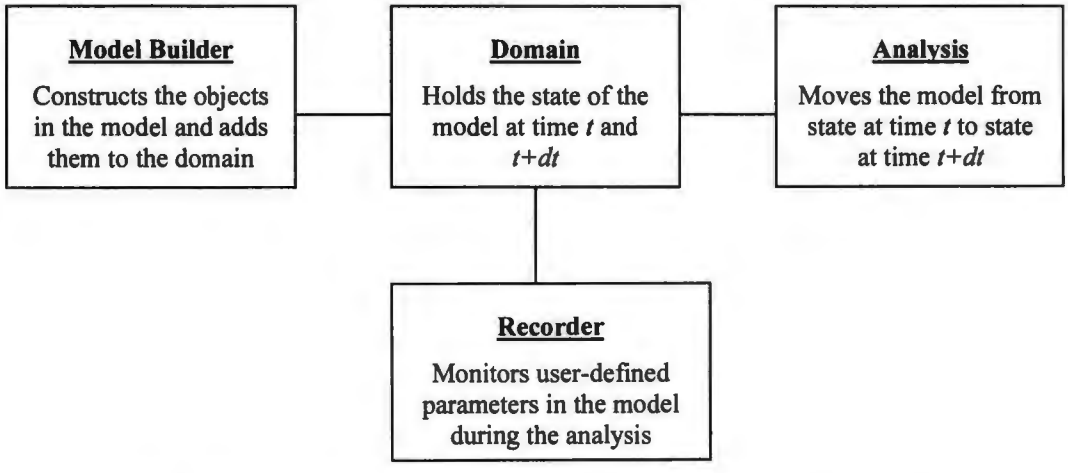

Fig. 4.1. OpenSees framework for the finite element analysis

4.3. Modeling of Shear Wall Structure

In this study the shear wall resting on a shallow foundation is modeled using an elastic beam-column element in OpenSees. For an elastic beam-column element the Young's modulus of the material, cross-sectional area and area moment of inertia of the cross-section of the element are required. As shown in Fig. 4.2 footing dimension used in this study are length of the footing, L = 4 m, and width of the footing, B = 2 m. The height of center of gravity of the structure, or effective height of the structure is considered equal to 8 m. Young's modulus of concrete is considered as 20 GPa and cross section of the shear wall structure as shown in Fig. 4.2 (b) taken as 2.5 m by 1 m. The detail of the OpenSees numerical model used in this study has been described in section 4.5.

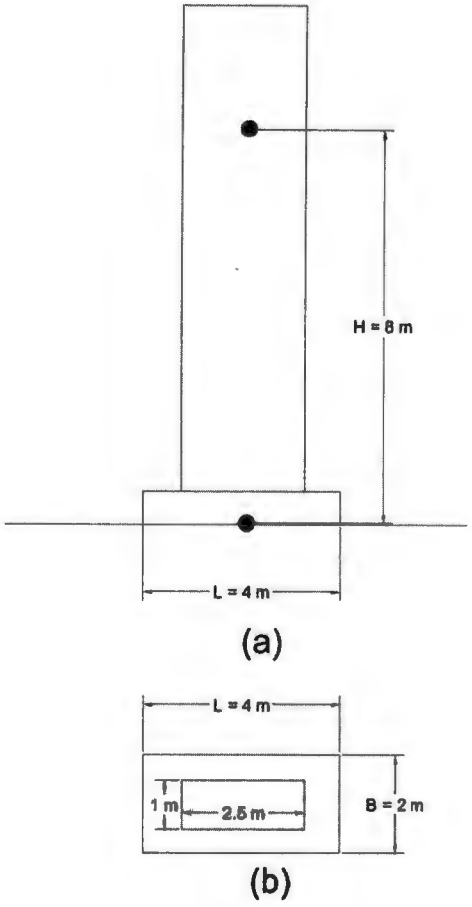

Fig. 4.2. Shear wall-footing system with dimensions (a) elevation view and (b) plan view

Fig. 4.3 presents normalized base acceleration time history with 1.0 g maximum ground acceleration. By scaling this acceleration time history three (0.27 g, 0.55 g and 0.98 g maximum ground accelerations) acceleration time histories have been obtained to perform numerical simulations with different shaking intensities. Fig. 4.4 shows the response spectra (with 5% damping ratio) of the applied base acceleration in the numerical simulations.

Table 4.1 presents fixed-base period and flexible-base period of the shear-wall structure resting on different types of soil. The fixed-base period has been calculated using the following equation

$$T_n = 2\pi\sqrt{m/k} \qquad (4.1)$$

where m = mass of the shear-wall structure and k is the stiffness of the structure obtained from

$$K = 3EI/h^3 \qquad (4.2)$$

where E = Young's modulus of the concrete = 20 GPa, I = Area moment of inertia of the shear-wall structure = 1.33 m^4 and h = height of center of gravity of the structure = 8 m.

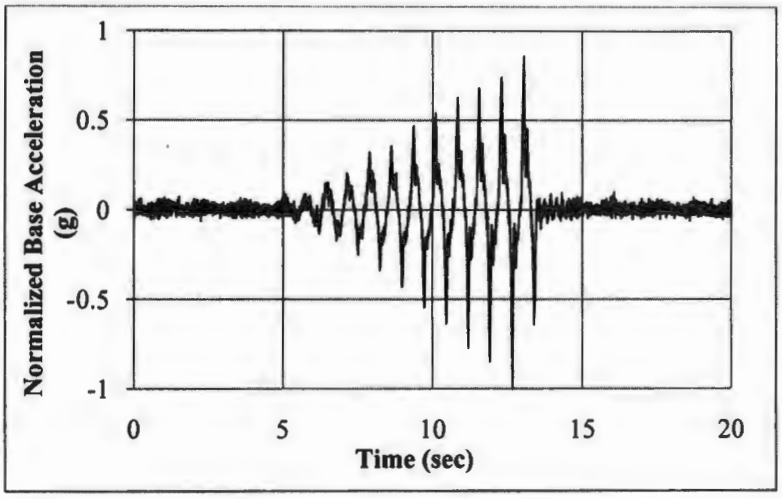

Fig. 4.3. Acceleration time history used in the numerical simulations (time history is normalized by the peak acceleration)

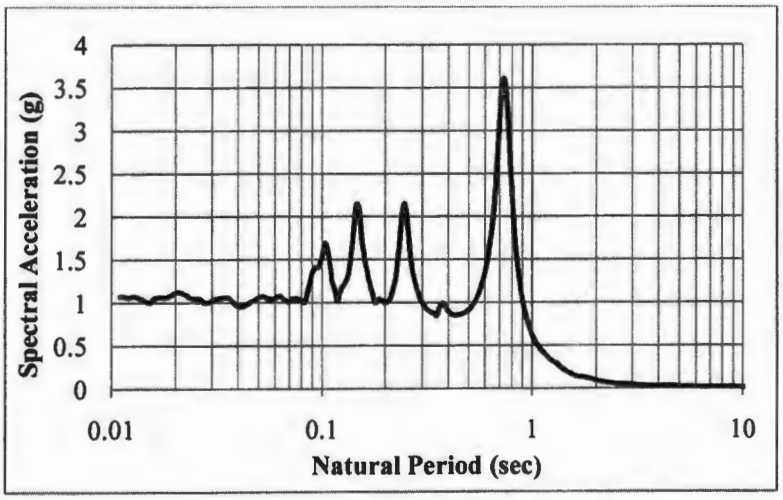

Fig. 4.4. Acceleration response spectra with 5% elastic damping

Flexible-base period is calculated based on the initial stiffness of the structure-soil system (elastic) in OpenSees. Period lengthening ratio is calculated from the basic definition of ratio between the flexible-base period and fixed-base period of the CIM model. To verify the period lengthening ratio obtained from the numerical simulations, period lengthening ratio is also calculated using the following equation (Veletsos and Meek, 1974):

$$\frac{T}{T_n} = \sqrt{(1 + \frac{K}{K_h} + \frac{Kh^2}{K_\theta})} \qquad (4.3)$$

where, T is flexible-base period of a surface foundation, T_n is fixed-base period, K is the stiffness of the structure can be calculated using equation (4.2), h is effective height of the structure, K_h and K_θ are the horizontal and the rotational stiffness of the foundation respectively.

Table 4.1. Period of the shear-wall structure

Soil Type	Applied Mass (Mg)	Fixed Base Period (sec)	Flexible Base Period (sec)	Period Lengthening Ratio	
				CIM	Veletsos and Meek (1974)
Dense Sand	115	0.17	0.30	1.75	2.01
Medium Dense Sand	28.8	0.09	0.19	2.19	2.34
Loose Sand	14.6	0.06	0.17	2.8	3.05
Stiff Clay	61	0.12	0.23	1.88	2.12
Medium Stiff Clay	30.6	0.09	0.21	2.43	2.50
Soft Clay	15.3	0.06	0.20	3.27	3.32

4.4. Concept of CIM

Fig. 4.5 presents the idea of macro-model in the footing-soil interface element. Substituting the rigid footing and adjacent soil in the zone of influence, the contact interface model is placed at the footing–soil interface. The contact interface model, developed to study the dynamic soil-shallow foundation-structure behavior, contains the

relations that correlate the forces (V, H, and M) and deformations (s, u, and θ) at the footing–soil boundary during the application of combined cyclic loading. Using the concept of macro-element model, considering the footing and soil under the footing as a single element, the model was developed by Gajan and Kutter (2009) to study the load-displacement behavior of footing during dynamic loading.

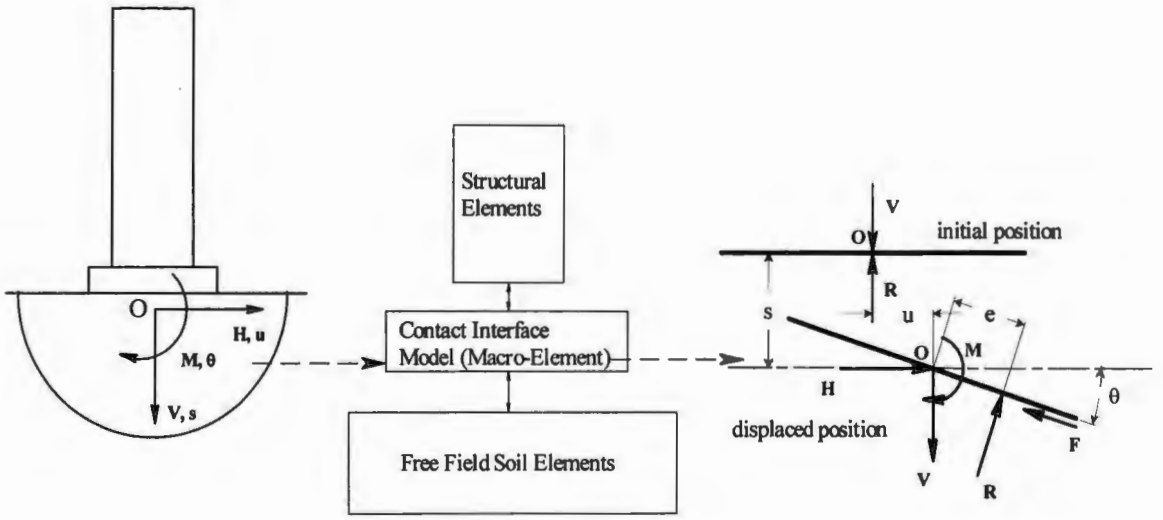

Fig. 4.5. Concept of macro-element contact interface model and forces and displacements at footing-soil interface during combined loading (Gajan et al. 2007)

According to Gajan and Kutter (2009) when combined loading is applied on foundation that creates soil yielding and footing uplift at the same time, the contact interface model accounts for coupling between forces and displacements. The CIM was originally developed by Gajan and Kutter (2009) for cyclic moment loading (vertical loading, V = constant and horizontal loading, H = 0) by considering the geometry of the footing–soil contact area and incorporating the coupling between vertical load and moment using critical contact area ratio (which is ratio between actual area of the footing and minimum area of the footing required to have contact with the soil to support the vertical and shear loads). After that shear-sliding model was build up by including the combination

between vertical–shear and moment–shear by interaction diagrams in normalized *V–H–M* (vertical–shear–moment) space and the modified critical contact area ratio. As a final point, the CIM is completed to common loading conditions in vertical–shear–moment space.

Gajan et al. (2010) presented application and validation of the CIM along with BNWF model (described in chapter 2). Performance of CIM has been evaluated by performing numerical simulations for shear wall structure system and validated by the test results obtained from centrifuge testing. They concluded that CIM can capture the hysteretic features obtained during experiment. Even though CIM under-predicted the maximum moment of the soil-footing system, it predicted reasonably well the energy dissipation characteristics observed during the experiment.

4.5. OpenSees Numerical Model

OpenSees simulations are carried out for the simple shear wall-footing system. CIM in the finite element analysis framework has been presented in Fig. 4.6 which shows the structure-soil system, modeled in OpenSees for dynamic base shaking. The shear wall is modeled using an elastic beam-column element in OpenSees as the wall is rigid and stiff compared to the soil. The footing and soil around the footing is modeled using the material "Soil Footing Section" and "Zero Length Section" element. According to Gajan (2006) the Soil Footing Section material need to be incorporated with a Zero Length Section element to characterize the two-dimensional footing-soil interface that has three degrees of freedom of forces and displacements. As shown in Fig. 4.5, the Soil Footing Section material combines nonlinear coupled relationships between the vertical, shear and moment forces and the subsequent displacements settlement, sliding and rotation at the footing-soil interface. The Zero Length Section element connects two nodes at the same location (node

1 and node 2 in Fig. 4.6) with node 1 being fixed in all three degrees of freedom. The bottom end of the elastic beam column element is connected to the Soil Footing Section at node 2.

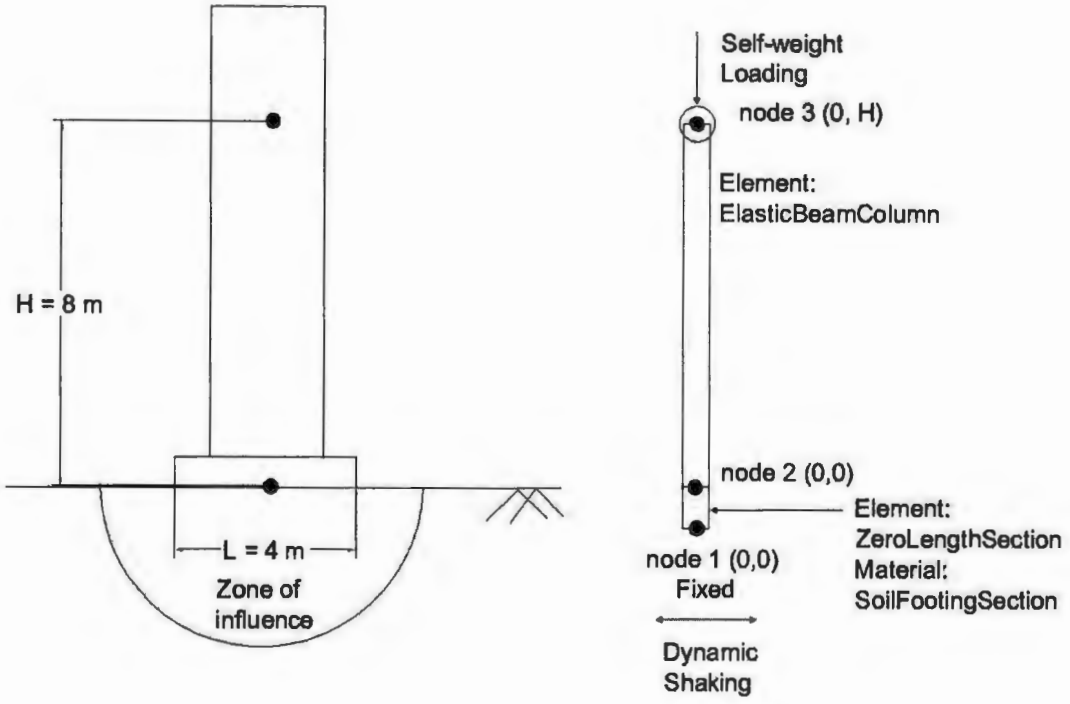

Fig. 4.6. CIM in the OpenSees finite element framework

For dynamic shaking simulations, the total mass of the structure is applied at node 3, which is the height of center of mass of the structure (in this study this height has been considered as 8m), to simulate the inertial forces transferred from structure to soil in vertical, horizontal and rotational directions. Once the self-weight of the structure is applied in node 3, the measured free field acceleration time histories obtained from the centrifuge tests performed by Gajan et al. (2007) are applied at the fixed node in the bottom (node 1) in OpenSees simulations. OpenSees recorders are used to record the stress resultants and displacements at the base center point of the footing during the application of loading.

4.6. Contact Interface Modeling Input Parameters

According to Gajan et al. (2007) the input parameters of the contact interface model can be described as following:

a) Ultimate vertical load (V_{ULT}): The maximum vertical load that can be applied to the footing, which occurs with full footing-soil contact.

b) Length of footing (L): The linear dimension of the footing in the plane of rocking or in the direction of shaking.

c) Initial vertical stiffness (K_v): The initial vertical stiffness of the footing in full contact with soil for pure vertical loading.

d) Initial horizontal stiffness (K_h): The initial shear stiffness of the footing in full contact with the soil for pure shear loading.

e) Elastic rotation limit ($\theta_{elastic}$): The maximum amplitude of rotation for which no settlements occur.

f) Rebound ratio (R_v): R_v is an empirical factor to account for the elastic rebound and bulging of soil into the gap associated with the plastic compression in neighboring loaded areas.

g) Footing node spacing (ΔL): ΔL specifies the distance between the footings nodes internally created in the model.

The equations used to calculate the CIM input parameters are:

Ultimate vertical load of the foundation (sand) from Das (2008),

$$V_{ult} = L \times B \times 0.5 \times \gamma \times B \times N_\gamma \times F_{\gamma s} \quad (4.4)$$

Ultimate vertical load of the foundation (clay) from Das (2008),

$$V_{ult} = L \times B \times C_u \times N_c \times F_{cs} \quad (4.5)$$

where L is length of the footing, B is width of the footing, γ is unit weight of soil, Nc and Nγ are bearing capacity factors depend on friction angle of soil, Fγs and Fcs are shape factors depend on foundation geometry and Cu is undrained shear strength of clay.

Initial vertical stiffness from FEMA 356,

$$K_v = \frac{G \times B}{1-\nu}[1.55(\frac{L}{B})^{0.75} + 0.8] \qquad (4.6)$$

and initial horizontal stiffness from FEMA 356,

$$K_h = \frac{G \times B}{2-\nu}[3.4(\frac{L}{B})^{0.65} + 1.2] \qquad (4.7)$$

where G is shear modulus of soil and υ is poison's ratio of soil (in this study $\upsilon = 0.4$ for sandy soils and $\upsilon = 0.5$ for clayey soil).

Other constant CIM input parameters used in this study are:

Dimension of the footing (in the direction of shaking), L = 4.0 m

Rebound ratio, $R_v = 0.1$ (Gajan et al. 2007)

Elastic rotation limit, $\theta_{elastic} = 0.001$ rad (Gajan et al. 2007)

Mesh spacing, $\Delta L/L = 0.0025$ (Gajan et al. 2007).

4.7. Values of the CIM Input Parameters Used in this Study

To study the sensitivity of the CIM input parameters, considering four CIM input parameters, Vult, Kv, Kh, and Rv and applied vertical load (Vapp) on the structure as random input parameters numerical simulations have been performed for sandy soils and clayey soils. Both sandy and clayey soils were divided into three categories each based on their strength and stiffness: dense sand, medium dense sand, loose sand, stiff clay, medium stiff clay, and soft clay. All types of soils have been simulated by three different maximum ground shaking intensities 0.27 g, 0.55 g and 0.98 g. Mean and COV values of the five random input parameters for each case have been presented in table 4.2 and table 4.3

respectively for sandy soils and clayey soils. Table 4.4 presents value of the constant CIM input parameters. In addition to the studies depicted here, to study the sensitivity of mesh spacing on the CIM, ΔL/L was assumed random (ΔL/L = 0.005, 0.0025 and 0.00125) and simulated by 0.55 g maximum ground acceleration for dense sand and stiff clay soil only with six random input parameters (Vult, Kv, Kh, Rv, Vapp and ΔL).

Table 4.2. Random CIM input parameters for sandy soils

Input Parameter	Dense Sand		Medium Dense Sand		Loose Sand	
	Mean	COV (%)	Mean	COV (%)	Mean	COV (%)
Vult (MN)	11	54.4	3	48.2	1.1	34.2
Kv (MN/m)	1000	23.2	557	25	307	22.6
Kh (MN/m)	956	23	400	25.5	221	23
Rv	0.1	50-100	0.1	50-100	0.1	50-100
Vapp (MN)	1.13	15	0.283	15	0.143	15

Table 4.3. Random CIM input parameters for clayey soils

Input Parameter	Stiff Clay		Medium Stiff Clay		Soft Clay	
	Mean	COV (%)	Mean	COV (%)	Mean	COV (%)
Vult (MN)	6.8	27.4	3.4	27.4	1.7	27.4
Kv (MN/m)	835	26.5	426	26.5	217	26.5
Kh (MN/m)	601	26.5	306	26.5	156	26.5
Rv	0.1	50-100	0.1	50-100	0.1	50-100
Vapp (MN)	0.6	15	0.3	15	0.15	15

Table 4.4. Constant CIM input parameters

Input Parameter	Mean	COV
$\theta_{elastic}$ (rad)	0.001	0
L (m)	4	0
ΔL/L	0.0025	0

4.8. Output Calculations

After performing numerical simulations using the CIM input's following outputs can be achieved

a) Cyclic Moment

b) Cyclic Rotation

c) Cyclic Settlement

d) Cyclic Shear Force

d) Cyclic Sliding and

e) Vertical Load (constant – controlled by the weight of the structure).

In this study, only the first three outputs are considered to study the sensitivity of these parameters when probabilistic input parameters are used in CIM. It should be noted that the shear force is proportional to the moment at the base center of the footing and sliding is not significant for relatively slender structures (when compared with rotation).

In this study four outputs are evaluated for each simulation: ultimate moment, settlement, and rotation at the base center of the footing and energy dissipation beneath the footing. Rotation and settlement are obtained directly from the output of simulation. The maximum settlement is obtained from the settlement vs. rotation plot. Rotation is calculated by averaging the difference between the maximum positive and maximum negative rotations. To calculate the theoretical maximum moment following equation is used

$$\text{Ultimate Moment} = \frac{V_{app} L}{2}\left[1 - \frac{1}{FS}\right] \qquad (4.8)$$

where V_{app} is the applied vertical load, L is the length of the footing and FS is the factor of safety.

Using the output data, moment vs. rotation is plotted and from the plot the peak moment is selected as the ultimate moment in this study as shown in Fig. 4.7 (a). By

integrating the area of the hysteresis loop in the moment-rotation plot energy dissipation beneath the footing is calculated.

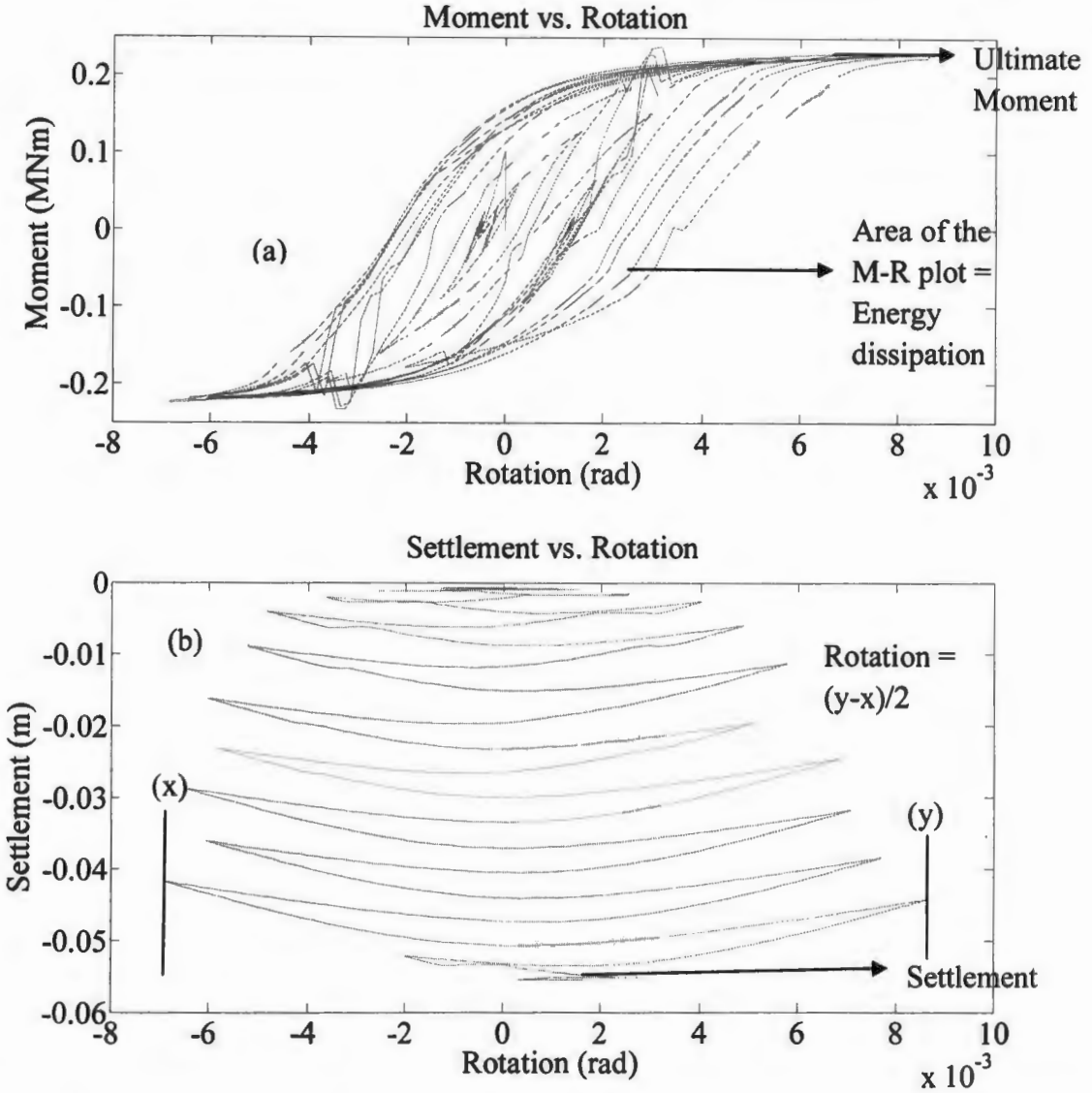

Fig. 4.7. Example output at the base center point of the footing: (a) Moment vs. Rotation plot (b) Settlement vs. Rotation plot for soft clay with a maximum ground acceleration of 0.55 g (Values of the input parameters for this particular simulation are Vult = 2.26e+6 MN, L = 4 m, Kv = 2.17e+8 MN/m, Kh = 1.06e+8 MN/m, $\theta_{elastic}$ = 0.001 rad, Rv = 0.1 and ΔL = 0.01 m. Applied vertical load in this simulation is 0.15 MN)

CHAPTER 5. PROBABILISTIC NUMERICAL SIMULATIONS

5.1. Introduction

Different probabilistic methods are used to study the effects of uncertainties in soil properties on the seismic behavior of soil-foundation system through CIM numerical simulations. The probabilistic methods used in this study include Tornado diagram method, First Order Second Moment (FOSM) method, Spider plot method and Monte Carlo Simulation technique. Each method is described briefly and the input parameter matrices for each method are presented.

5.2. Tornado Diagram Analysis

Tornado diagram method is used to identify the input parameter that contributes the biggest to a particular output result. In other words, Tornado diagram quantifies the sensitivity of each output results to random input variables. By using Tornado diagrams, designers can easily evaluate which input parameters need to be given more attention and consideration when designing a system.

In the Tornado diagram analysis, in addition to the deterministic mean value of an input parameter, two other extreme values are selected: the 84^{th} percentile and 16th percentile (mean ± 1 standard deviation) (Na et al. 2008). The responses of the numerical model are evaluated by this method using these two extreme values for a certain selected random variable, while all other random input variables are kept in their mean value. The absolute difference of these two response values corresponding to the two extreme values of that random variable, which is termed as swing of the response corresponding to the selected random variable, is then calculated. This calculation procedure is repeated for all

random variables. If the total number of random input parameters is "n", then the required number of simulations for Tornado diagram analysis is "2.n+1".

Table 5.1 presents the input matrix for Tornado diagram method of soft clay with five random input parameters (Vult, Kv, Kh, Rv and Vapp) and other constant input parameters (the bold numbers represent the mean values). To demonstrate the relative contribution of each variable to a particular output result, swings are plotted in a figure from the top to the bottom in a descending order according to their size. Longer swing implies that the corresponding variable has larger effect on that particular output than those with shorter swing. The vertical line in the plot presents the mean value of the output.

Table 5.1. Input matrix for Tornado diagram method with five random input parameters (Soft Clay)

Vult (MN)	Kv (MN/m)	Kh (MN/m)	Rv	Vapp (MN)
1.128	217	156	0.1	0.15
1.7	147	156	0.1	0.15
1.7	217	106	0.1	0.15
1.7	**217**	**156**	**0.1**	**0.15**
1.7	217	207	0.1	0.15
1.7	287	156	0.1	0.15
2.26	217	156	0.1	0.15
1.7	217	156	0.05	0.15
1.7	217	156	0.2	0.15
1.7	217	156	0.1	0.173
1.7	217	156	0.1	0.13
Note: Constant input parameters:				
$\theta_{elastic}$ = 0.001 rad, L = 4 m, and ΔL = 0.01 m				

Similar input matrices are created for other types of soil as well. Numerical simulations are performed for shear wall-shallow foundation systems supported by dense sand, medium dense sand, loose sand, stiff clay, medium clay and soft clay with maximum ground accelerations 0.27 g, 0.55 g and 0.98 g (input acceleration time histories are presented in the previous chapter). Eleven simulations are performed for each of the above mentioned cases to study the effects of the CIM input parameters on the response of the

soil-foundation system by changing the five major input parameters (Vult, Kv, Kh, Rv and Vapp). To study the effect of CIM node spacing, structures supported by dense sand and stiff clay type soil are subjected to shakes with 0.55 g maximum acceleration with node spacing as an additional random variable (ΔL = 0.02 m, ΔL = 0.01 m, and ΔL = 0.005 m). In that case total thirteen simulations are performed (2 x 6 + 1).

Fig. 5.1 presents an example Tornado diagram for foundation settlement on soft clay subjected to 0.55 g maximum ground acceleration time history. As can be seen from the plot, the initial vertical stiffness (Kv) has the biggest effect on settlement, and rebound ratio (Rv) and applied vertical load (Vapp) respectively show second and third biggest effect on settlement. The effects of ultimate vertical load (Vult) and initial horizontal stiffness (Kh) on settlement are negligible.

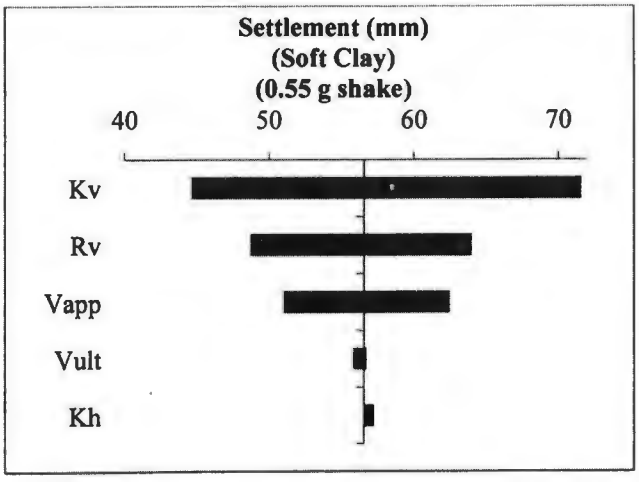

Fig. 5.1. Tornado diagram for settlement of foundation supported by soft clay subjected to ground shaking with maximum acceleration of 0.55 g

5.3. First Order Second Moment (FOSM) Method

The FOSM method is one of the most widely applied methods in engineering design. As FOSM method considers the first-order terms of the Taylor series expansion

about the mean value of each input variable and requires up to the second moment (variance) of the uncertain variables, it is defined as first order second moment method. While Tornado diagram method presents the variation of a particular output in absolute terms, FOSM presents the relative contribution of each random variable on a particular output.

A detailed derivation of FOSM method is presented in Baynes (2005) and a brief description is presented in the following. The derivation of FOSM method begins by considering an output variable, Y, that is a function of input variables X_i (for i = 1 to N) such that

$$Y = g(X_1, X_2, ..., X_N) \tag{5.1}$$

This relationship can be expanded using a Taylor series of the form

$$\begin{aligned} Y = {} & f(\mu_{X_1}, \mu_{X_2}, \ldots, \mu_{X_N}) + \frac{1}{1!}\sum_{i=1}^{N}(X_i - \mu_{X_i})\frac{\delta g}{\delta X_i} \\ & + \frac{1}{2!}\sum_{i=1}^{N}\sum_{j=1}^{N}(X_i - \mu_{X_i})(X_j - \mu_{X_j})\frac{\delta^2 g}{\delta X_i \delta X_j} \\ & + \frac{1}{3!}\sum_{i=1}^{N}\sum_{j=1}^{N}\sum_{k=1}^{N}(X_i - \mu_{X_i})(X_j - \mu_{X_j})(X_k - \mu_{X_k})\frac{\delta^3 g}{\delta X_i \delta X_j \delta X_k} \end{aligned} \tag{5.2}$$

where μ_{Xi} is the mean value of input variable X_i. Since $(X_i - \mu_{Xi})$ is smaller (when compared to the first term) when the random value is close to the mean value, by ignoring the higher order terms, Taylor series can be written as

$$Y \approx f(\mu_{X_1}, \mu_{X_2}, \ldots, \mu_{X_N}) + \frac{1}{1!}\sum_{i=1}^{N}(X_i - \mu_{X_i})\frac{\delta g}{\delta X_i} \tag{5.3}$$

From statistics,

$$\mu_Y \approx f(\mu_{X_1}, \mu_{X_2}, \ldots, \mu_{X_N}) \tag{5.4}$$

and $$\sigma_Y^2 \approx \sum_{i=1}^{N}\sum_{j=1}^{N}\mathrm{cov}(X_i, X_j)\frac{\delta g}{\delta X_i}\frac{\delta g}{\delta X_j} \qquad (5.5)$$

where μ_Y and σ_Y^2 are the mean and variance of the output Y. Rearranging equation 5.5 so that the input variable variances are isolated gives a relationship that is used to determine the contribution of each input variable to the overall output variable variance (Baynes, 2005). It is expressed as

$$\sigma_Y^2 \approx \sum_{i=1}^{N}\sigma_{X_i}^2\left(\frac{\delta g}{\delta X_i}\right)^2 + \sum_{i=1}^{N}\sum_{j\neq i}^{N}\rho_{X_iX_j}\frac{\delta g}{\delta X_i}\frac{\delta g}{\delta X_j} \qquad (5.6)$$

where σ_{Xi}^2 is the variance of input X_i and $\rho_{X_iX_j}$ is the correlation coefficient between two random input variables X_i and X_j. The quantity $\delta g/\delta X_i$ in equation 5.6 is called the variation of g to the input variable X_i. When two random input variables have strong correlation, then to describe their contribution to the output, the second term of the equation is used. For the random variables with no correlation among them only the first term in the right hand side of equation 5.6 is used to calculate the effect of random input variables on the output variance. After obtaining the total variance, variance of each random variable is normalized by that total variance so that the total normalized variance gives a sum value of one in the plot.

In the numerical model CIM, the variance of the response parameter (Y) (due to an example input parameter K_V) as a function of input parameters in the FOSM method can be approximated as

$$\sigma_Y^2 \approx \sigma_{K_v}^2\left(\frac{\delta g}{\delta K_v}\right)^2 + \rho_{K_vK_h}\frac{\delta g}{\delta K_v}\frac{\delta g}{\delta K_h} + \rho_{K_vV_{ult}}\frac{\delta g}{\delta K_v}\frac{\delta g}{\delta V_{ult}} \qquad (5.7)$$

where σ_{Kv}^2 is the variance of Kv, ρ_{KvKh} is the correlation coefficient between Kv and Kh, and ρ_{KvVult} is the correlation coefficient between Kv and Vult, which are calculated by using equation (3.10). In this study Kv, Kh and Vult are assumed to be correlated and coefficient of correlations between these parameters are calculated. In all the cases, unit value of coefficient of correlation is found.

In this study finite difference approach is used to approximate the partial derivatives. The derivative at a point is evaluated by using one increment above and below of the mean value of the random input variable, which is expected to better capture some of the non-linear behavior of the function over a range of likely values. For example,

$$\frac{\delta g}{\delta K_v} = \frac{g(\mu_{Kv} + \Delta K_v) - g(\mu_{Kv} - \Delta K_v)}{2\Delta K_v} \qquad (5.8)$$

where, ΔK_v is the standard deviation of input parameter K_v.

Simulations are performed for shear wall-shallow foundation systems by varying each CIM input parameter individually to approximate the partial derivatives in the equation. Similar to Tornado diagram method, for "n" random input parameters, "2.n+1" simulations are performed in FOSM method. The same set of simulations (presented in section 5.2 for Tornado diagram method) are used in FOSM method as well; however additional post processing is performed to calculate the derivatives in equation 5.7. Table 5.2 presents the input matrix for FOSM method to study the response of shear wall-shallow foundation systems resting on medium dense sand with five random input parameters (Vult, Kv, Kh, Rv and Vapp) and other constant input parameters (bold row presents the mean value of all the parameters).

Similar to Tornado diagram method, in FOSM method, other input matrices are created to study the response of shear wall-shallow foundation systems where foundation is resting on different types of soil subjected to different maximum ground acceleration. The effect of mesh spacing on shallow foundation resting on dense sand and stiff clay type soil are also studied using the FOSM method.

Table 5.2. Input matrix for FOSM method with five random input parameters (Medium Dense Sand)

Vult (MN)	Kv (MN/m)	Kh (MN/m)	Rv	Vapp (MN)
5.66	557	400	0.1	0.283
3.04	750	400	0.1	0.283
3.04	557	539	0.1	0.283
3.04	**557**	**400**	**0.1**	**0.283**
3.04	557	286	0.1	0.283
3.04	398	400	0.1	0.283
1.68	557	400	0.1	0.283
3.04	557	400	0.05	0.283
3.04	557	400	0.2	0.283
3.04	557	400	0.1	0.325
3.04	557	400	0.1	0.241
Note: Constant input parameters:				
θelastic = 0.001 rad, L = 4 m, and ΔL = 0.01 m				

Fig. 5.2 presents an example FOSM plot for foundation energy dissipation on medium dense sand subjected to 0.98 g maximum ground acceleration. In this case, Vapp shows the largest relative contribution on energy dissipation (more than 70%), while Vult shows the least contribution.

5.4. Spider Plot Method

To evaluate the sensitivity of the outputs of a model to the input variables and how the outputs are related to random input variables, spider plot is a very effective technique. While Tornado diagram method presents the variation of a particular output in absolute terms and FOSM presents the relative contribution of each random input variable on a

particular output, Spider plot method reveals the relationships between the inputs and outputs (whether the relationships are linear or nonlinear, for example). In a spider plot, the variation of input parameters (as a percentage of mean) are shown in the x-axis and the corresponding variation in output (as a percentage of mean output) are plotted in the y-axis.

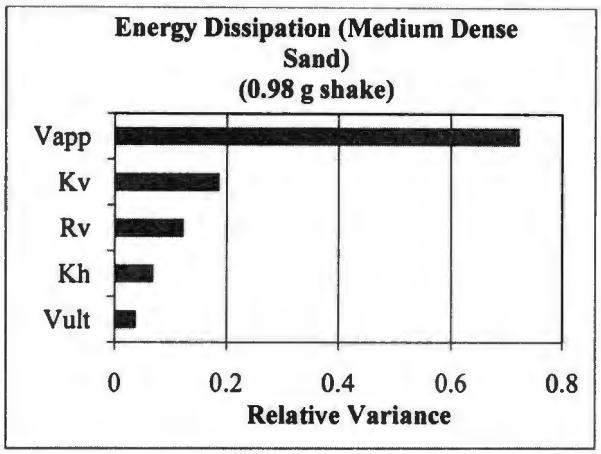

Fig. 5.2. FOSM plot for energy dissipation of shallow foundation supported by medium dense sand subjected to ground shaking with maximum acceleration of 0.98 g

In order to clearly examine the relationships between outputs and inputs, in this study, five values are chosen for each input parameter (μ, $\mu \pm 0.5\ \sigma$, and $\mu \pm \sigma$). Table 5.3 presents the input matrix for Spider plot method of dense sand with five random input parameters (Vult, Kv, Kh, Rv and Vapp) and other constant input parameters (bold row presents the mean value of all the input parameters). In addition to the eleven simulations conducted for Tornado diagram method and FOSM method, ten additional simulations ($\mu \pm 0.5\ \sigma$ for five random input variables) have been carried out for Spider plot method.

To study response of shallow foundation resting on different types of soil similar input matrices are created in spider plot method. Twenty one (4 x 5 + 1) simulations are performed for each types of soil subjected to maximum ground accelerations of 0.27 g, 0.55 g and 0.98 g. Considering the same COV value of mesh spacing as used in the

Tornado method, the effect of mesh spacing on shallow foundation resting on dense sand and stiff clay type soil is studied using spider plot method.

Table 5.3. Input matrix for Spider plot method with five random input parameters (Dense Sand)

Vult (MN)	Kv (MN/m)	Kh (MN/m)	Rv	Vapp (MN)
22.6	1000	719	0.1	1.13
11	1329	719	0.1	1.13
11	1000	956	0.1	1.13
11	**1000**	**719**	**0.1**	**1.13**
11	1000	539	0.1	1.13
11	750	719	0.1	1.13
5.66	1000	719	0.1	1.13
11	1000	719	0.2	1.13
11	1000	719	0.2	1.13
15.6	1000	719	0.1	1.13
11	1158	719	0.1	1.13
11	1000	833	0.1	1.13
11	1000	629	0.1	1.13
11	874.4	719	0.1	1.13
7.84	1000	719	0.1	1.13
11	1000	719	0.075	1.13
11	1000	719	0.15	1.13
11	1000	719	0.1	1.3
11	1000	719	0.1	1.21
11	1000	719	0.1	0.96
11	1000	719	0.1	1.05
Note: Constant input parameters:				
θelastic = 0.001 rad, L = 4 m, ΔL = 0.01 m and Vapp = 1.13 MN				

Fig. 5.3 presents an example spider plot for foundation settlement on dense sand subjected to 0.98 g maximum ground acceleration. In Fig. 5.3, x-axis presents the percent variation of all random input parameters (percentage of mean) and y-axis presents the percent variation of a particular output (settlement as percentage of mean settlement). The plot clearly presents that the settlement is strongly dependant on Kv, while the second and third biggest influencing input parameters are Rv and Vapp respectively. The plot also

reveals the relationships between settlement and Kv, and settlement and Vapp are almost linear, while the relationship between settlement and Rv is slightly nonlinear. The settlement does not vary much with the change of Kh and Vult in this particular case.

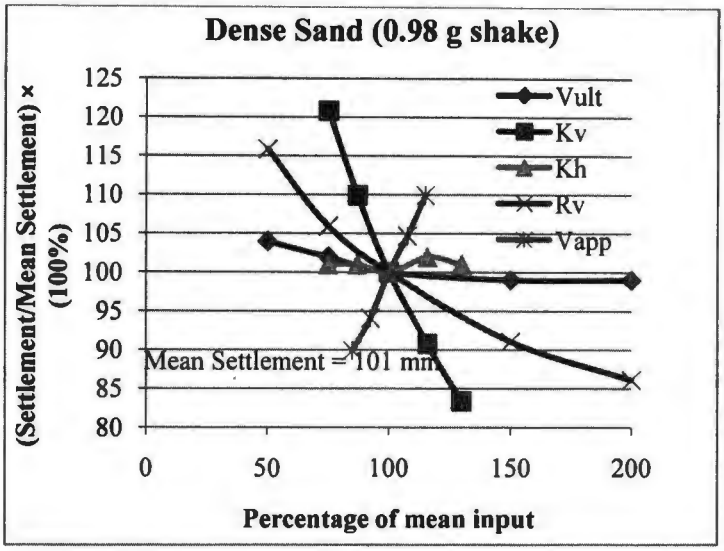

Fig. 5.3. Spider plot for settlement of foundation supported by dense sand subjected to ground shaking with maximum acceleration of 0.98 g

5.5. Monte-Carlo Simulation Method

To study the effect of uncertainties in soil properties (CIM input parameters) on the seismic performance of soil foundation systems (CIM output parameters), the Monte Carlo Simulation technique is the most effective method among the different probabilistic methods used in this study. The previous three methods (Tornado diagram, FOSM, and Spider plot) vary each random input variable at a time (μ, $\mu \pm 0.5\ \sigma$, and $\mu \pm \sigma$, etc), while keeping all other input parameters at mean values. Monte-Carlo simulation method considers all different possibilities by combining all possible combinations of random input variables. If the number of input parameters is "n" and each input parameters has "x" possible values, then the required number of simulations for Monte-Carlo technique is "x^n".

The Monte Carlo Simulation technique supplies a predicted probability distribution of the output variable for all probability of exceedence. This helps the engineers and the designers to approximate the probability of outcomes close to the mean and also helps to look at the probability of the outcome at the end of the distribution. Prediction of the entire distribution, rather than only the moments of the distribution, is important to engineers who are often concerned with the value that has a low probability of exceedence (Baynes, 2005).

Monte Carlo Simulation method is particularly suitable for numerical simulations of problems that are too complicated to solve analytically. Different steps used in this study to solve the problem by Monte Carlo Method are depicted in the following:

i. One deterministic model, which is CIM in OpenSees in this study, is selected.

ii. To avoid large number of simulations and evaluation of subsurface uncertainty only Vapp has been considered as constant in the Monte Carlo Simulation method. Four major input parameters (V_{ult}, K_v, K_h and R_v) are selected as random variable for large scale study. Few small scale studies are performed (specifically for dense sand and stiff clay) by varying two other parameters (applied vertical load and mesh spacing) in addition to the four above mentioned major input parameters.

iii. Three different values (μ, ($\mu + \sigma$) and ($\mu - \sigma$)) for each input parameters are evaluated.

iv. For a specific type of soil with a particular ground shaking, $3^4 = 81$ simulations (where number of random input parameters = 4) are performed in large scale study.

v. For each output, mean and standard deviation are determined

$$\mu_x = \frac{1}{n}\sum x_i \qquad (5.9)$$

$$\sigma_x = \sqrt{\frac{1}{n-1}\sum_{i=1}^{n}(x_i - \mu_x)^2} \qquad (5.10)$$

vi. Assuming normal distribution, probability density function is plotted using the following equation

$$f_x(x) = \frac{1}{\sigma_x\sqrt{2\pi}}\exp\left[-\frac{1}{2}\left(\frac{x-\mu_x}{\sigma_x}\right)^2\right], -\infty < x < +\infty \qquad (5.11)$$

vii. Cumulative distribution function is plotted with the following equation:

$$F_X(x) = P[X \le x] = \int_{-\infty}^{x} f_X(x)\,dx \qquad (5.12)$$

Table 5.4 presents the values of the four major input parameters (μ, (μ + σ) and (μ - σ)) those are used to create the input matrix for stiff clay in Monte Carlo Simulation method. Input matrix was created using the random values (for four major parameters) and constant values (for four other parameters) and a total of eighty one (3^4) simulations were carried out for each soil type.

Table 5.4. Values used to create the input matrix for Monte Carlo Analysis method with four random input parameters (Stiff Clay)

	Vult (MN)	Kv (MN/m)	Kh (MN/m)	Rv
μ	6.8	835	601	0.1
μ - σ	4.5	563	405	0.05
μ + σ	9.0	1105	795	0.2
Note: Constant input parameters:				
θelastic = 0.001 rad, L = 4 m, ΔL = 0.01 m and Vapp = 0.6 MN				

To study shallow foundation response using Monte Carlo Simulation method similar input matrices are created for foundation resting on other types of soil. Considering the same COV values of vertical load and mesh spacing as used in the Tornado method, the effect of applied vertical load and mesh spacing on shallow foundation resting on dense sand and stiff clay type soil is studied using Monte Carlo Simulation method.

Fig. 5.4 presents an example PDF and CDF plot of foundation energy dissipation for stiff clay subjected to 0.27 g maximum ground acceleration. From the simulation results, mean and standard deviation are calculated for each output and the PDF and CDF of each output are then calculated using equation (5.11) and (5.12) respectively. In Fig. 5.4, in the direction-axis, left side scale presents the value of the probability density function and the right side scale presents the value of cumulative density function. To verify the normal distribution assumption of the output, CDF curve has been compared with the result obtained from numerical simulations (solid squares in Fig. 5.4). As can be seen from Fig. 5.4, using the CDF relationship, the probability of occurrence and exceedence of energy dissipation with a particular value can be calculated. For example, the probability of not exceeding the energy dissipation value of 17 MN.m.rad is 20% whereas the probability of exceeding that value is 80%.

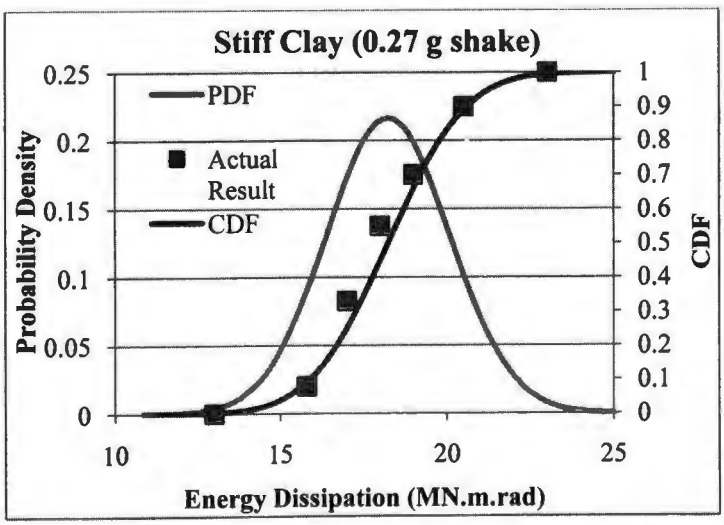

Fig. 5.4. PDF and CDF plot for energy dissipation of foundation supported by stiff clay subjected to ground shaking with maximum acceleration of 0.27 g

Table 5.5 presents the number of simulations performed in the Monte Carlo simulation analysis for each case. The table shows the values of maximum ground shaking

with the name of the input parameters varied in the Monte Carlo analysis and the number of simulations performed for each type of soil.

Table 5.5. Number of simulations performed in the Monte Carlo analysis

Soil Type	Maximum Ground Acceleration	Random Input Parameters	Number of Simulations
Dense Sand	0.27 g	R_v, K_h, K_v and V_{ult}	81
	0.55 g	R_v, K_h, K_v, V_{ult} and V_{app}	243
	0.98 g	R_v, K_h, K_v and V_{ult}	81
Medium Dense Sand	0.27 g	R_v, K_h, K_v and V_{ult}	81
	0.55 g	R_v, K_h, K_v and V_{ult}	81
	0.98 g	R_v, K_h, K_v and V_{ult}	81
Loose Sand	0.27 g	R_v, K_h, K_v and V_{ult}	81
	0.55 g	R_v, K_h, K_v and V_{ult}	81
	0.98 g	R_v, K_h, K_v and V_{ult}	81
Stiff Clay	0.27 g	R_v, K_h, K_v and V_{ult}	81
	0.55 g	R_v, K_h, K_v, V_{ult} and V_{app}	243
	0.98 g	R_v, K_h, K_v and V_{ult}	81
Medium Stiff Clay	0.27 g	R_v, K_h, K_v and V_{ult}	81
	0.55 g	R_v, K_h, K_v and V_{ult}	81
	0.98 g	R_v, K_h, K_v and V_{ult}	81
Soft Clay	0.27 g	R_v, K_h, K_v and V_{ult}	81
	0.55 g	R_v, K_h, K_v and V_{ult}	81
	0.98 g	R_v, K_h, K_v and V_{ult}	81
Dense Sand	0.55 g	R_v, K_h, K_v, V_{ult} and ΔL	243
Stiff Clay	0.55 g	R_v, K_h, K_v, V_{ult} and ΔL	243

CHAPTER 6. RESULTS AND DISCUSSIONS

6.1. Introduction

The purpose of this chapter is to discuss the results of probabilistic numerical simulations in terms of the seismic performance of soil-foundation systems and how sensitive they are to the soil properties. The sensitivities of the ultimate moment capacity of the soil-foundation system (Mult), settlement (s) and rotation (θ) at the base center point of the foundation and the energy dissipation (ED) characteristics of the soil-foundation systems are discussed. In addition to the applied vertical load (Vapp) on the foundation, the four major random input parameters for numerical simulations (CIM), derived from shear strength and shear stiffness of soil, considered in this study include ultimate vertical load (Vult), initial vertical stiffness (Kv), initial horizontal stiffness (Kh) and rebound ratio (Rv).

Selected results are presented in terms of Tornado diagrams, FOSM diagrams, Spider plots, probability density function (PDF) plots, and cumulative density function (CDF) plots. The PDF and CDF plots have been obtained from the small scale Monte Carlo Simulation (MCS) technique. The MCS has been performed only to study the effect of subsurface uncertainties considering Vult, Kv, Kh and Rv as random parameters and all other parameters including Vapp as constant. Results that are not included in this chapter are included in Appendix. Figures of the outputs are presented in the order of shaking intensity variation and soil strength variation. Plots are arranged with the increment of shaking intensity from top to bottom and with the decrement of soil strength from left to right.

At the end of the chapter, sensitivity of the CIM model to mesh spacing and mean and COV values of the outputs as a function of shaking intensity for all types of soil have been presented.

6.2. Sensitivity Study of Ultimate Moment Capacity

To study the sensitivity of the ultimate moment capacity of the soil-foundation system to the CIM input parameters, in addition to the four major CIM input parameters (Vult, Kv, Kh, and Rv), the applied vertical load imposed on the structure has also been varied. Fig 6.1 presents the Tornado diagrams of the output ultimate moment of the soil-foundation system resting on sandy soils. Fig 6.2, Fig 6.3 and Fig 6.4 respectively present Tornado diagrams, Spider plots, and PDF and CDF plots of the ultimate moment capacity of the soil-foundation system resting on clayey soils. The plots have been arranged with the increment of shaking intensity from top to bottom (0.27 g, 0.55 g and 0.98 g maximum ground acceleration) and with the decrement of soil strength from left to right (strong, medium strong, and weak soils).

From the Tornado diagrams (Fig. 6.1 and Fig. 6.2), it can be seen that the ultimate moment capacity of the soil-foundation system is more sensitive to the applied vertical load on the foundation than any other input parameters for all types of soils and for all shaking intensities. Though not presented in this chapter, FOSM diagrams reveal that the contribution of Vapp itself ranges from 75% to 95% in most of the cases, while all other input parameters contribute the rest (please see Fig. A.1 and A.3 in Appendix), even though the COV of Vapp is 15% while the COV of all other input parameters range from 30% to 100%. This is expected because, as shown in the theoretical ultimate moment equation

($M_u = \frac{V_{app} L}{2}\left[1 - \frac{1}{FS}\right]$), moment capacity is more sensitive to applied vertical load than any other parameters for relatively higher FSv values (the FSv values considered in this study range from 5 to 20 for sandy soils and 7.5 to 15 for clayey soils). The other input parameters that slightly affect the ultimate moment include Vult and Kv, however their effects on ultimate moment decreases as the shaking intensity increases.

In order to study the nature of the relationship between ultimate moment and Vapp, Fig. 6.3 presents the results for clayey soils in terms of normalized Vapp and normalized ultimate moment (both normalized to their respective means). As can be seen from Fig. 6.3, the relationship between normalized ultimate moment and normalized Vapp is almost linear. This is because for relatively higher FSv values (FSV $\approx$ 10) and for constant geometry of the footing (L), the ultimate moment is almost linearly related to Vapp. Similar linear relationships obtained between normalized ultimate moment and normalized Vapp for sandy soils as well regardless of the shaking intensity (please see Fig. A.2 in Appendix).

Fig. 6.4 presents the PDF and CDF distribution of the ultimate moment assuming that the output ultimate moment follows the normal distribution and using the theoretical equations for PDF and CDF (described in Chapter 5). It should be noted that PDF and CDF relationships were obtained using the output of the Monte-Carlo simulations, where Vapp was kept constant and Vult, Kv, Kh, and Rv were varied. Also plotted in Fig. 6.4 are the CDF values calculated purely based on the simulation output results (solid symbols) in order to verify that the normal distribution assumption is valid. The PDF plots (Fig 6.4) for the ultimate moment of foundation on clayey soils show that with the increase of shaking intensity the dispersion value of the ultimate moment capacity decreases (in other words,

the uncertainty in ultimate moment capacity decreases). This is because, for higher shaking intensities, the foundation reaches close to the theoretical moment capacity sooner (when compared with small shakes), and hence the small dispersion in calculated moment capacities. From the CDF plots ultimate moment capacity for a particular probability of exceedence can also be found. From the CDF plots and the results obtained from the numerical simulations it can be concluded that the normal distribution assumption of ultimate moment capacity is reasonably valid. Similar characteristics are found for footings resting on sand as well (Appendix Fig. A.4).

6.2.1. Special Study with Undrained Shear Strength of Clay COV = 50%:

In the previous section (6.2), results are presented for clayey soils with COV of undrained shear strength 33%. In order to further explore the effect of undrained shear strength of clay (which, in turn, controls Vult, Kv and Kh), a special study was carried for foundations resting on clayey soils with COV of undrained shear strength of 50%. This study has been performed for foundations resting on medium stiff clay soil subjected to 0.55 g maximum ground shaking acceleration. Results of this study are presented in Fig. 6.5 and the results reinforce the conclusions derived in section 6.2. Comparing the results presented in Fig. 6.2 to 6.4 with the results presented in Fig. 6.5 clearly shows that the ultimate moment is less sensitive to undrained shear strength (in other words, Vult, Kv and Kh) when compared with applied vertical load (same COV value for Vapp (15%) has been used and the COV of Vult, Kv and Kh has been changed from 27% to 40%). It should be noted that this is only true for relatively higher FSv values (the design FSv values used in seismically active zones).

From these results it can be concluded that ultimate moment capacity is more sensitive to applied vertical load than soil properties (steep slopes in spider plots). Since the uncertainty in applied vertical load is typically much smaller than the uncertainties in soil properties, the ultimate moment capacity of the soil-foundation system during seismic loading is predictable with reasonable accuracy.

6.3. Sensitivity Study of Energy Dissipation (ED)

Fig. 6.6 and Fig. 6.7 respectively present Tornado diagrams and Spider plots of the output energy dissipation of soil-foundation system resting on sandy soil. Fig. 6.8, Fig. 6.9 and Fig. 6.10 respectively present Tornado diagrams, FOSM plots, and PDF and CDF plots of the energy dissipation of soil-foundation system resting on clayey soils. Fig. 6.11 and Fig. 6.12 respectively present the FOSM plots of energy dissipation of soil-foundation system resting on sandy soils and clayey soils considering only four (Vult, KV, Kh and Rv) random input parameters. The plots have been arranged with the increment of shaking intensity from top to bottom (0.27 g, 0.55 g and 0.98 g maximum ground acceleration) and with the decrement of soil strength from left to right (strong, medium strong, and weak soils).

From the Tornado diagrams (Fig. 6.6 and Fig. 6.8) it can be seen that Vapp and Kv are the key input parameters that contribute to the energy dissipation of the soil-foundation system and Vapp has largest relative contribution and Kv has second largest relative contribution to the energy dissipation in most of the cases. FOSM diagrams (Fig. 6.9) for clayey soils reveal that the relative contribution of Vapp on energy dissipation ranges from 40% to 60% and the relative contribution of Kv ranges from 20% to 50%. The other input

parameters that slightly affect the energy dissipation include Rv and Vult. Almost similar characteristics have been observed for foundations resting on sandy soils (Appendix A.5).

In order to study the nature of the relationship between energy dissipation and input parameters, Fig. 6.7 presents the results for sandy soils in terms of normalized input parameters and normalized energy dissipation. As can be seen from Fig. 6.7, the relationships between normalized energy dissipation, and normalized Vapp and normalized Kv are almost linear. This linear relationship observed since Vapp has almost linear relationship with moment (section 6.2) and the variation of rotation is very small with the change of Vapp (Appendix A.13) (energy dissipation has been obtained from the integrated area of the hysteresis loop in the moment-rotation plot). Similarly Kv has slightly linear effect on moment and strong linear relationship with rotation therefore linear relationship has been obtained between normalized energy dissipation and normalized Kv. The effect of Vult and Kh on energy dissipation is almost negligible. Similar relationships obtained between normalized energy dissipations and normalized input parameters for clayey soils as well (Fig. A.7 in Appendix).

Fig. 6.10 presents the PDF and CDF distribution of the energy dissipation assuming that the output energy dissipation follows the normal distribution and using the theoretical equations for PDF and CDF (described in Chapter 5). Also plotted in Fig. 6.10 are the CDF values calculated purely based on the simulation output results (solid symbols) in order to verify that the normal distribution assumption is valid. From the CDF plots energy dissipation values for a particular probability of exceedence can also be found. From the CDF plots and the results obtained from the numerical simulations it can be concluded that the normal distribution assumption of energy dissipation is reasonably valid.

In order to study the effects of soil properties alone on the amount of energy dissipation, simulations were carried out with four random input parameters (Vult, Kv, Kh, and Rv), while keeping Vapp as constant. The results of these simulations are presented in Fig. 6.11 and Fig. 6.12. It can be concluded that when Vapp is constant, Kv (which is a function of shear modulus of the soil and the geometry of the footing) contributes to the energy dissipation the most and it is followed by Rv.

6.3.1. Special Study with Undrained Shear Strength of Clay COV = 50%:

In the previous section (6.3), results are presented for clayey soils with COV of undrained shear strength 33%. In order to further explore the effect of undrained shear strength of clay, a special study was carried for foundations resting on clayey soils with COV of undrained shear strength 50%. This study has been performed for foundations resting on medium stiff clay soil subjected to 0.55 g maximum ground shaking acceleration. Results of this study are presented in Fig. 6.13. As can be seen from the figure, when the COV of undrained shear strength is 50%, the contribution of Kv to the energy dissipation becomes significant when compared to the contribution by Vapp (with COV = 15%).

6.4. Sensitivity Study of Settlement

Fig. 6.14 and Fig. 6.15 respectively present FOSM plots and Spider plots of the output settlement of soil-foundation system resting on sandy soils. Fig. 6.16 and Fig. 6.17 respectively present FOSM plots, and PDF and CDF plots of the settlement of soil-foundation system resting on clayey soils. The plots have been arranged with the increment of shaking intensity from top to bottom (0.27 g, 0.55 g and 0.98 g maximum ground

acceleration) and with the decrement of soil strength from left to right (strong, medium strong, and weak soils).

From the FOSM plots (Fig. 6.14 and Fig. 6.16) it can be seen that Kv and Rv are the key input parameters that contribute to the variation of settlement. Kv has largest relative contribution and Rv has second largest contribution on the settlement in most of the cases. In the FOSM plots the contribution of Kv on settlement ranges from 30% to 80% whereas the contribution of Rv on settlement for small shaking intensity (0.27 g) is less than 10% and for bigger shaking intensities (0.55 g and 0.98 g) it varies from 20% to 35%. In CIM, the actual rebounding of the soil is proportional to Rv and the amount of total settlement. As the total settlement increases with shaking intensity, the effect of Rv on settlement also increases. The other input parameters that slightly affect the settlement include Vapp and Vult.

In order to study the nature of the relationship between settlement and input parameters, Fig. 6.15 presents the results for sandy soils in terms of normalized input parameters and normalized settlement (both normalized to their respective means). As can be seen from Fig. 6.15, the relationships between normalized settlement and normalized Vapp and Kv are almost linear. This linear relationship has been observed since with the increase of Vapp, settlement increases, and with the increase of Kv, settlement decreases. However nonlinear relationship between normalized settlement and normalized Rv has been obtained since the COV values of Rv used in the simulations are relatively high (50% to 100%) in all cases. Spider plots and FOSM plots also reveal that the effects of Vult and Kh on settlement are negligible. Similar relationships obtained between normalized

settlements and normalized input parameters for clayey soils as well (Fig. A.10 in Appendix).

Fig. 6.17 presents the PDF and CDF distribution of the settlement assuming that the output settlement follows normal distribution and using the theoretical equations for PDF and CDF (described in Chapter 5). Also plotted in Fig. 6.17 are the CDF values calculated purely based on the simulation output results (solid symbols) in order to verify that the normal distribution assumption is valid. From the PDF and CDF plots, settlement value for a particular probability of exceedance can be computed. From the CDF plots and the results obtained from the numerical simulations it can be concluded that the normal distribution assumption of settlement is reasonably valid.

6.4.1. Special Study with Undrained Shear Strength of Clay COV = 50%:

In the previous section (6.4), results are presented for clayey soils with COV of undrained shear strength 33%. In order to further explore the effect of undrained shear strength of clay, a special study was carried for foundations resting on clayey soils with COV of undrained shear strength 50%. This study has been performed for foundations resting on medium stiff clay soil subjected to 0.55 g maximum ground shaking acceleration. Results of this study are presented in Fig. 6.18 and the results reinforce the conclusions derived in section 6.4. Comparing the results presented in Fig. 6.16 with the results presented in Fig. 6.18, it can be seen that the Kv and Rv are the key parameters that contribute to the settlement the most. However, the relative contribution of Kv in Fig. 6.18 becomes even more significant (as compared to Fig. 6.16), because Kv depends on undrained shear strength and the COV value of undrained shear strength used in this study is 50%.

6.5. Sensitivity Study of Rotation

Fig. 6.19 and Fig. 6.22 respectively present Tornado diagrams, and PDF and CDF plots of the output rotation of soil-foundation system resting on sandy soils. Fig. 6.20 and Fig. 6.21 present Tornado diagrams and FOSM plots of the rotation of the soil-foundation system resting on clayey soils. The plots have been arranged with the increment of shaking intensity from top to bottom (0.27 g, 0.55 g and 0.98 g maximum ground acceleration) and with the decrement of soil strength from left to right (strong, medium strong, and weak soils).

From the Tornado diagrams (Fig. 6.19 and Fig. 6.20), it can be seen that Rv and Kv are the key input parameters that contribute to the rotation of the foundation and Rv has largest relative contribution and Kv has second largest relative contribution to the rotation in most of the cases. In the FOSM plots (Fig. 6.21) the contribution of Rv on rotation ranges from 25% to 70% whereas the contribution of Kv on rotation varies from 10% to 40%.

Fig. 6.22 presents the PDF and CDF distribution of the rotation assuming that the output rotation follows the normal distribution and using the theoretical equations for PDF and CDF (described in Chapter 5). Also plotted in Fig. 6.22 are the CDF values calculated purely based on the simulation output results (triangular symbols) in order to verify that the normal distribution assumption is valid. From the CDF plots, rotation value for a particular probability of exceedance can be computed. From the CDF plots and the results obtained from the numerical simulations it can be concluded that the normal distribution assumption of rotation is reasonably valid.

6.5.1. Special Study with Undrained Shear Strength of Clay COV = 50%:

In the previous section (6.5), results are presented for clayey soils with COV of undrained shear strength 33%. In order to further explore the effect of undrained shear strength of clay, a special study was carried for foundations resting on clayey soils with COV of undrained shear strength 50%. This study has been performed for foundations resting on medium stiff clay soil subjected to 0.55 g maximum ground shaking acceleration. Results of this study are presented in Fig. 6.23 and the results reinforce the conclusions derived in section 6.5. Comparing the results presented in Fig. 6.23 with the results presented in Fig. 6.20 and Fig. 6.21 it can be depicted that the Kv and Rv are the key parameters that contribute to the rotation of the foundation. As can be seen from the spider plots in Fig. 6.23, the rotation of the foundation is not much sensitive to the input parameters (normalized rotation varies from 95% to 103%). The rotation of the foundation is mainly dictated by the intensity of shaking.

6.6. Sensitivity of Mesh Spacing

To study the sensitivity of the CIM mesh spacing, the input parameter ΔL has been varied as well (0.02 m, 0.01 m, and 0.005 m). Spacing between the nodes in CIM was changed to find the effect of node spacing to the outputs. This study is performed for dense sand and stiff clay soils with 0.55 g maximum ground shaking. From Fig. 6.24 and Fig. 6.25, it can be seen that influence of mesh spacing (after reaching a critical value) on the outputs is negligible in both cases.

6.7. Mean and COV of the Outputs and the Effect of Shaking Intensity

The mean and COV of the outputs have been obtained from the Monte Carlo simulation technique performed in this study. Fig. 6.26 and Fig. 6.27 respectively present

6.5.1. Special Study with Undrained Shear Strength of Clay COV = 50%:

In the previous section (6.5), results are presented for clayey soils with COV of undrained shear strength 33%. In order to further explore the effect of undrained shear strength of clay, a special study was carried for foundations resting on clayey soils with COV of undrained shear strength 50%. This study has been performed for foundations resting on medium stiff clay soil subjected to 0.55 g maximum ground shaking acceleration. Results of this study are presented in Fig. 6.23 and the results reinforce the conclusions derived in section 6.5. Comparing the results presented in Fig. 6.23 with the results presented in Fig. 6.20 and Fig. 6.21 it can be depicted that the Kv and Rv are the key parameters that contribute to the rotation of the foundation. As can be seen from the spider plots in Fig. 6.23, the rotation of the foundation is not much sensitive to the input parameters (normalized rotation varies from 95% to 103%). The rotation of the foundation is mainly dictated by the intensity of shaking.

6.6. Sensitivity of Mesh Spacing

To study the sensitivity of the CIM mesh spacing, the input parameter ΔL has been varied as well (0.02 m, 0.01 m, and 0.005 m). Spacing between the nodes in CIM was changed to find the effect of node spacing to the outputs. This study is performed for dense sand and stiff clay soils with 0.55 g maximum ground shaking. From Fig. 6.24 and Fig. 6.25, it can be seen that influence of mesh spacing (after reaching a critical value) on the outputs is negligible in both cases.

6.7. Mean and COV of the Outputs and the Effect of Shaking Intensity

The mean and COV of the outputs have been obtained from the Monte Carlo simulation technique performed in this study. Fig. 6.26 and Fig. 6.27 respectively present

the mean and COV values of the outputs for sandy and clayey soils as a function of shaking intensity. In the plots μ_1 = mean value of the output for dense sand or stiff clay, μ_2 = mean value of the output for medium dense sand or medium stiff clay and μ_3 = mean value of the output for loose sand or soft clay. Table 6.1 presents the COV values of the random CIM input parameters, and table 6.2 and table 6.3 respectively present COV values of the four outputs obtained for different maximum ground accelerations. As can be seen from table 6.2 and table 6.3, and Fig. 6.26 and 6.27, the COV of the ultimate moment and rotation of the foundation is less than 10% for all types of soils and for all shaking intensities considered in this study. The COV values of energy dissipation and settlement of the foundation varies considerably from about 5% to 50% depending on the type of soil and intensity of shaking. From the plots it can be seen that, except for the rotation of the footing (the output with lowest COV values), for all other outputs, COV values are higher for smallest intensity shaking than the medium and large intensity shakes. Though the actual (absolute) variations in the outputs for larger shaking events may increase, as the mean value becomes bigger, the COV values of the output for larger shaking events become smaller.

Table 6.1. COV values of the random CIM input parameters used in this study

	Vult (%)	Kv (%)	Kh (%)	Rv (%)
Dense Sand	54.4	23.2	23.0	50-100
Medium Dense Sand	48.2	25.0	25.5	50-100
Loose Sand	34.2	22.6	23.0	50-100
Stiff Clay	27.4	26.5	26.5	50-100
Medium Stiff Clay	27.4	26.5	26.5	50-100
Soft Clay	27.4	26.5	26.5	50-100

Table 6.2. COV values of the CIM outputs for sandy soils in different maximum ground accelerations

	Settlement (%)	Rotation (%)	Energy Dissipation (%)	Ultimate Moment (%)
Dense Sand (0.27 g)	10.4	4.5	31.8	9.3
Medium Dese Sand (0.27 g)	54.5	5.7	27.2	1.7
Loose Sand (0.27 g)	47.4	2.9	23.3	3.6
Dense Sand (0.55 g)	11.8	2.5	15.4	5.1
Medium Dese Sand (0.55 g)	27.4	3.6	4.0	2.6
Loose Sand (0.55 g)	24.1	3.5	4.1	4.8
Dense Sand (0.98 g)	18.5	2.3	8.9	4.6
Medium Dese Sand (0.98 g)	26.8	3.1	5.5	1.7
Loose Sand (0.98 g)	23.8	3.3	5.5	3.6

Table 6.3. COV values of the CIM outputs for clayey soils in different maximum ground accelerations

	Settlement (%)	Rotation (%)	Energy Dissipation (%)	Ultimate Moment (%)
Stiff Clay (0.27 g)	25.2	2.2	9.2	4.9
Medium Stiff Clay (0.27 g)	26.8	2.4	9.0	5.8
Soft Clay (0.27 g)	28.9	2.7	8.3	5.8
Stiff Clay (0.55 g)	20.8	3.3	8.2	4.3
Medium Stiff Clay (0.55 g)	20.6	3.6	7.7	1.7
Soft Clay (0.55 g)	21.2	3.6	7.1	3.7
Stiff Clay (0.98 g)	24.8	3.1	6.6	2.1
Medium Stiff Clay (0.98 g)	24.6	3.3	6.6	3.5
Soft Clay (0.98 g)	24.9	3.3	6.4	3.4

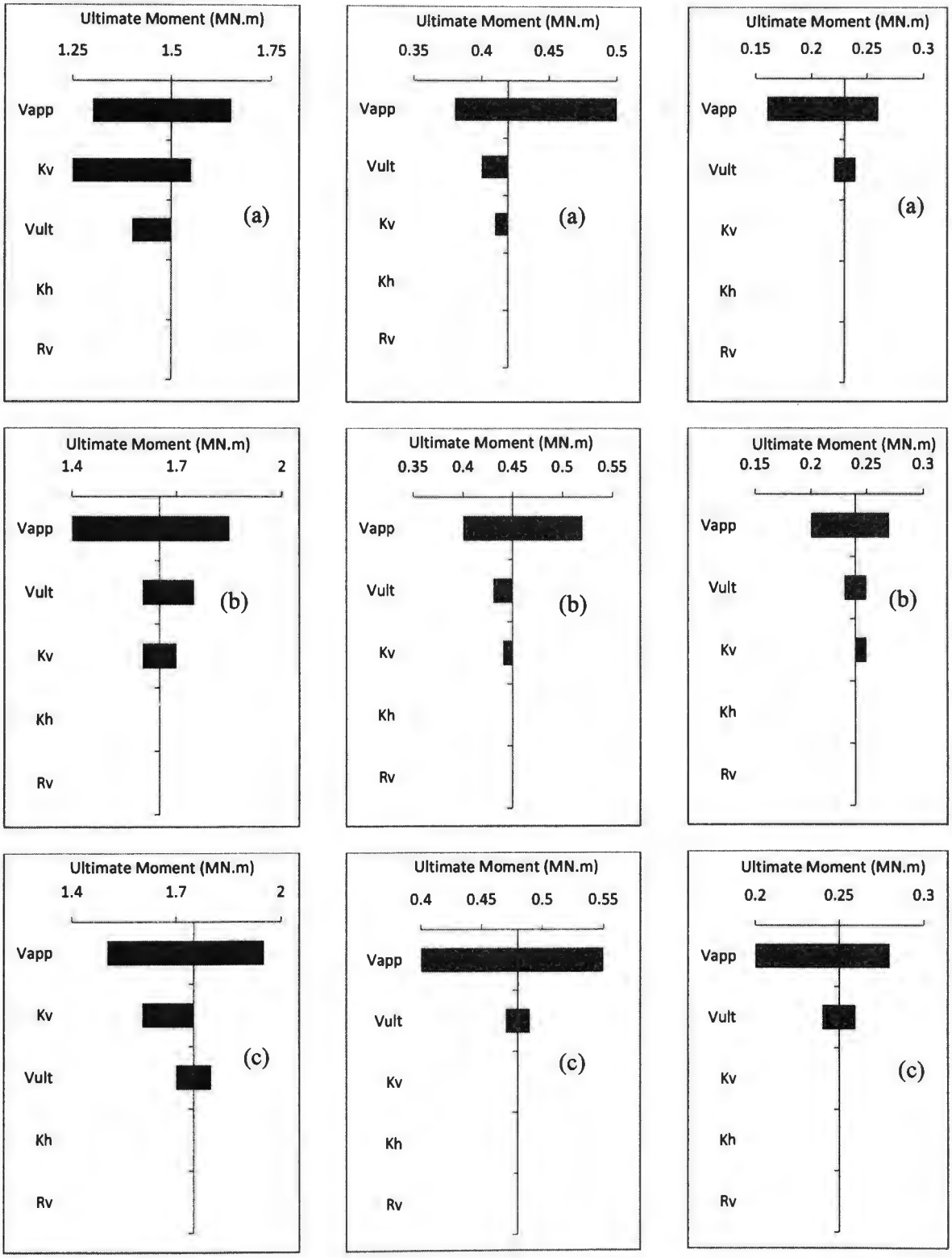

Dense Sand Medium Dense Sand Loose Sand

Fig. 6.1. Tornado plots of ultimate moment capacity of soil-foundation system resting on sandy soils subjected to (a) 0.27 g (b) 0.55 g and (c) 0.98 g maximum ground shaking

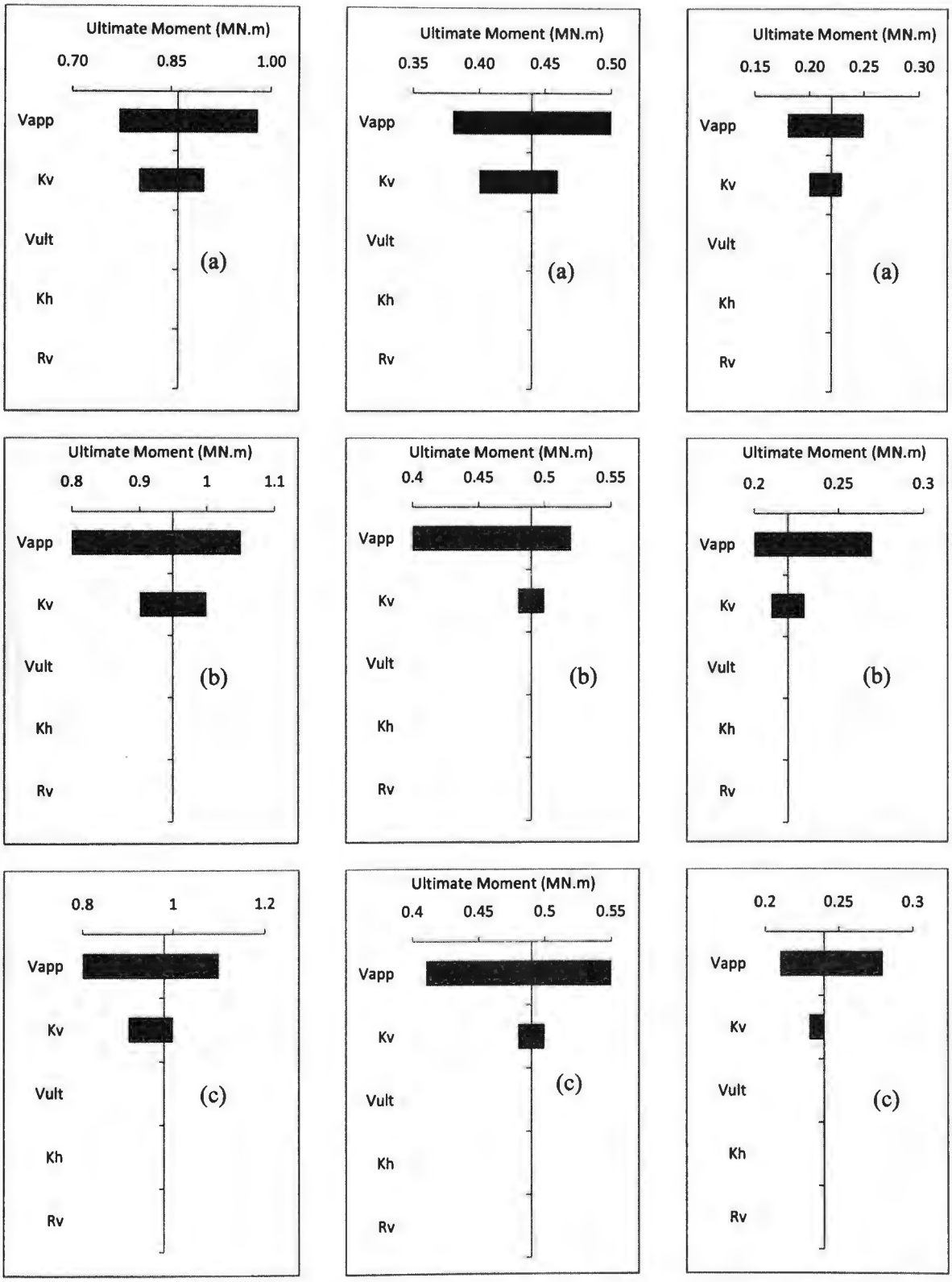

Stiff Clay Medium Stiff Clay Soft Clay

Fig. 6.2. Tornado plots of ultimate moment capacity of soil-foundation system resting on clayey soils subjected to (a) 0.27 g (b) 0.55 g and (c) 0.98 g maximum ground shaking

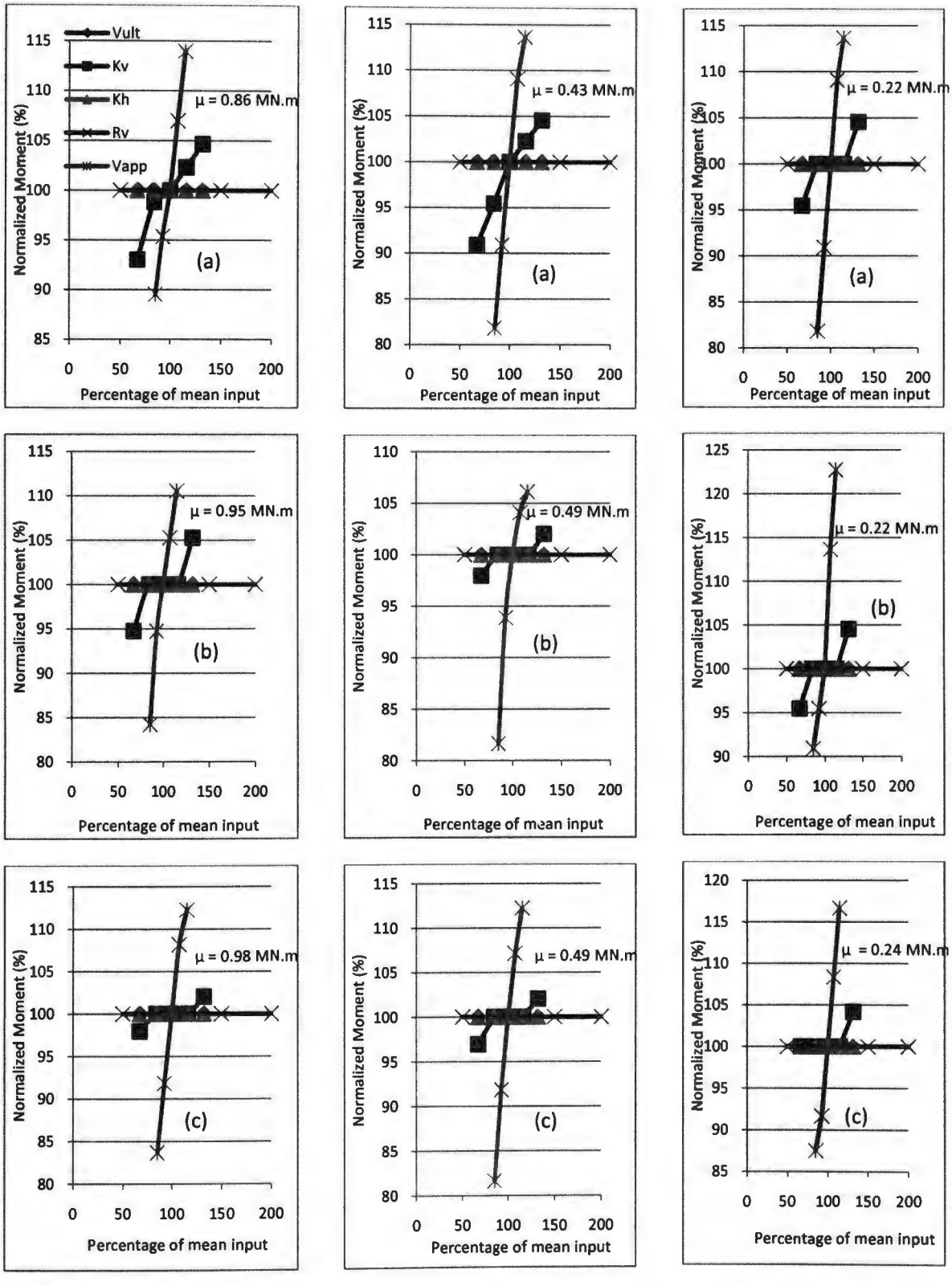

Stiff Clay Medium Stiff Clay Soft Clay

Fig. 6.3. Spider plots of ultimate moment capacity of soil-foundation system resting on clayey soils subjected to (a) 0.27 g (b) 0.55 g and (c) 0.98 g maximum ground shaking

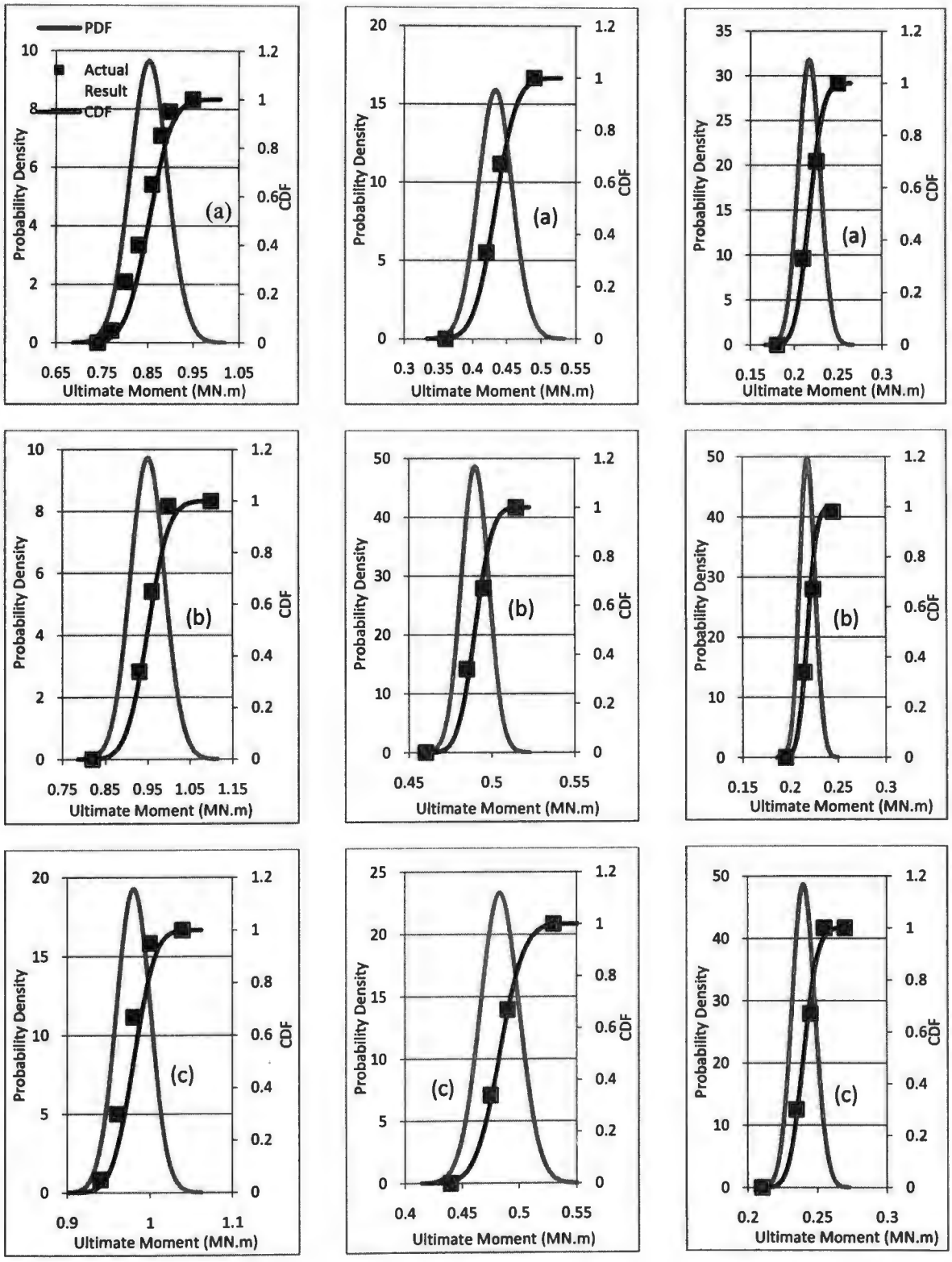

Fig. 6.4. PDF and CDF plots of ultimate moment capacity of soil-foundation system resting on clayey soils subjected to (a) 0.27 g (b) 0.55 g and (c) 0.98 g maximum ground shaking

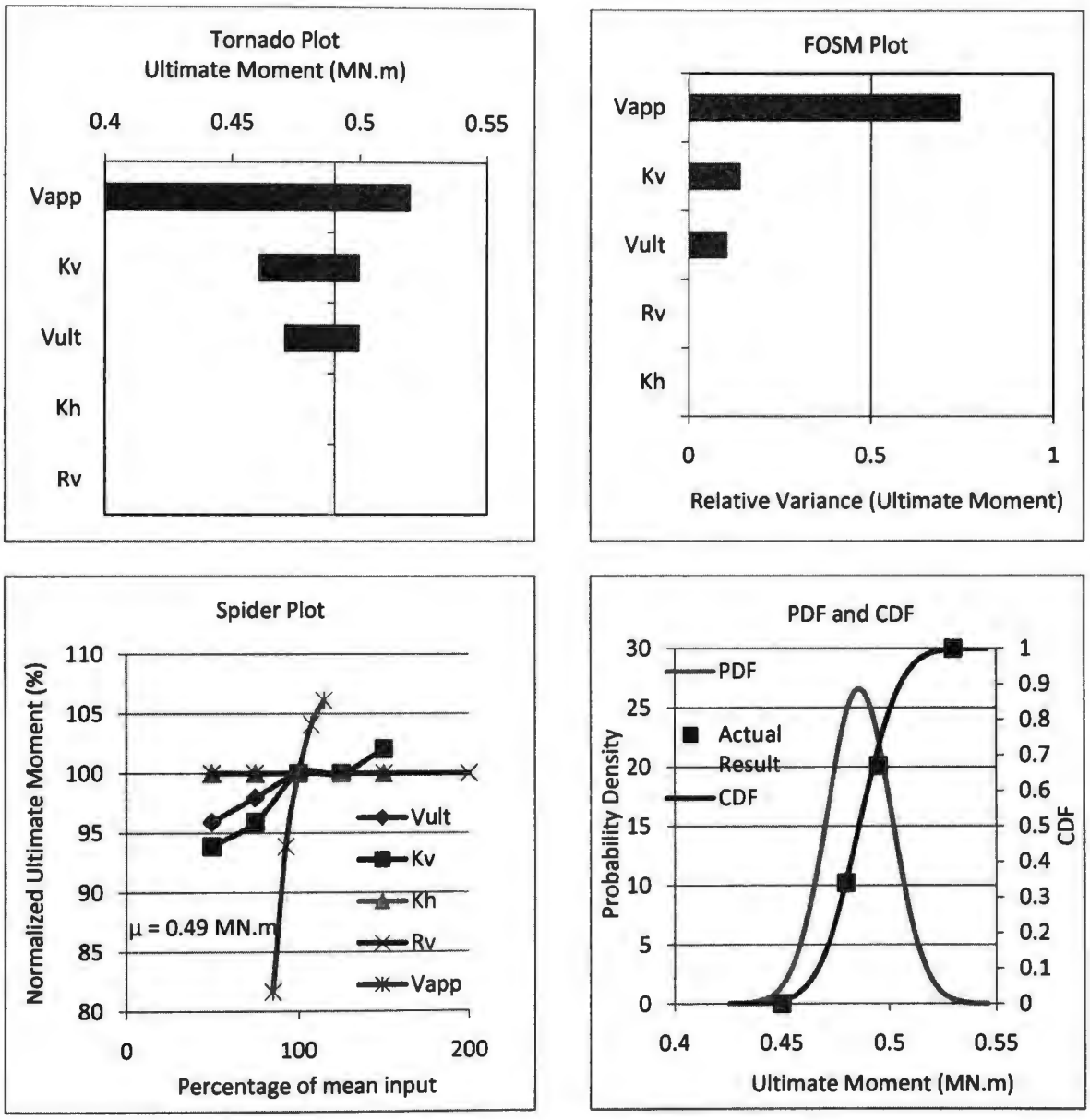

Fig. 6.5. Plots of ultimate moment capacity of soil-foundation system resting on medium stiff clay soil subjected to 0.55 g maximum ground shaking

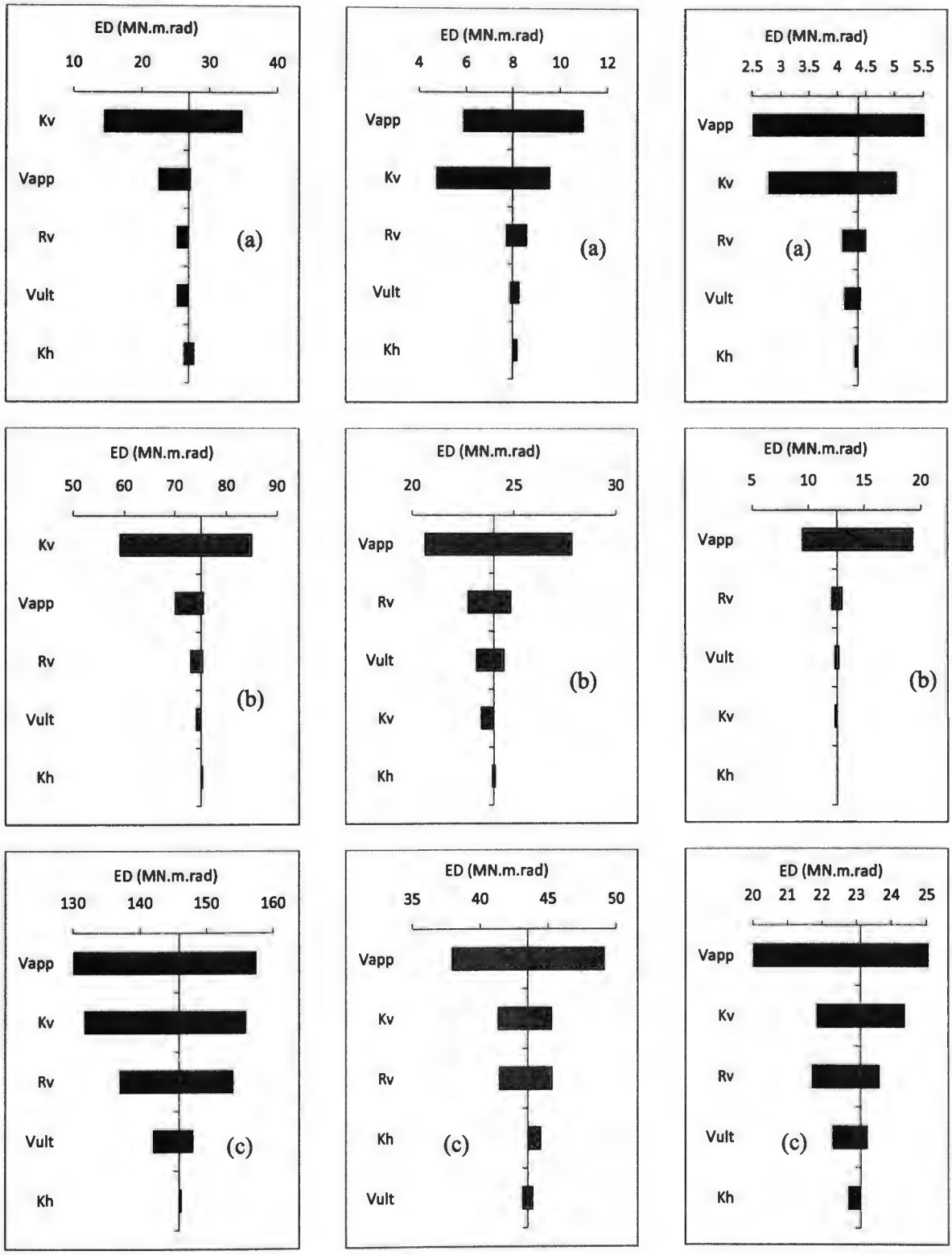

Dense Sand Medium Dense Sand Loose Sand

Fig. 6.6. Tornado plots of energy dissipation of soil-foundation system resting on sandy soils subjected to (a) 0.27 g (b) 0.55 g and (c) 0.98 g maximum ground shaking

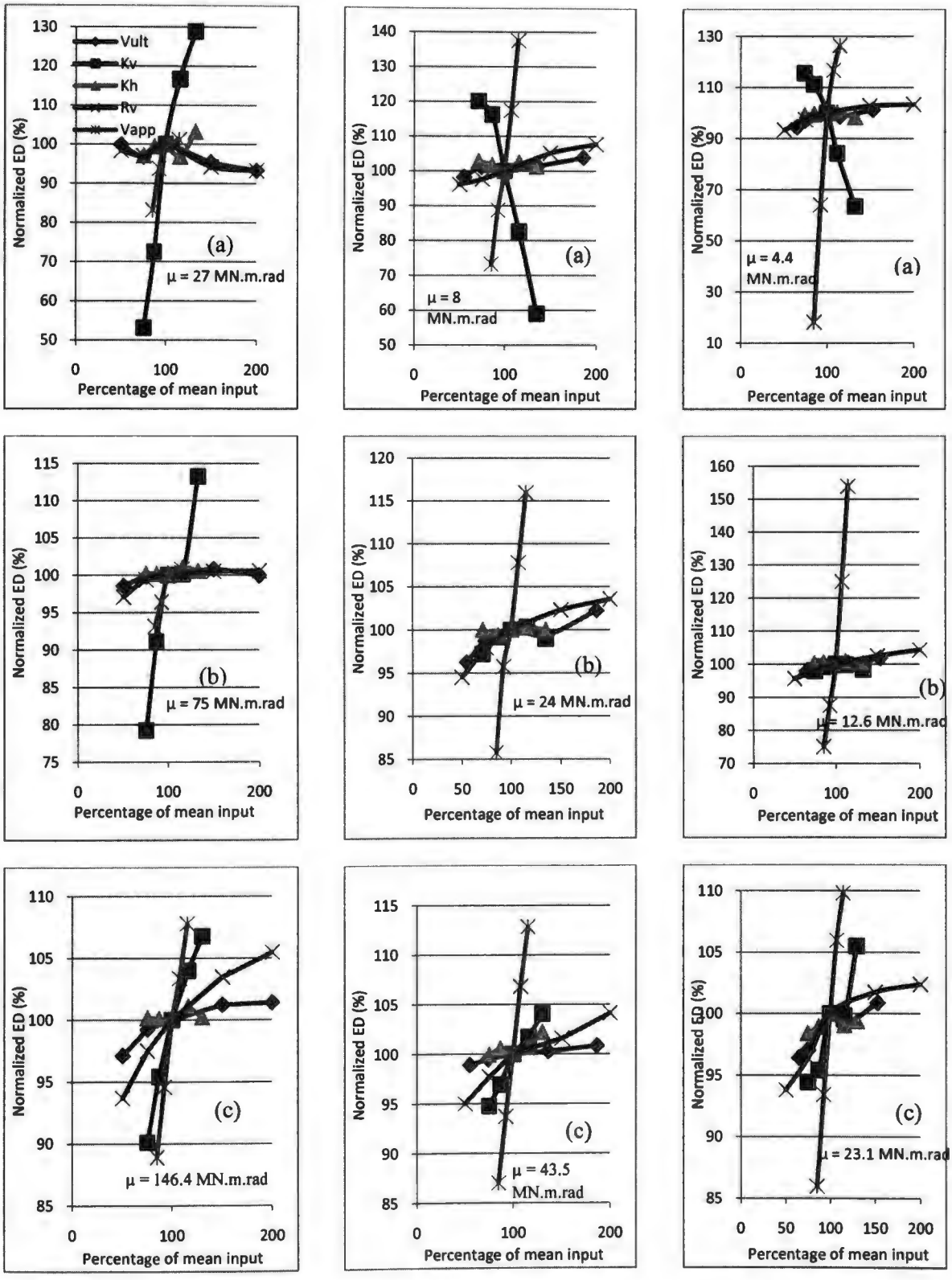

Fig. 6.7. Spider plots of energy dissipation of soil-foundation system resting on sandy soils subjected to (a) 0.27 g (b) 0.55 g and (c) 0.98 g maximum ground shaking

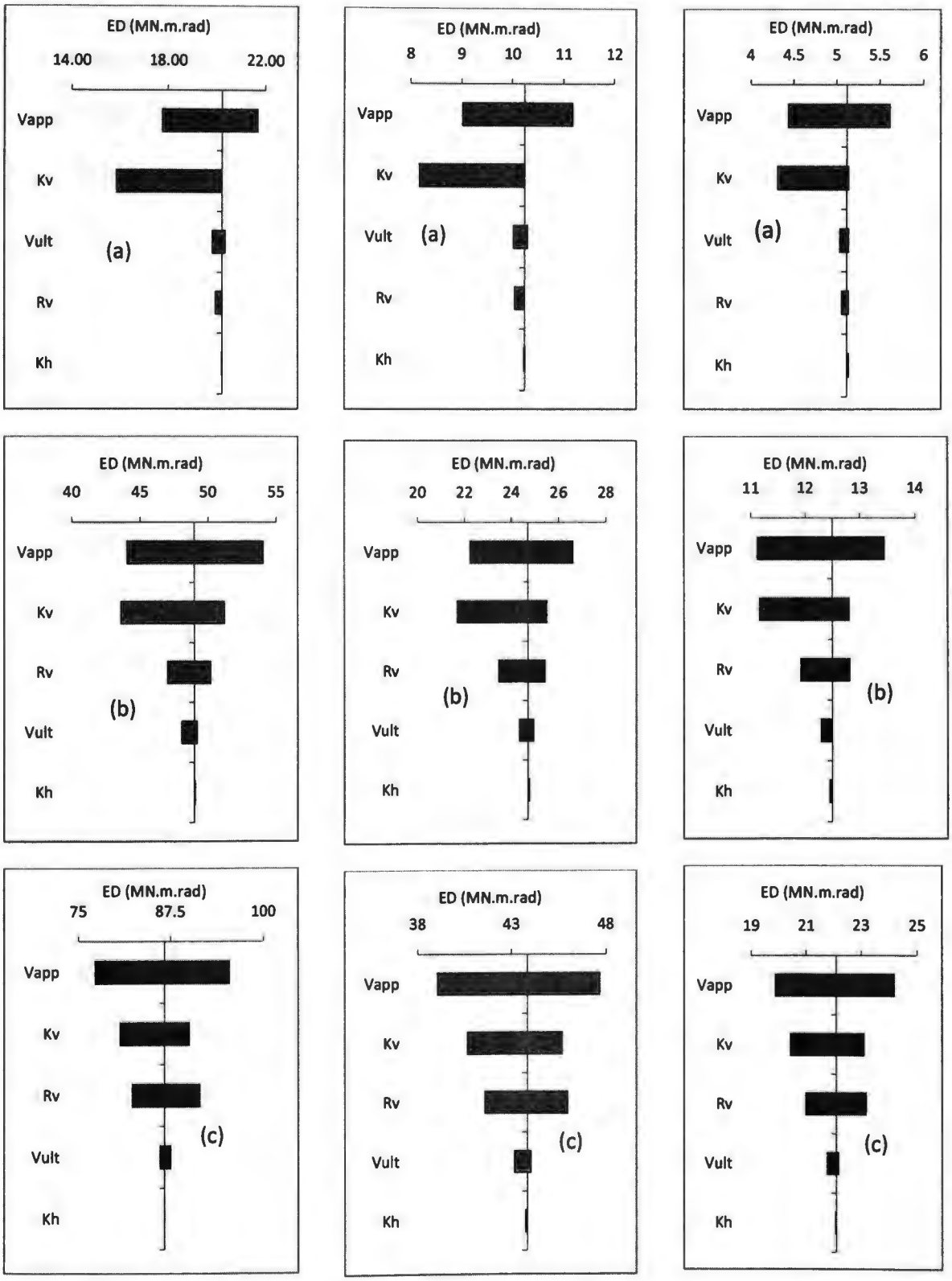

Stiff Clay Medium Stiff Clay Soft Clay

Fig. 6.8. Tornado plots of energy dissipation of soil-foundation system resting on clayey soils subjected to (a) 0.27 g (b) 0.55 g and (c) 0.98 g maximum ground shaking

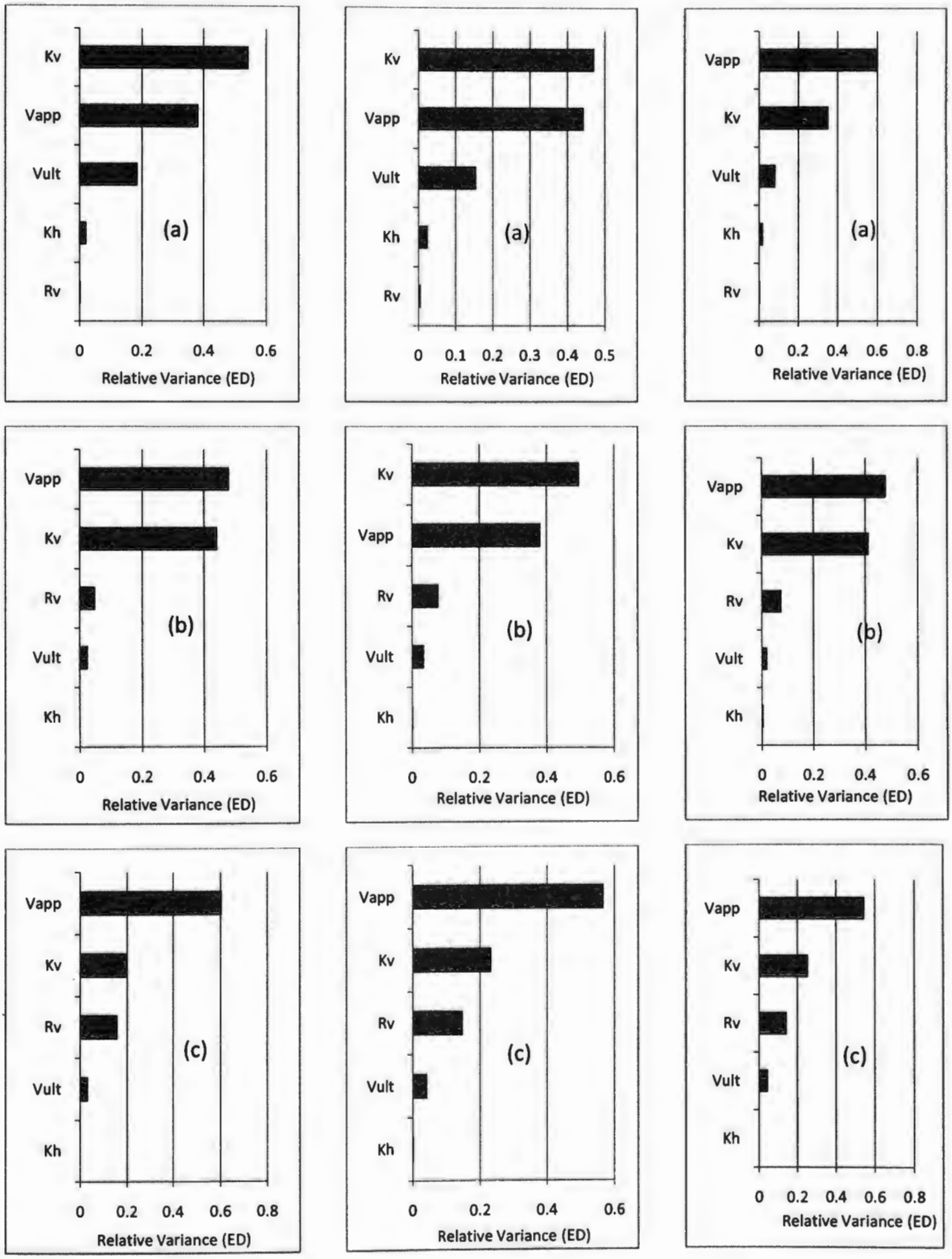

Stiff Clay Medium Stiff Clay Soft Clay

Fig. 6.9. FOSM plots of energy dissipation of soil-foundation system resting on clayey soils subjected to (a) 0.27 g (b) 0.55 g and (c) 0.98 g maximum ground shaking

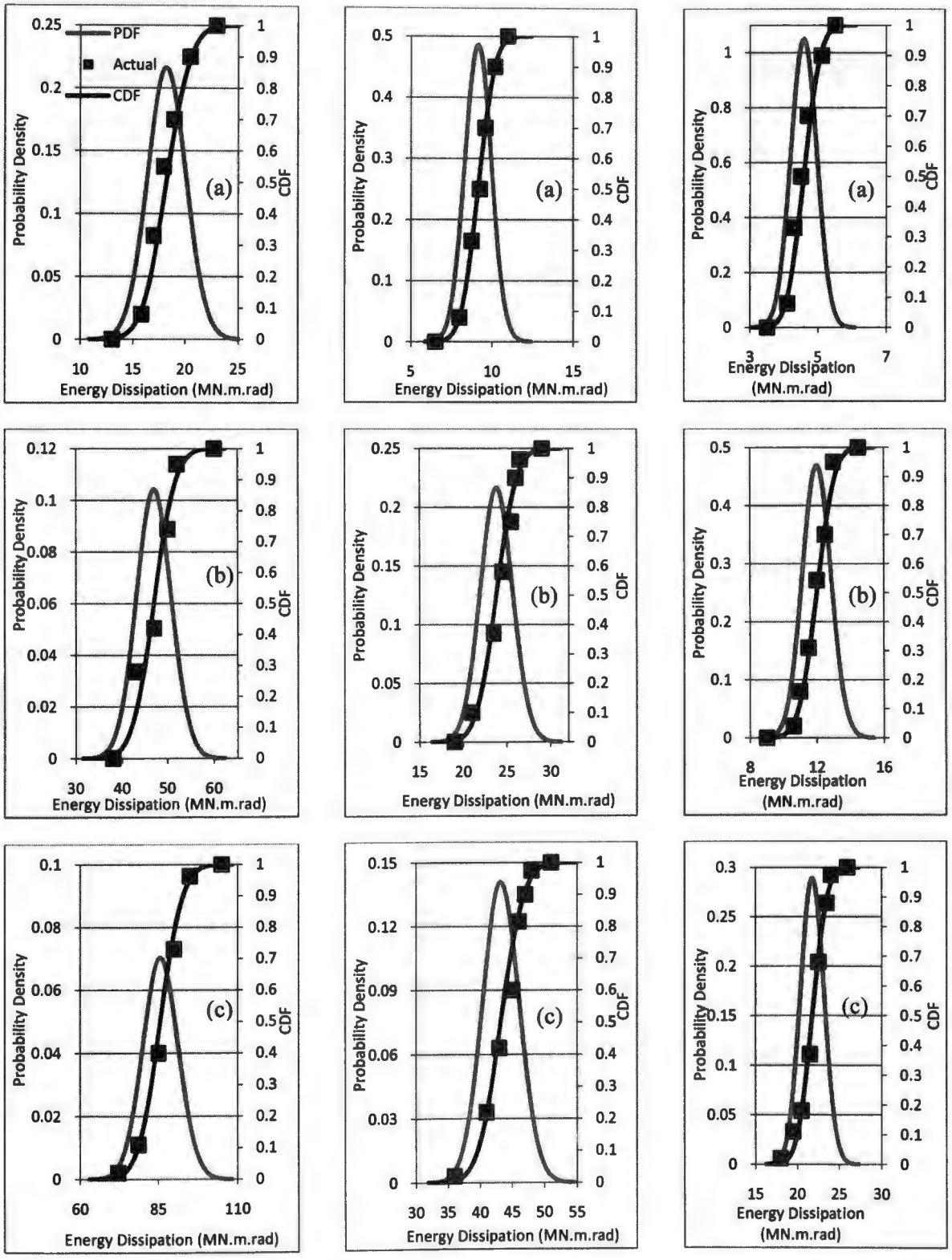

Stiff Clay Medium Stiff Clay Soft Clay

Fig. 6.10. PDF and CDF plots of energy dissipation of soil-foundation system resting on clayey soils subjected to (a) 0.27 g (b) 0.55 g and (c) 0.98 g maximum ground shaking

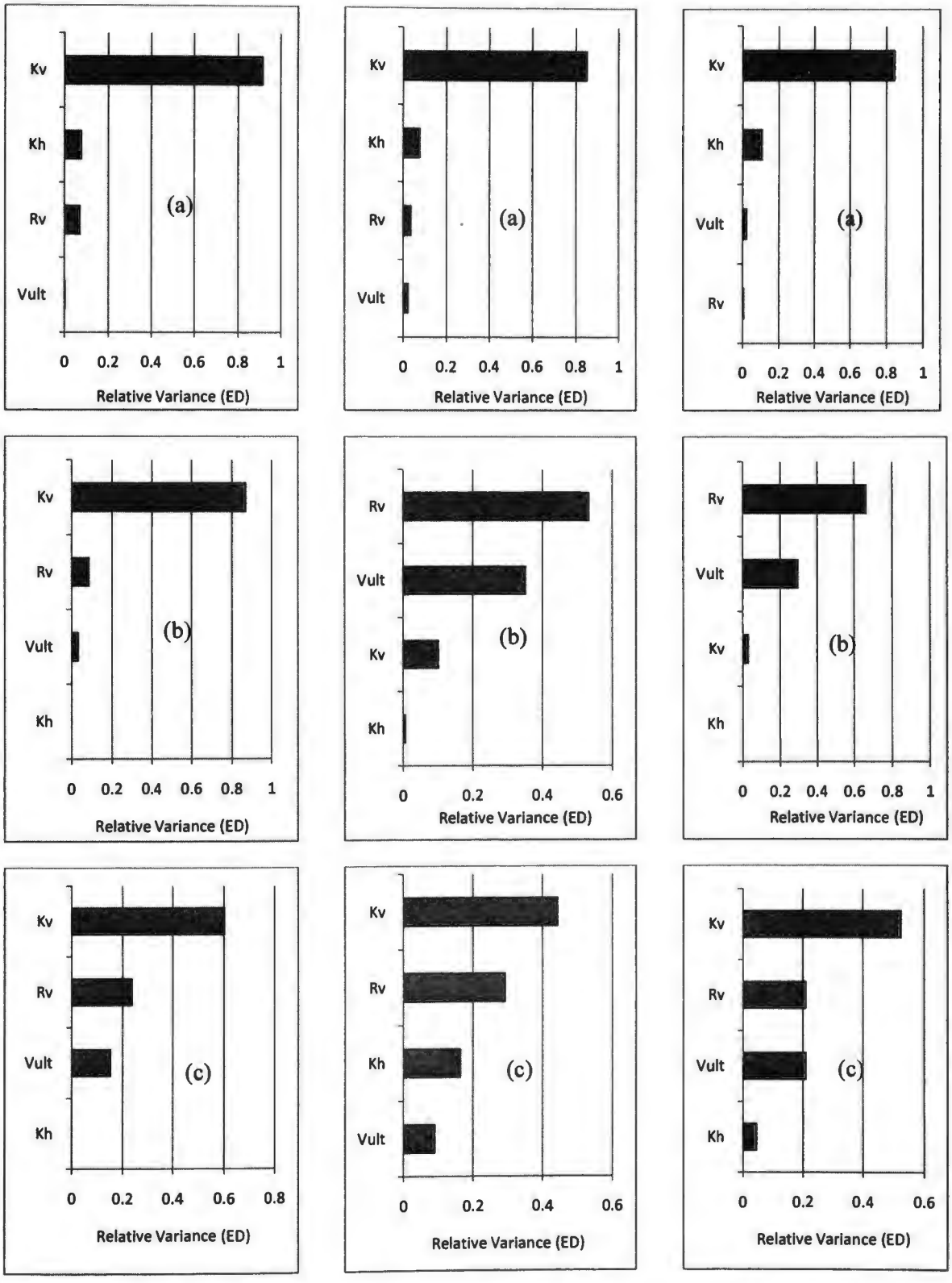

Dense Sand Medium Dense Sand Loose Sand

Fig. 6.11. FOSM plots of energy dissipation of soil-foundation system resting on sandy soils subjected to (a) 0.27 g (b) 0.55 g and (c) 0.98 g maximum ground shaking

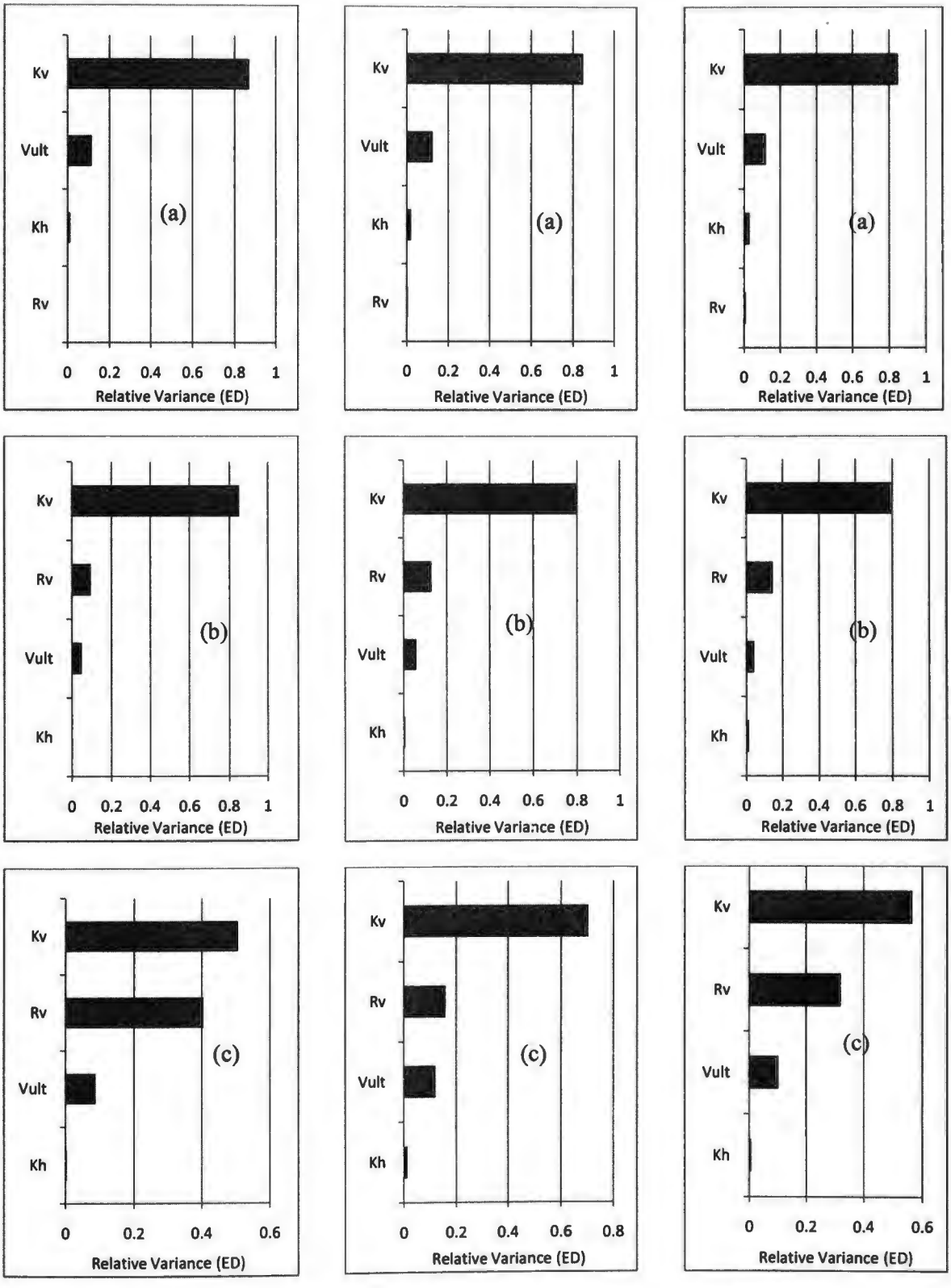

Stiff Clay Medium Stiff Clay Soft Clay

Fig. 6.12. FOSM plots of energy dissipation of soil-foundation system resting on clayey soils subjected to (a) 0.27 g (b) 0.55 g and (c) 0.98 g maximum ground shaking

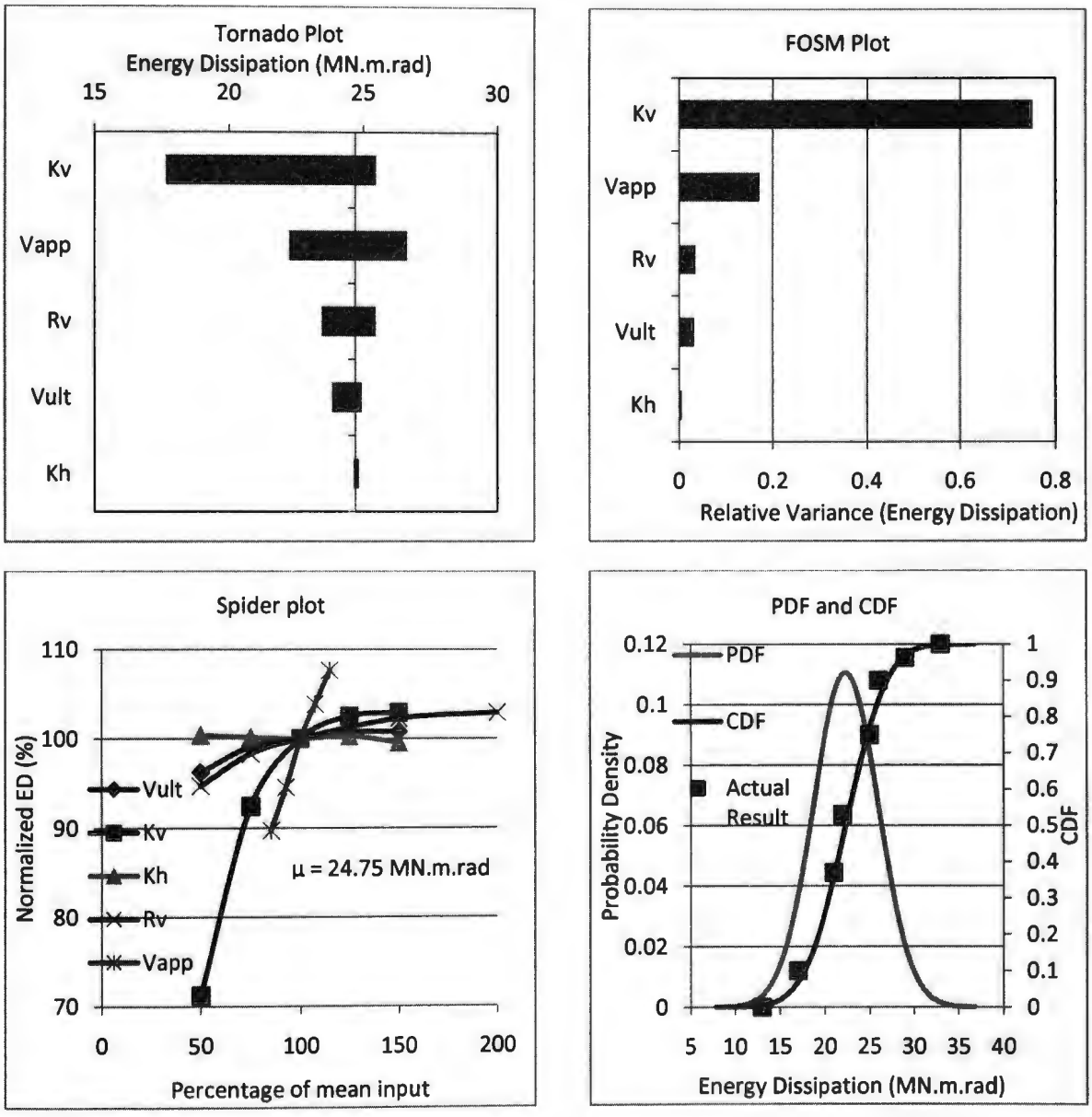

Fig. 6.13. Plots for energy dissipation of soil-foundation system resting on medium stiff clay soil subjected to 0.55 g maximum ground shaking

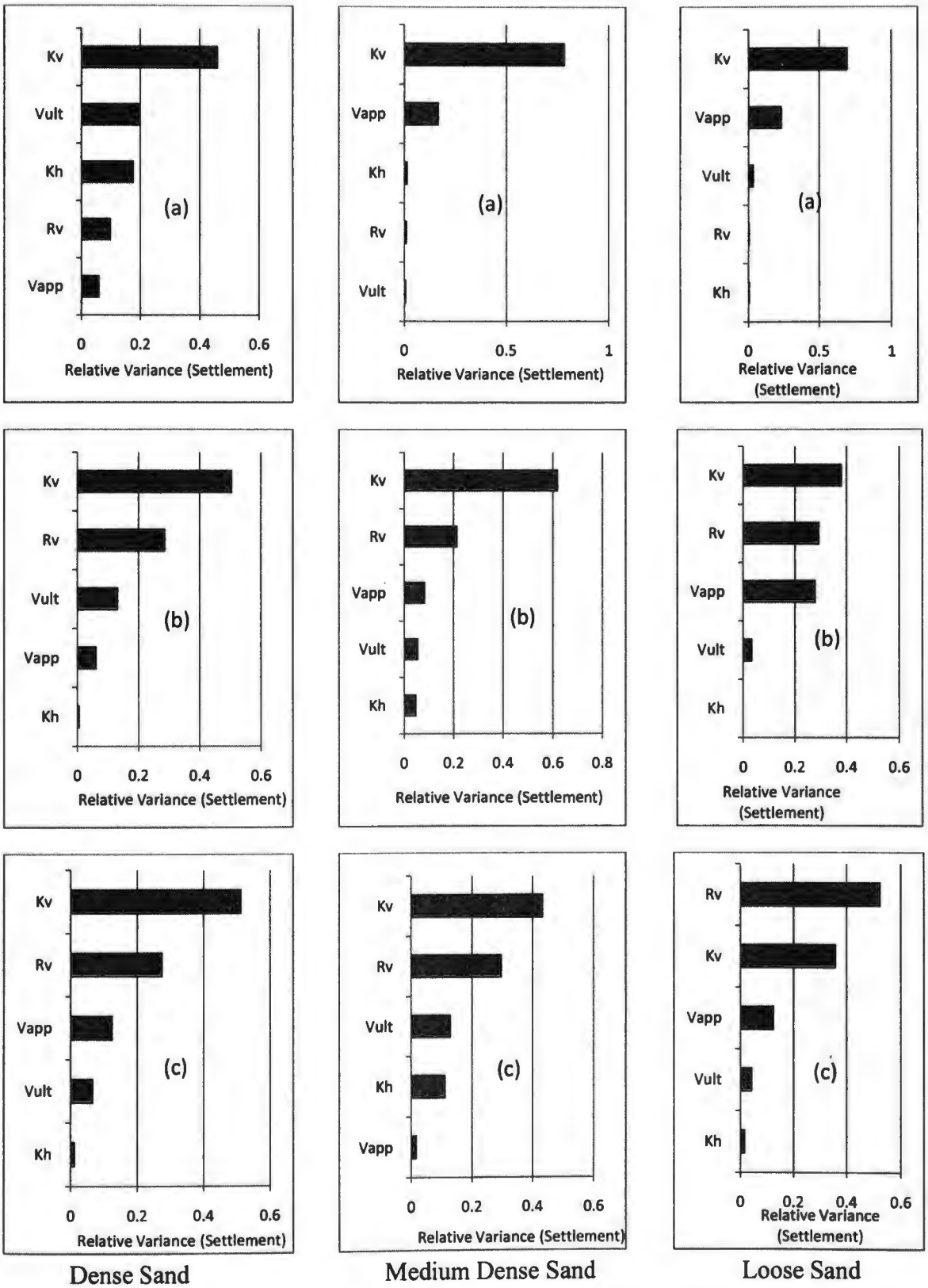

Dense Sand Medium Dense Sand Loose Sand

Fig. 6.14. FOSM plots of settlement of soil-foundation system resting on sandy soils subjected to (a) 0.27 g (b) 0.55 g and (c) 0.98 g maximum ground shaking

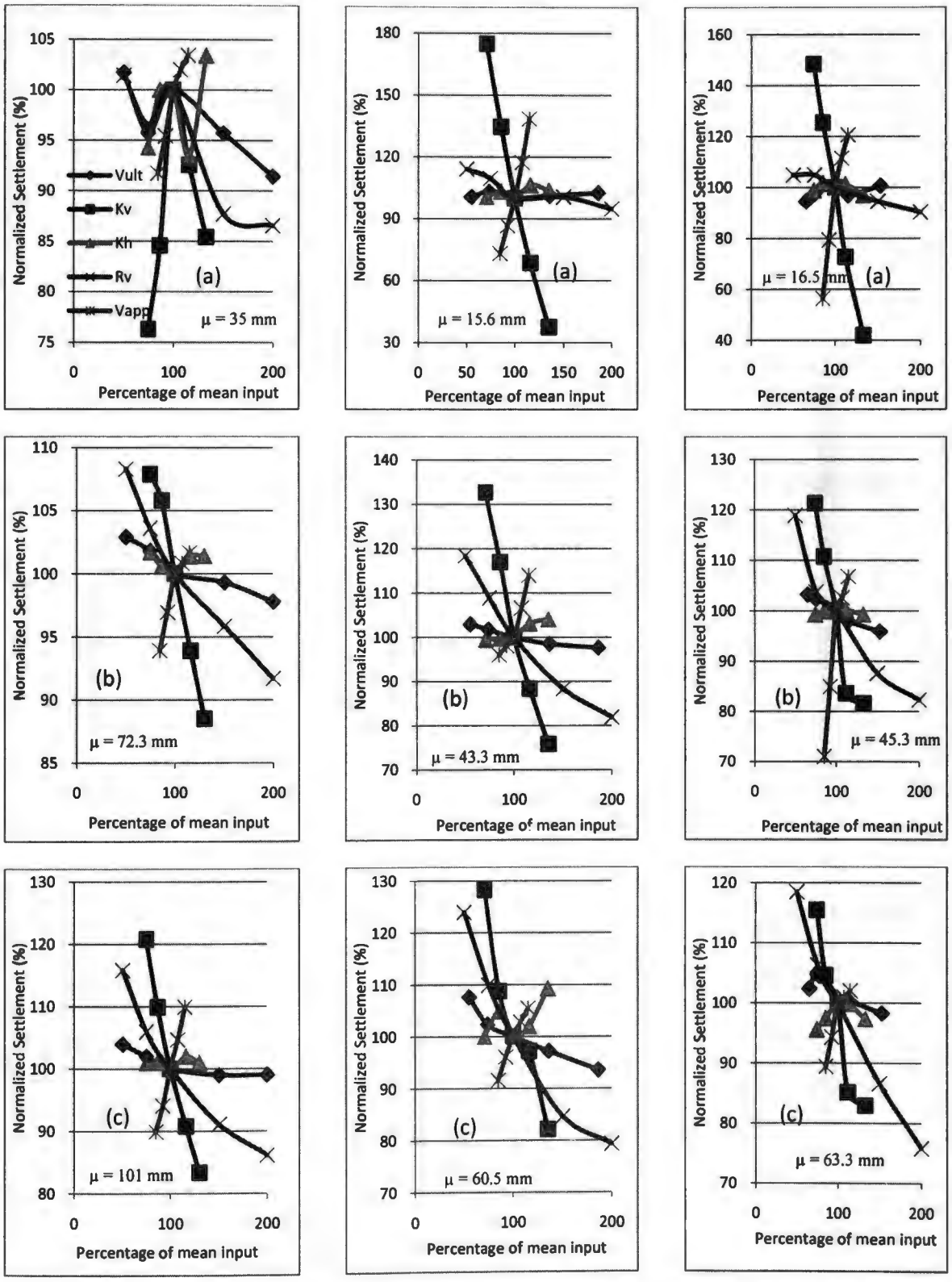

Dense Sand Medium Dense Sand Loose Sand

Fig. 6.15. Spider plots of settlement of soil-foundation system resting on sandy soils subjected to (a) 0.27 g (b) 0.55 g and (c) 0.98 g maximum ground shaking

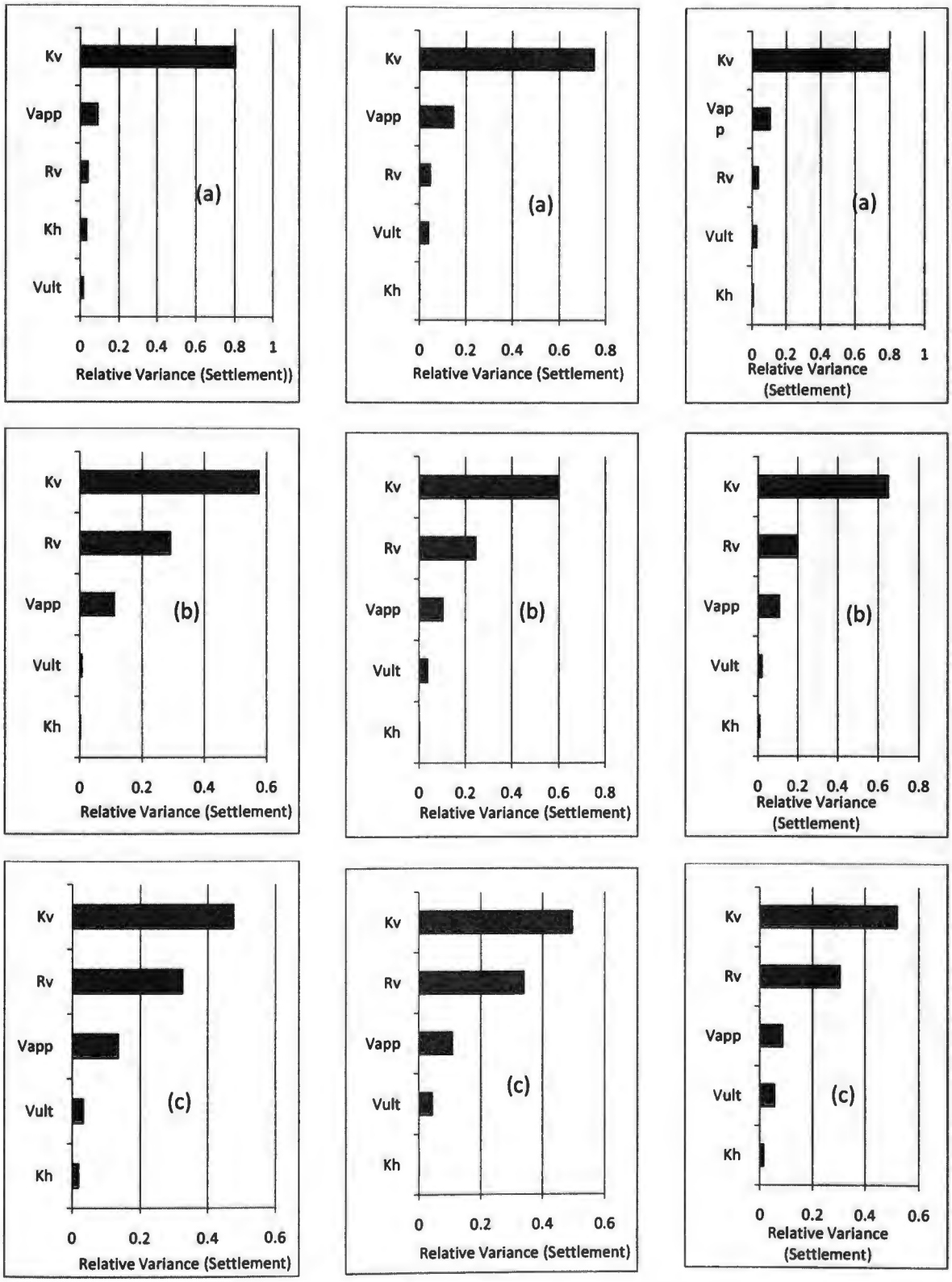

Stiff Clay Medium Stiff Clay Soft Clay

Fig. 6.16. FOSM plots of settlement of soil-foundation system resting on clayey soils subjected to (a) 0.27 g (b) 0.55 g and (c) 0.98 g maximum ground shaking

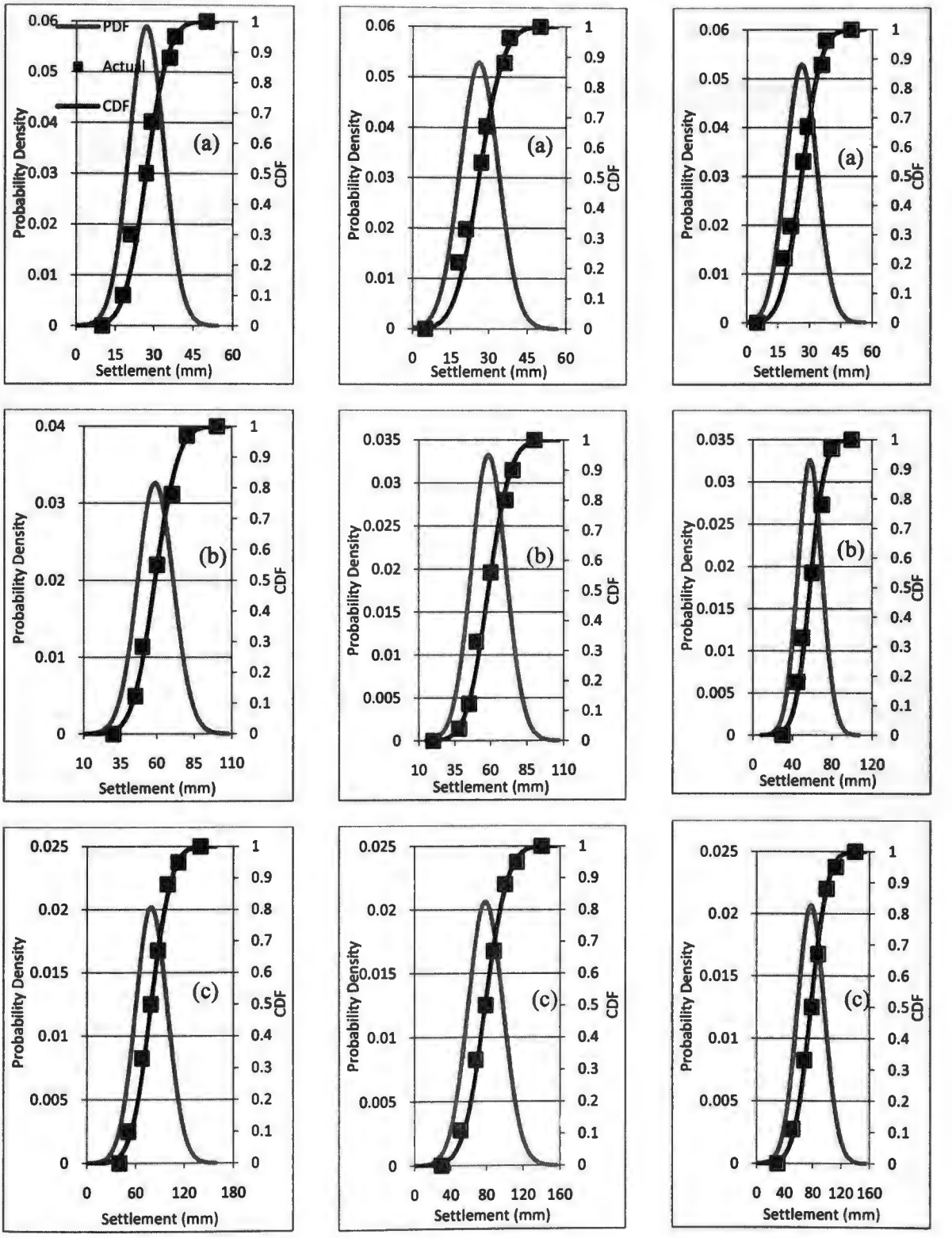

Fig. 6.17. PDF and CDF plots of settlement of soil-foundation system resting on clayey soils subjected to (a) 0.27 g (b) 0.55 g and (c) 0.98 g maximum ground shaking

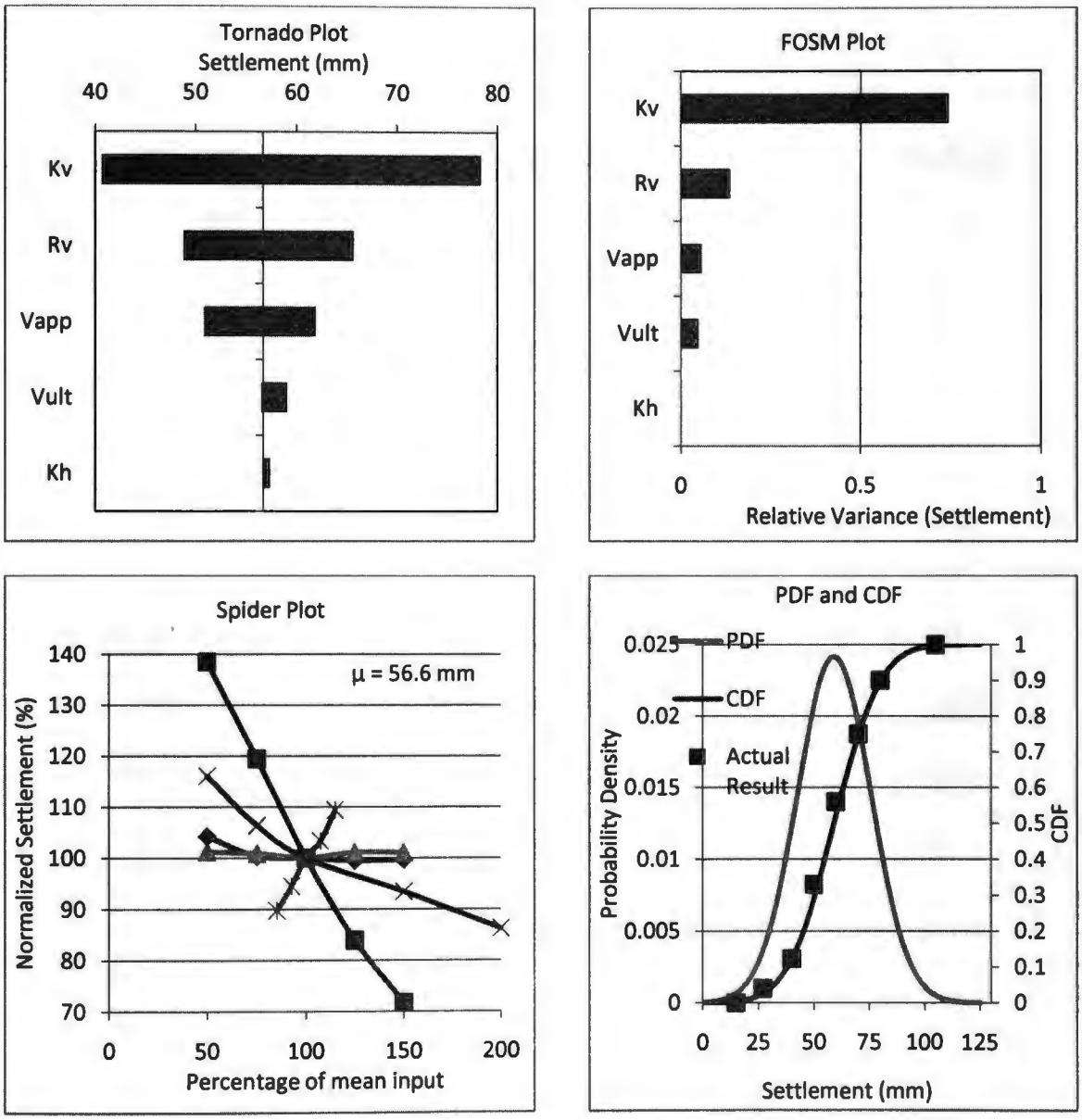

Fig. 6.18. Plots for settlement of soil-foundation system resting on medium stiff clay subjected to 0.55 g maximum ground shaking

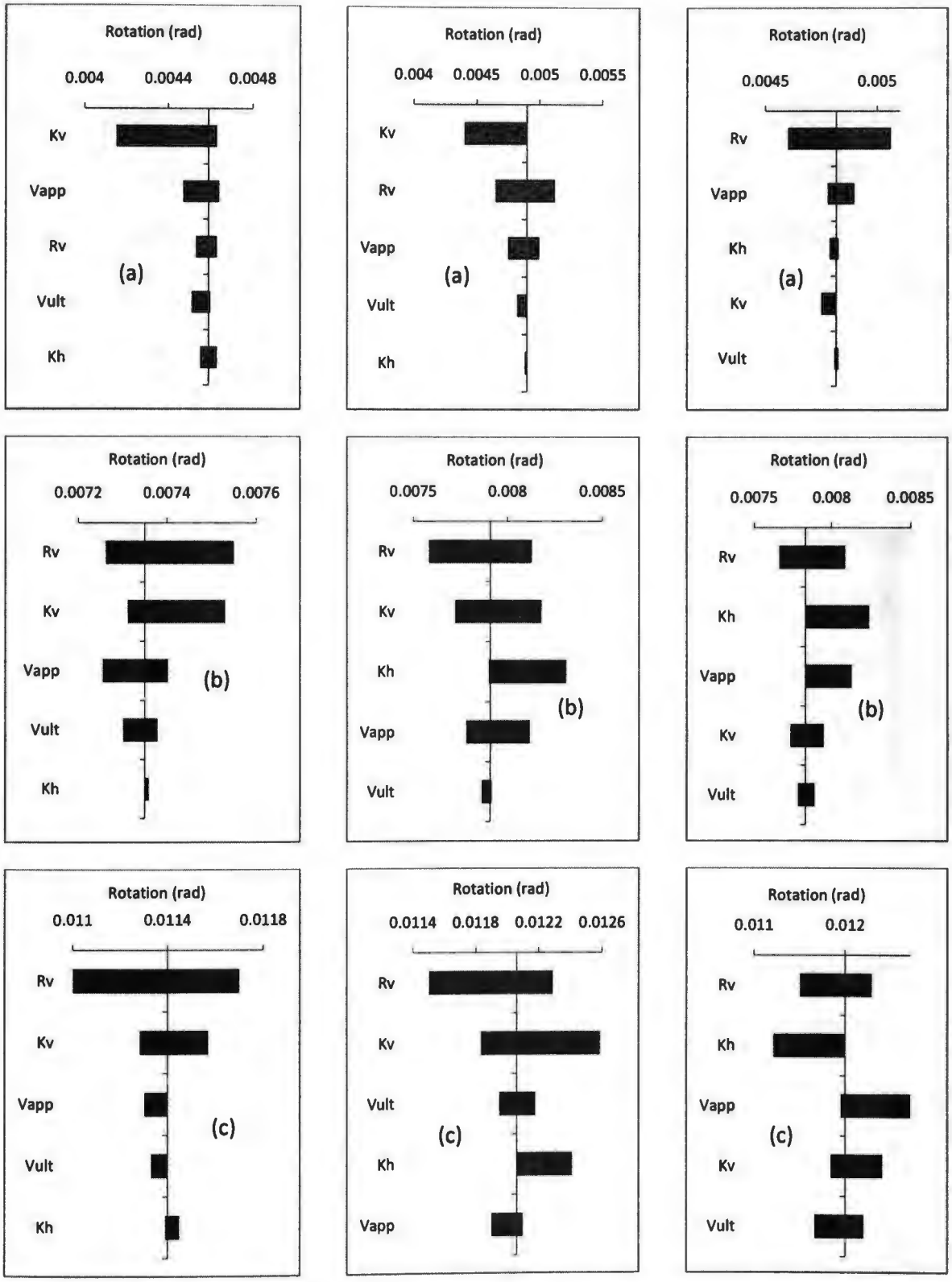

Dense Sand Medium Dense Sand Loose Sand

Fig. 6.19. Tornado plots of rotation of soil-foundation system resting on sandy soils subjected to (a) 0.27 g (b) 0.55 g and (c) 0.98 g maximum ground shaking

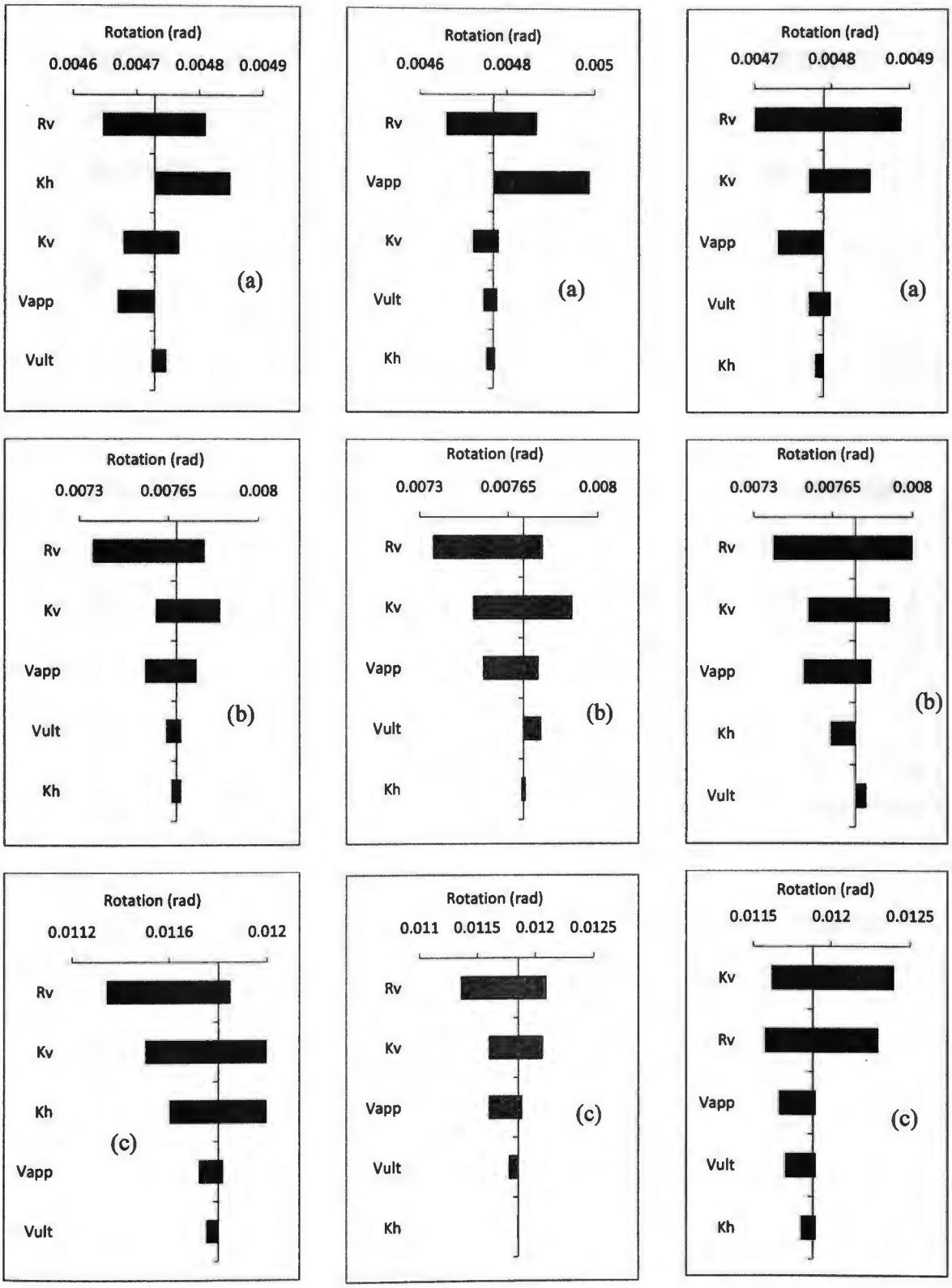

Stiff Clay Medium Stiff Clay Soft Clay

Fig. 6.20. Tornado plots of rotation of soil-foundation system resting on clayey soils subjected to (a) 0.27 g (b) 0.55 g and (c) 0.98 g maximum ground shaking

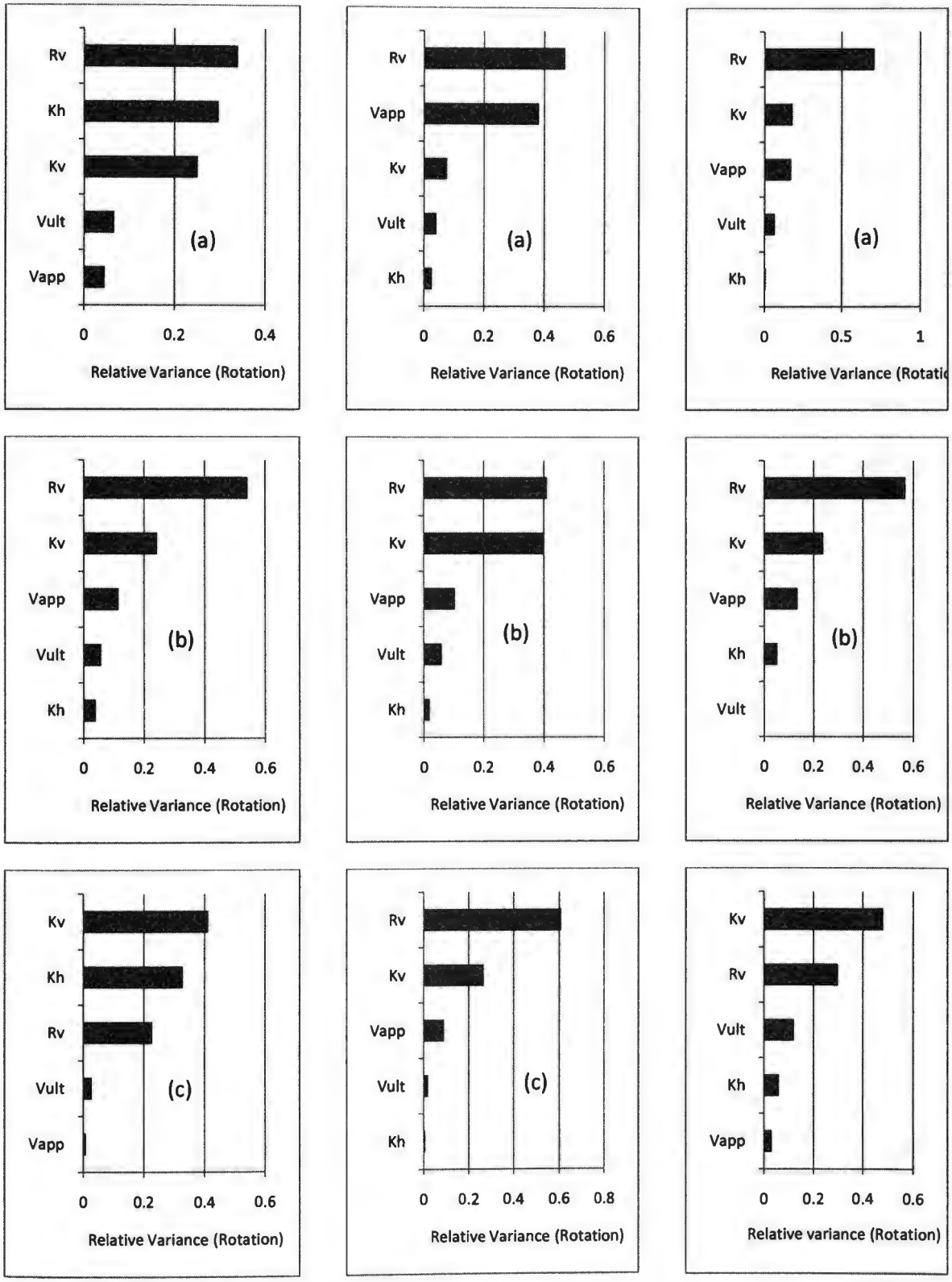

Stiff Clay Medium Stiff Clay Soft Clay

Fig. 6.21. FOSM plots of rotation of soil-foundation system resting on clayey soils subjected to (a) 0.27 g (b) 0.55 g and (c) 0.98 g maximum ground shaking

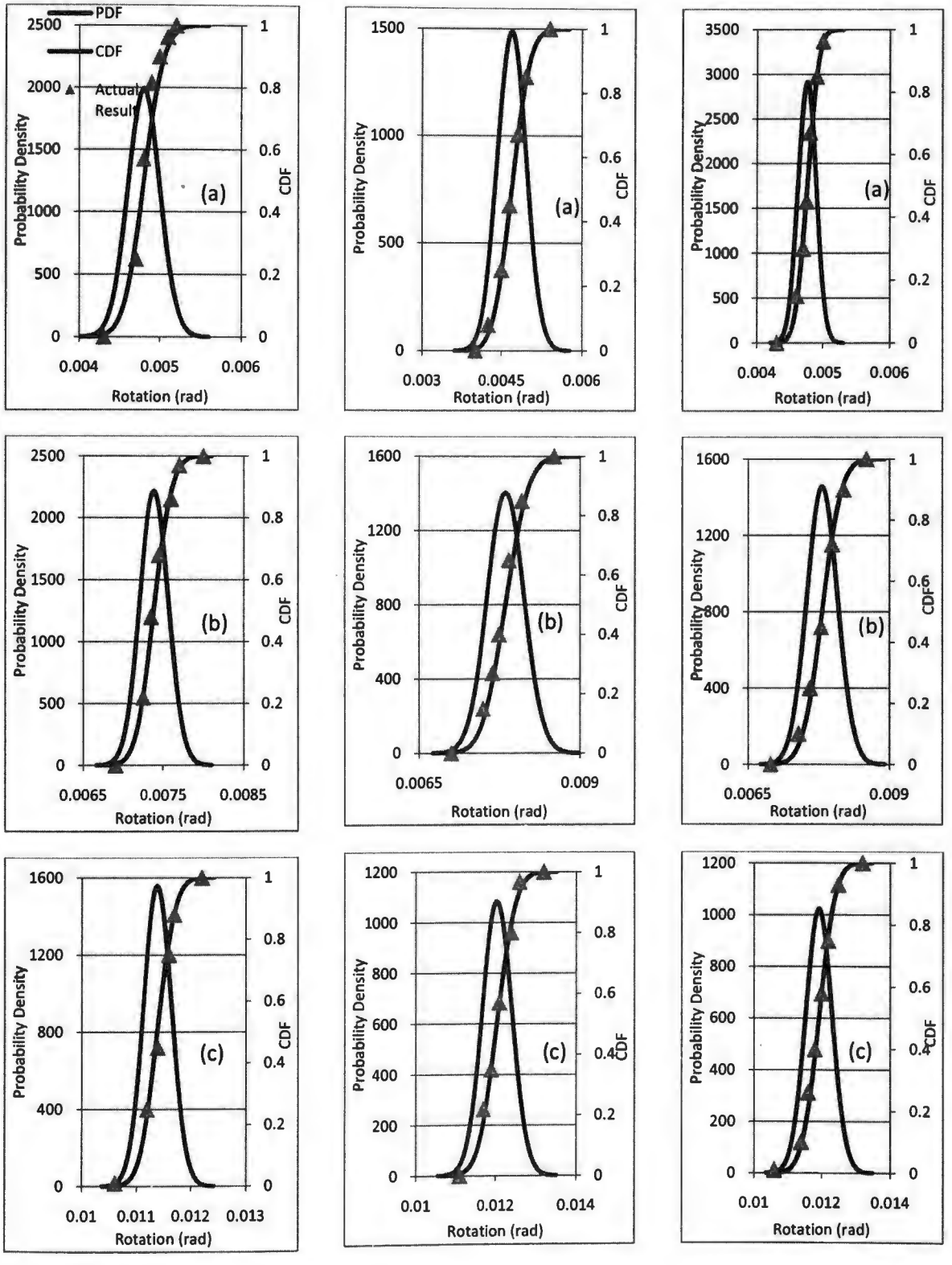

Fig. 6.22. PDF and CDF plots of rotation of soil-foundation system resting on sandy soils subjected to (a) 0.27 g (b) 0.55 g and (c) 0.98 g maximum ground shaking

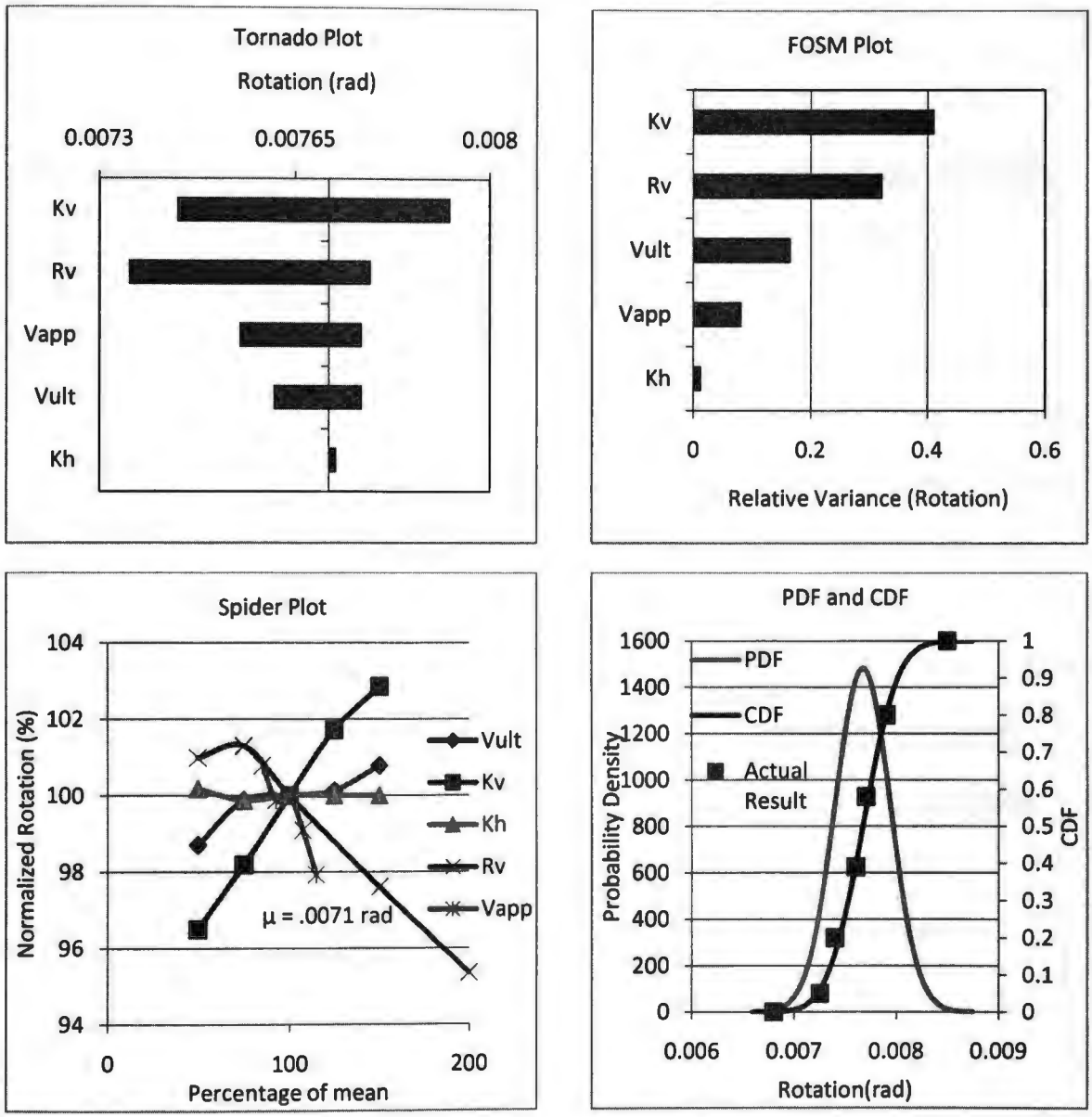

Fig. 6.23. Plots for rotation of soil-foundation system resting on medium stiff clay soil subjected to 0.55 g maximum ground shaking

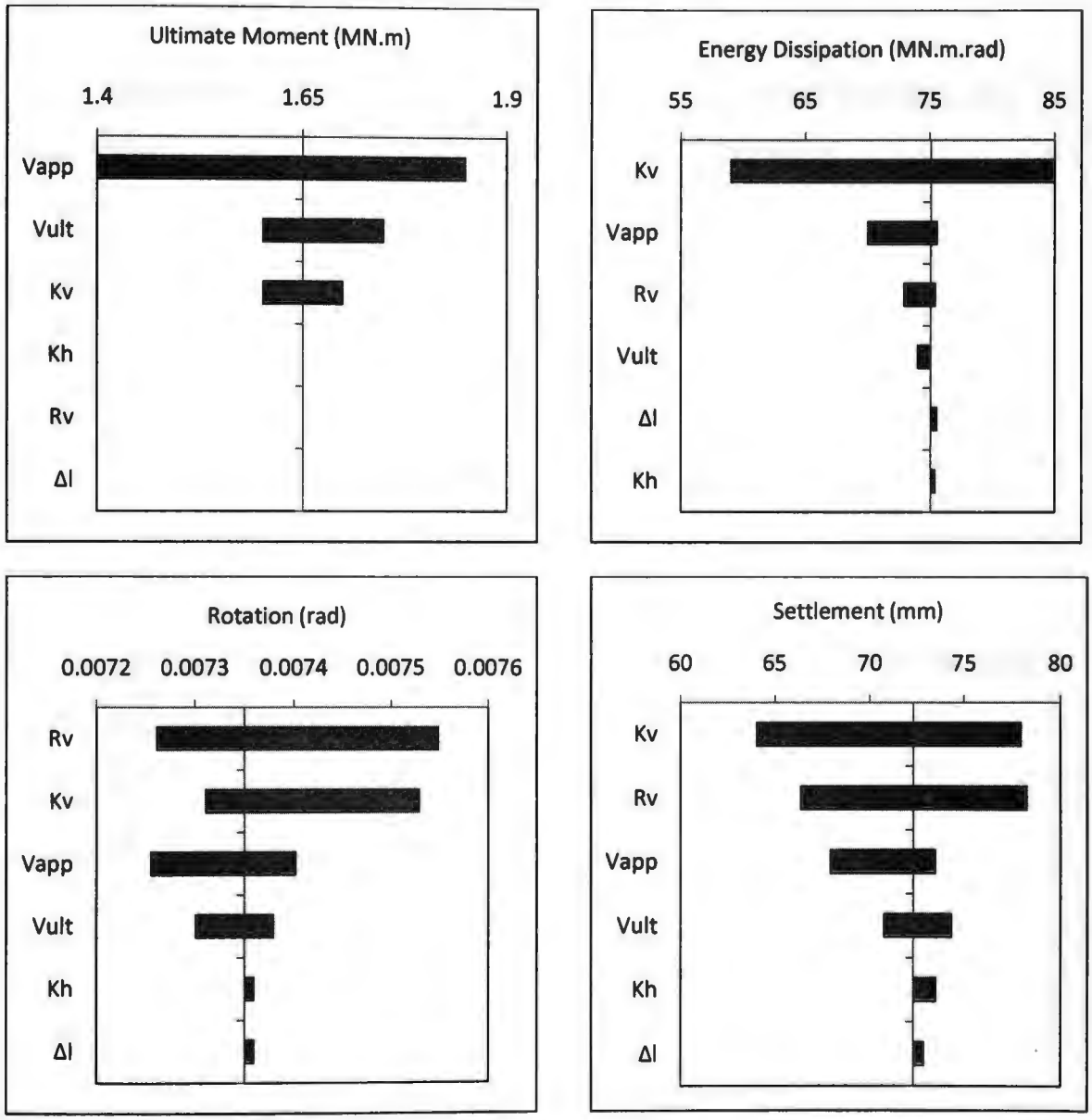

Fig. 6.24. Tornado plots of the outputs (with six random inputs) for soil-foundation system resting on dense sand with maximum ground acceleration 0.55 g

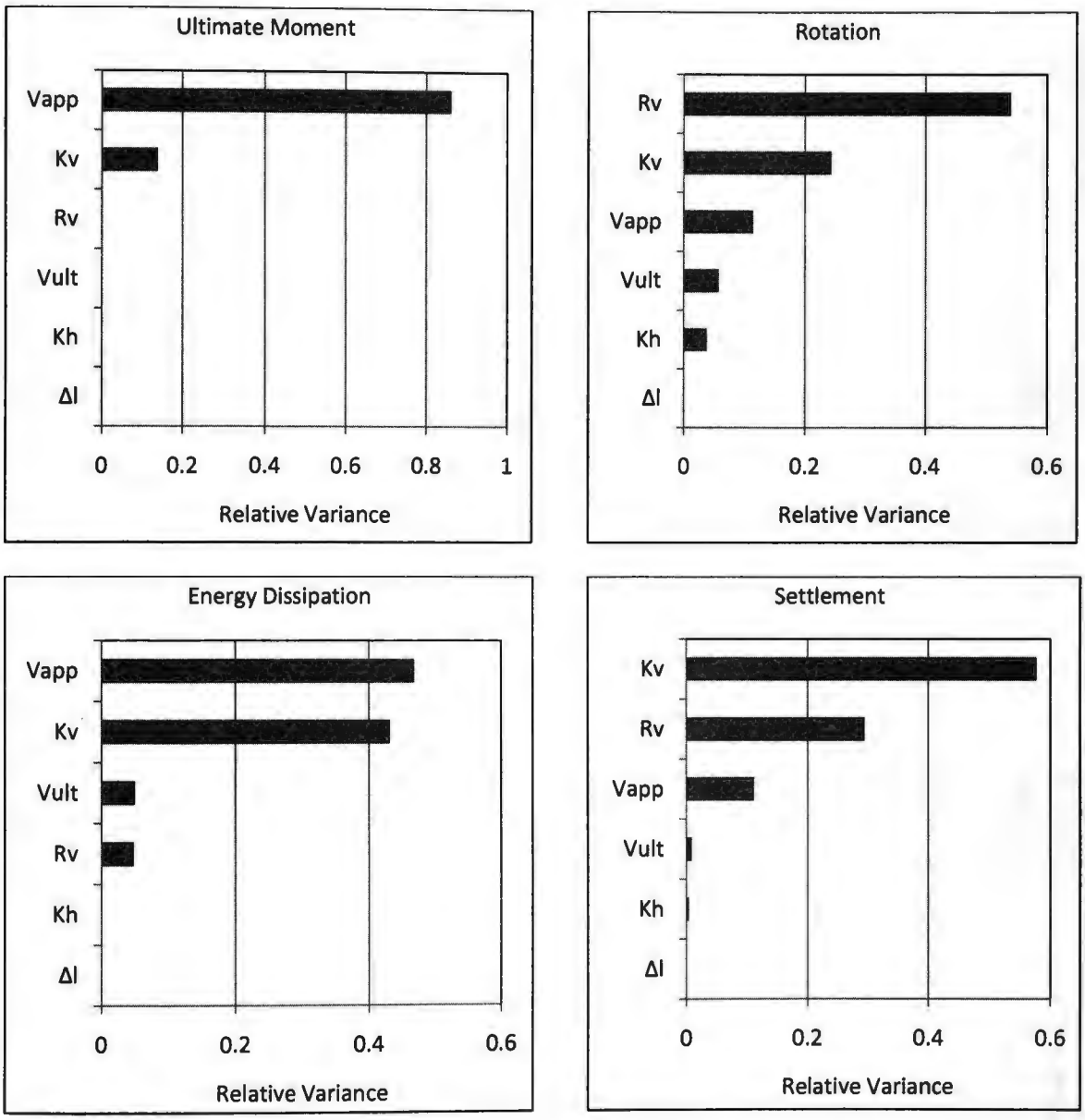

Fig. 6.25. FOSM plots of the outputs (with six random inputs) for soil-foundation system resting on stiff clay with maximum ground acceleration 0.55 g

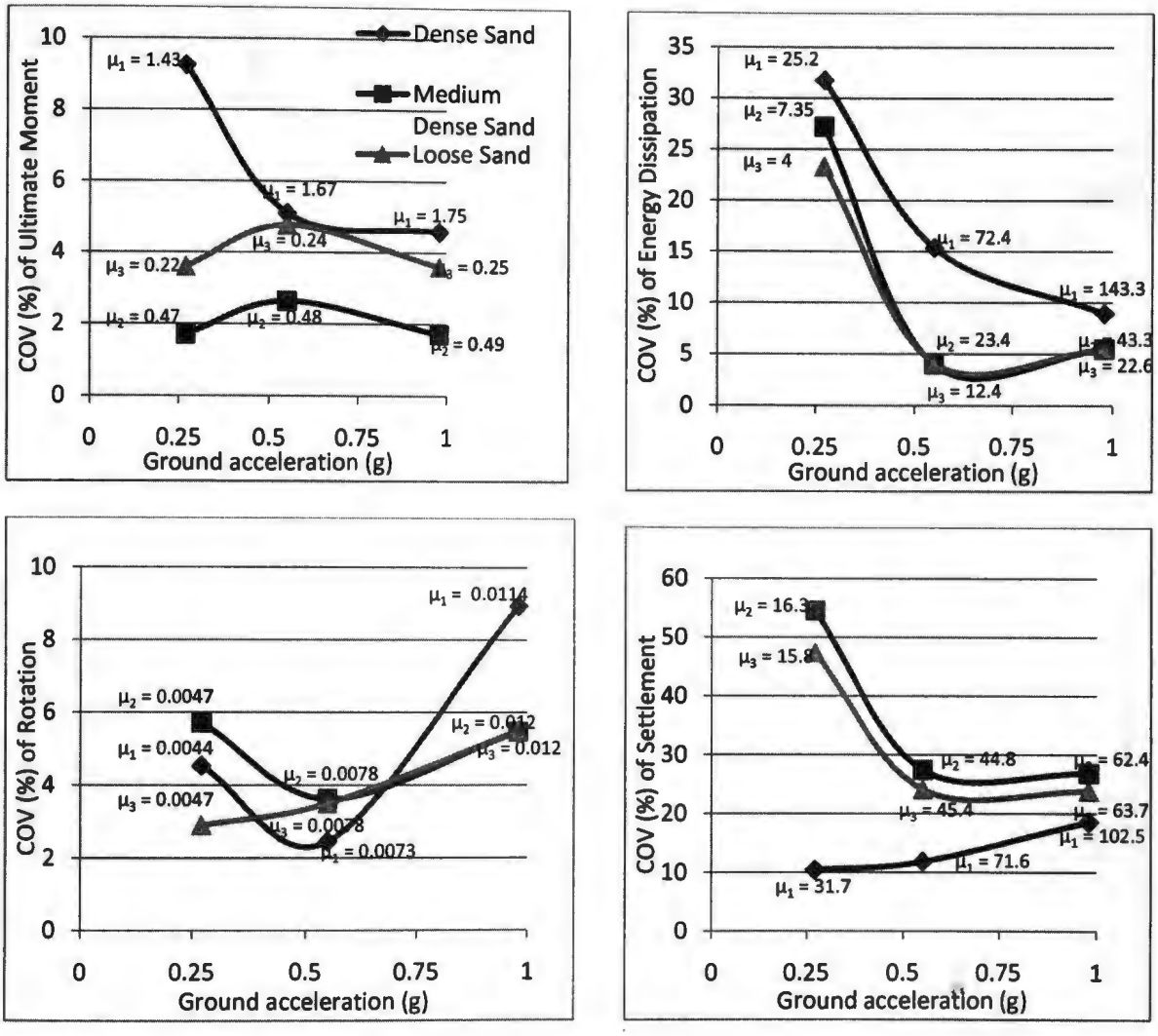

Fig. 6.26. COV of the ultimate moment (MN.m), energy dissipation (MN.m.rad), rotation (rad) and settlement (mm) for soil-foundation system resting on sandy soils against maximum ground shaking intensities

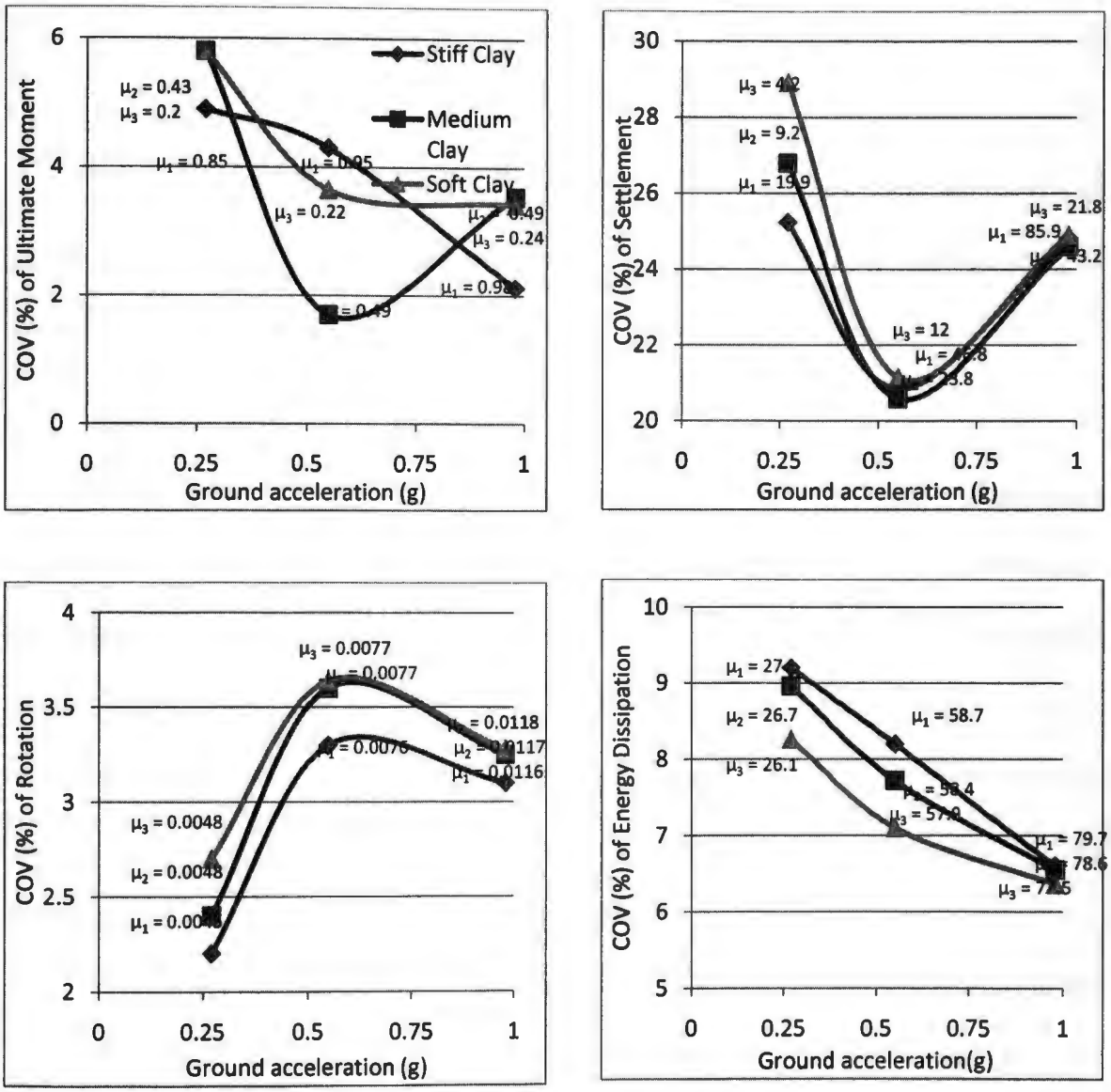

Fig. 6.27. COV of the ultimate moment (MN.m), energy dissipation (MN.m.rad), rotation (rad) and settlement (mm) for soil-foundation system resting on clayey soils against maximum ground shaking intensities.

CHAPTER 7. SUMMARY AND CONCLUSIONS

7.1. Introduction

This chapter summarizes the research program and presents a brief motivation of the research, objectives of this research and the conclusions derived from this research. At the end of this chapter, recommendations for future research are also presented.

7.2. Summary of Research Program

Recent research findings show that yielding of soil and mobilization of foundation load/moment capacities (rocking behavior of foundation) during earthquake loading can dissipate significant seismic energy beneath the foundation (and hence decrease the seismic energy transmitted to the structure and the resulting drift demands in the structure). However, current design practice of shallow foundations for seismic loading avoids yielding of soil and mobilization of ultimate load/moment capacity due to the following main reasons:

- Can the foundation load/moment capacity be reliable and predictable, amid subsurface uncertainties?
- Would the deformations beneath the foundation be tolerable and predictable, amid subsurface uncertainties?

The objectives of this research are two-fold: (1) to characterize the uncertainties in soil properties, in general, in a probabilistic framework (for sandy soils and clayey soils), and (2) to quantify the effects of uncertainties in soil properties on dynamic soil-shallow foundation system behavior, especially rocking behavior of foundations (moment-rotation-settlement behavior and energy dissipation characteristics), during seismic loading.

The research methodology includes systematic propagation of uncertainties in soil properties and loading conditions through soil-foundation interface to the dynamic behavior of the structure during seismic loading. A simple elastic shear wall-shallow foundation structural model, with aspect ratio of about 2.0 (effective height of the structure divided by the dimension of the footing in the direction of seismic loading), supported by dry sandy soils and saturated clayey soils was considered in this study. Probabilistic numerical simulations were carried out using OpenSees finite element framework, where the structural behavior is represented by an elastic beam column element and the soil-foundation system behavior is simulated by a recently developed Contact Interface Model (CIM).

The major random input parameters considered in this study include (1). Ultimate vertical load of the foundation for pure static vertical loading (Vult), derived from either friction angle of sand or undrained shear strength of clay, (2). Initial static vertical stiffness of soil (Kv), derived from the shear modulus of soil, (3). Initial static horizontal stiffness of soil (Kh), derived from the shear modulus of soil, (4). Rebounding ratio of the soil beneath the footing for cyclic loading (Rv), an empirical parameter calibrated using previous experimental studies, and (5). Applied vertical load on the foundation (Vapp) that results from the self weight of the structure. The initial static vertical factors of safety values (FSv = Vult/Vapp) used in this study ranges from 5.0 to 20.0. It should be noted that in seismically active zones, it is not the bearing capacity but the settlement controls the design, and hence these types of large values for stating bearing capacity factor of safety is practical.

The soil-foundation-structure system was subjected to different intensity of earthquake shaking events and the response of the system were recorded (moment at soil-foundation interface, settlement of the foundation, energy dissipation beneath the foundation and the drift demand (rotation) of the structure) Probabilistic sensitivity analyses have been carried out using Tornado Diagram analysis, Spider Plot analysis, First Order Second Moment (FOSM) analysis, and small scale Monte-Carlo simulations. The findings of this research are presented in the following section.

7.3. Conclusions

- The ultimate moment capacity of the soil-foundation system is more sensitive to the applied vertical load on the foundation (Vapp) than any other input parameters for all types of soils and for all shaking intensities. The contribution of Vapp itself ranges from 75% to 95%, while all other input parameters contribute the rest, though the COV of Vapp is 15% while the COV of all other input parameters range from 30% to 100%.
- For relatively larger FSv values, the relationship between ultimate moment and Vapp is almost linear. This study reinforces the previous research finding that the moment capacity of a rocking foundation is well defined and, unlike bearing capacity, moment capacity is less sensitive to the uncertainties in soil properties. Since the uncertainty in applied vertical load is typically much smaller than the uncertainties in soil properties, the ultimate moment capacity of the soil-foundation system during seismic loading is predictable with reasonable accuracy.
- Vapp and Kv are the key input parameters that contribute to the energy dissipation beneath the foundation with Vapp being the largest relative contributor

and Kv being the second largest relative contributor in almost all of the cases. The relative contribution of Vapp on energy dissipation ranges from 40% to 60% and the relative contribution of Kv ranges from 20% to 50%. The other input parameters that slightly affect the energy dissipation include Rv and Vult.

- When Vapp was kept constant, as expected, Kv (which is a function of shear modulus of the soil and the geometry of the footing) contributes to the energy dissipation the most and it is followed by Rv. When the COV of undrained shear strength was at 50%, the contribution of Kv to the energy dissipation becomes significant when compared to the contribution by Vapp (with COV = 15%).
- Kv and Rv are the key input parameters that contribute to the variation of settlement of the foundation during seismic shaking. Kv has largest relative contribution and Rv has second largest contribution on the settlement in almost all of the cases. The contribution of Kv on settlement ranges from 30% to 80% whereas the contribution of Rv on settlement for small shaking intensity (0.27 g) is less than 10%, and for bigger shaking intensities (0.55 g and 0.98 g), it varies from 20% to 35%.
- The rotation of the structure-foundation system during seismic loading is less sensitive to the soil properties and weight of the structure (normalized rotation – normalized as the percentage of mean- varies from 95% to 103% in all cases). The rotation of the foundation is mainly dictated by the intensity of shaking. Though not included in this study, the other key parameter that controls the rotation of the structure-foundation system is the aspect ratio of the structure.

- Monte-Carlo simulation results and the resulting PDF distributions reveal that all the outputs (the probabilistic response of the soil-foundation-structure system) follow normal distributions with reasonable accuracy. From the CDF, given the performance value of a particular output (e.g. settlement), the probability of occurrence/exceedence can be computed. On the other hand, given the probability of occurrence/exceedence, the limiting value of a particular output can be computed using CDF.
- Influence of mesh spacing (after reaching a critical value) on the outputs was found to be negligible for both sandy soils and clayey soils. The overall COV of the ultimate moment and rotation of the foundation was found to be less than 10% for all types of soils and for all shaking intensities considered in this study. The overall COV values of energy dissipation and settlement of the foundation varies about 5% to 50% depending on the type of soil and intensity of shaking.

7.4. Future Recommendations

For future research related to this topic, further probabilistic numerical simulations that include the following are recommended.

- Uncertainties in the empirical relationships that are used to obtain some of the model input parameters (transformation uncertainties)
- Uncertainties in structural properties
- Different structural and foundation geometry and different aspect ratios
- Structures with multiple columns.

REFERENCES

Baynes, L. (2005). "An evaluation of free field liquefaction analysis using OpenSees." MSc thesis, University of Washington, Seattle.

Bransby, M. F. and Randolph, M. F. (1997). "Shallow foundations subject to combined loadings." *IACMAG '97 - Ninth International Conference of the International Association for Computer Methods and Advances in Geomechanics*, Wuhan, China, 2-7 November 1997, 3, 1947-1952. The Netherlands: Balkema.

Chakraborty, S. and Dey, S. S. (1996). "Stochastic finite element simulation of random structure on uncertain foundation under random loading." *International Journal of Mechanical Science*, 38(11), 1209–18.

Cherubini, C. (2000). "Reliability evaluation of shallow foundation bearing capacity on c′, Φ′ soils." *Canadian Geotechnical Journal*, 37(1), 264-269.

Conniff, D. E. and Kiousis, P. D. (2007). "Elastoplastic medium for foundation settlements and monotonic soil–structure interaction under combined loadings." *International Journal for Numerical and Analytical Methods in Geomechanics*, 31(6), 789-807.

Cremer, C., Pecker A. and Davenne L. (2001). "Cyclic macro-element of soil structure interaction: Material and geometrical nonlinearities." *International Journal for Numerical and Analytical Methods in Geomechanics*, 25, 1257–1284.

Cremer, C., Pecker A. and Davenne L. (2002). "Modelling of non-linear dynamic behaviour of a shallow foundation with macro-element." *Journal of Earthquake Engineering*, 6(2), 175-212.

Das, B. M. (2008). "Principles of Foundation Engineering." Thomson-Engineering.

Duncan, J. M. (2000). "Factors of safety and reliability in geotechnical engineering." *Journal of Geotechnical and Geoenvironmental Engineering*, 126(4), 307-316.

Federal Emergency Management Agency (2000). "Prestandard and commentary for the seismic rehabilitation of buildings." FEMA publication 356, November 2000.

Fenton, G. A. and Griffiths, D. V. (2005). "Three-dimensional probabilistic foundation settlement." *Journal of Geotechnical and Geoenvironmental Engineering*, 131(2), 232-239.

Fenton, G. A., Griffiths, D. V. and Cavers, W. (2005). "Resistance factors for settlement design." Canadian *Geotechical Journal*, 42(5), 1422-1436.

Griffiths, D. V. and Fenton, G. A. (2007). Probabilistic Methods in Geotechnical Engineering. Springer, New York.

Gajan, S. (2006). "Physical and Numerical Modeling of Nonlinear Cyclic Load-Deformation Behavior of Shallow Foundations Supporting Rocking Shear Walls." PhD thesis, University of California, Davis.

Gajan, S., Hutchinson, T., Kutter, B., Raychowdhury, P., Ugalde, J. A. and Stewart, J. (2007). "Numerical Models for Analysis and Performance-Based Design of Shallow Foundations Subjected to Seismic Loading." *Report for Pacific Earthquake Engineering Research Centre*, PEER 2007/04, May 2008.

Gajan, S. and Kutter, B. L. (2008). "Capacity, settlement, and energy dissipation of shallow footings subjected to rocking." *Journal of Geotechnical and Geoenvironmental Engineering, ASCE*, 134(8), 1129-1141.

Gajan, S. and Kutter, B. L. (2009). "Contact interface model for shallow foundations subjected to combined cyclic loading." *Journal of Geotechnical and Geoenvironmental Engineering, ASCE*, 135(3), 407-419.

Gajan, S., Raychowdhury, P., Hutchinson, T. C., Kutter, B. L. and Stewart, J. P. (2010). "Application and validation of practical tools for nonlinear soil-foundation interaction analysis." *Earthquake Spectra*, 26(1), 111-129.

Gajan, S. and Saravanathiiban, D. S. (2011). "Modeling of energy dissipation in structural devices and foundation soil during seismic loading." *Soil Dynamics and Earthquake Engineering*, 31, 1106–1122.

Grange, S., Kotronis, P. and Mazars, J. (2008). "A macro-element for a circular foundation to simulate 3D soil–structure interaction." *International Journal for Numerical and Analytical Methods in Geomechanics,* 32(10), 1205–1227.

Hara, A., Ohta, T., Niwa, M., Tanaka, S. and Banno, T. (1974). "Shear modulus and shear strength of cohesive soils." *Soils and Foundations*, 14(3), 1-12.

Harr, M. E. (1977). "Mechanics of particulate media—a probabilistic approach." McGraw-Hill, New York, N.Y.

Jimenez, R. and Sitar, N. (2009). "The importance of distribution types on finite element analyses of foundation settlement." *Computers and Geotechnics*, 36(3), 474-483.

Jones, A. L., Kramer, S. L. and Arduino, P. (2002). "Estimation of uncertainty in geotechnical properties for performance-based earthquake engineering." *Report for Pacific Earthquake Engineering Research Centre*, PEER 2002/16, December 2002, Berkeley, Calif.

Kellezi, L., Kudsk, G. and Hofstede, H. (2007). "FE skirted footings analyses for combined loads and layered soil profile." *Proceedings of European Conference on Soil Mechanics and Geotechnical Engineering in Madrid,* Spain, 24-27 September 2007, 341-346.

Kramer, S. L. (1996). Geotechnical Earthquake Engineering. Prentice-Hall, Inc., New Jersey.

Kulhawy, F. H. and Mayne, P. W. (1990). "Manual on estimating soil properties for foundation design." *EPRI EL-6800, Research Project, 1493-6*, Final Report. Electric Power Research Institute, Palo Alto, CA.

Lacasse, S. and Nadim, F. (1996). "Uncertainties in characterizing soil properties." In Charles D. Shackelford and Priscilla P. Nelson, editors, *Uncertainty in Geologic Environment: From Theory to Practice,* Proceedings of Uncertainty '96, July 31-August 3, 1996, Madison, Wisconsin, volume 1 of *Geotechnical Special Publication No. 58*, 49–75. ASCE, New York, 1996.

Loukidis, D., Chakraborty, T. and Salgado, R. (2008). "Bearing capacity of strip footings on purely frictional soil under eccentric and inclined loads." *Canadian Geotechnical Journal*, 45(6), 768-787.

Lumb, P. (1966). "The variability of natural soils." *Canadian Geotechnical Journal*, 3, 74–97.

Lutes, L. D., Sarkani, S. and Jin, S. (2000). "Response variability of an SSI system with uncertain structural and soil properties." *Engineering Structures*, 22, 605–620.

Massih, D., Soubra, A.H. and Low, B.K. (2008). "Reliability-based analysis and design of strip footings against bearing capacity failure." *Journal of Geotechnical and Geoenvironmental Engineering*, 134(7), 917–928.

Meyerhof, G.G. (1995). "Development of geotechnical limit state design." *Canadian Geotechnical Journal,* 32(1), 128-136.

Most, T. and Knabe, T. (2010). "Reliability analysis of the bearing failure problem considering uncertain stochastic parameters." *Computers and Geotechnics*, 37, 299-310.

Na, U. J., Ray Chaudhuri, S. and Shinozuka, M. (2008). "Probabilistic assessment for seismic performance of port structures." *Soil dynamics and earthquake engineering*, 28(2), 147-158.

Na, U. J., Ray Chaudhuri, S. and Shinozuka, M. (2009). "Effects of spatial variation of soil properties on seismic performance of port structures." *Soil dynamics and earthquake engineering*, 29(3), 537-545.

OpenSees (2010). Open System for Earthquake Engineering Simulation: OpenSees, Pacific Earthquake Engineering Research Center (PEER), University of California, Berkeley, http://opensees.berkeley.edu.

Paolucci, R., Shirato, M. and Yilmaz, M. T. (2007). "Seismic behavior of shallow foundations: shaking table experiments versus numerical modeling." *Earthquake Engineering and Structural Dynamics*, 34(7), 577-595.

PEER (2010). Pacific Earthquake Engineering Research Center, http://peer.berkeley.edu/.

Phoon, K. K. and Kulhawy, F. H. (1999a). "Characterization of geotechnical variability." *Canadian Geotechnical Journal*, 36, 612-624.

Phoon, K. K. and Kulhawy, F. H. (1999b). "Evaluation of geotechnical property variability." *Canadian Geotechnical Journal*, 36, 625-639.

Raychowdhury, P. and Hutchinson, T. C. (2009). "Performance evaluation of a nonlinear Winkler-based shallow foundation model using centrifuge test results." *Earthquake Engineering and Structural Dynamics*, 38, 679-698.

Raychowdhury, P. (2009). "Effect of soil parameter uncertainty on seismic demand of low-rise steel buildings on dense silty sand." *Soil Dynamics and Earthquake Engineering*, 29(10), 1367-1378.

Raychowdhury, P. and Hutchinson, T. C. (2010). "Sensitivity of shallow foundation response to model input parameters." *Journal of Geotechnical and Geoenvironmental Engineering*, 136(3), 538–541.

Ray Chaudhuri, S. and Gupta, V. K. (2002). "Variability in seismic response of secondary systems due to uncertain soil properties." *Engineering Structures*, 24, 1601–1613.

Sett, K., Unutmaz, B., Cetin, K. O., Koprivica, S. and Jeremic, B. (2010). "Soil Uncertainties and its Influence on Simulated $G=G_{max}$ and Damping Behavior." *Journal of Geotechnical and Geoenvironmental Engineering*, 137(3), 218-226.

Spiegel, M. R. and Stephens, L. J. (2007). Schaum's outline of Statistics. McGraw-Hill, New York, N.Y.

Srivastava, A. and Babu, G. L. S. (2009). "Effect of soil variability on the bearing capacity of clay and in slope stability problems." *Engineering Geology,* 108, 142–152.

Tomlinson, M. J. and Boorman, R. (1995). Foundation Design and Construction. Longman Publishing Group.

Touhei, T. and Ohmachi, T. (1994). "Modal analysis of a dam-foundation system based on an FE-BE method in the time domain." *Earthquake Engineering and Structural Dynamics,* 23, 1-15.

Valliappan, S. and Hakam, A. (2001). "Finite element analysis for optimal design of foundations due to dynamic loading." *International Journal for Numerical Methods in Engineering*, 52, 605–614.

Vanmarcke, E. H. (1977). "Probabilistic modeling of soil profiles." *Journal of the Geotechnical Engineering Division*, 103(11), 1227-1246.

Vanmarcke, E. H. (1984). "Random fields." M.I.T. Press, Cambridge, Massachusetts.

Veletsos, A.S. and Meek, J.W. (1974). "Dynamic behavior of building-foundation systems." *Earthquake Engineering and Structural Dynamics*, 3(2), 121–138.

Wegner, J. L. and Zhang, X. (2001). "Free-vibration analysis of a three-dimensional soil structure system." *Earthquake Engineering and Structural Dynamics*, 30, 43-57.

Wolff, T. F., Demsky, E. C., Schauer, J. and Perry, E. (1996). "Reliability assessment of dike and levee embankments." *In Uncertainty in the Geologic Environment: From Theory to Practice*, Proceedings of Uncertainty '96, ASCE Geotechnical Special Publication No. 58, C.D. Shackelford, P. P. Nelson, and M.J.S. Roth, eds. 1996, 636-650.

Yazdchi, M., Khalili, N. and Valliappan, S. (1999). "Dynamic soil–structure interaction analysis via coupled finite-element–boundary-element method." *Soil Dynamics and Earthquake Engineering*, 18, 499–517.

Zhang, J. and Tang, Y. C. (2007). "Finite element modeling of shallow foundations on nonlinear soil medium." *Structure Congress '07*, Long beach, May 2007.

APPENDIX A. OUTPUT PLOTS NOT PRESENTED IN CHAPTER 6

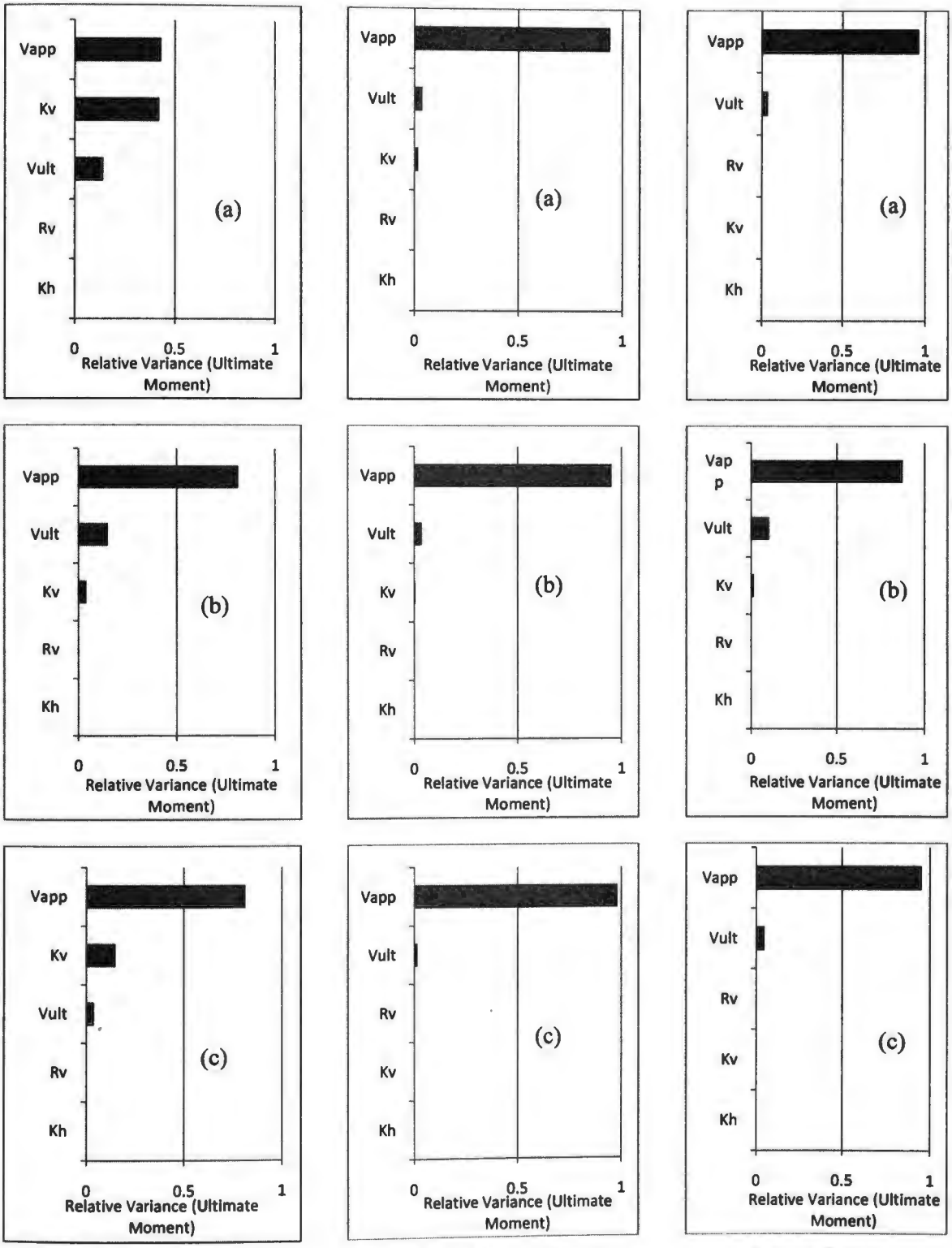

Dense Sand Medium Dense Sand Loose Sand

Fig. A.1. FOSM plots of ultimate moment capacity of soil-foundation system resting on sandy soils subjected to (a) 0.27 g (b) 0.55 g and (c) 0.98 g maximum ground shaking

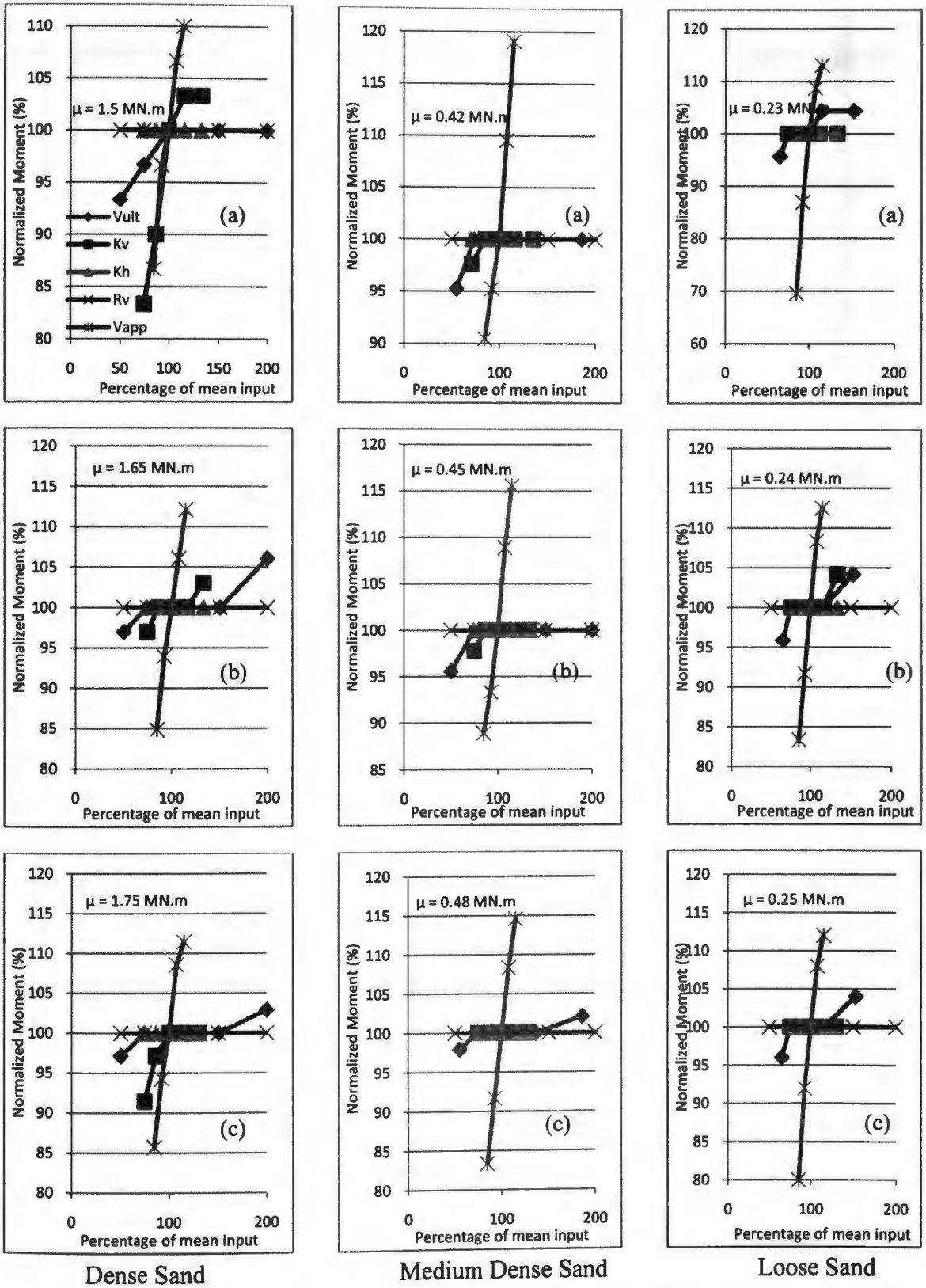

Fig. A.2. Spider plots of ultimate moment capacity of soil-foundation system resting on sandy soils subjected to (a) 0.27 g (b) 0.55 g and (c) 0.98 g maximum ground shaking

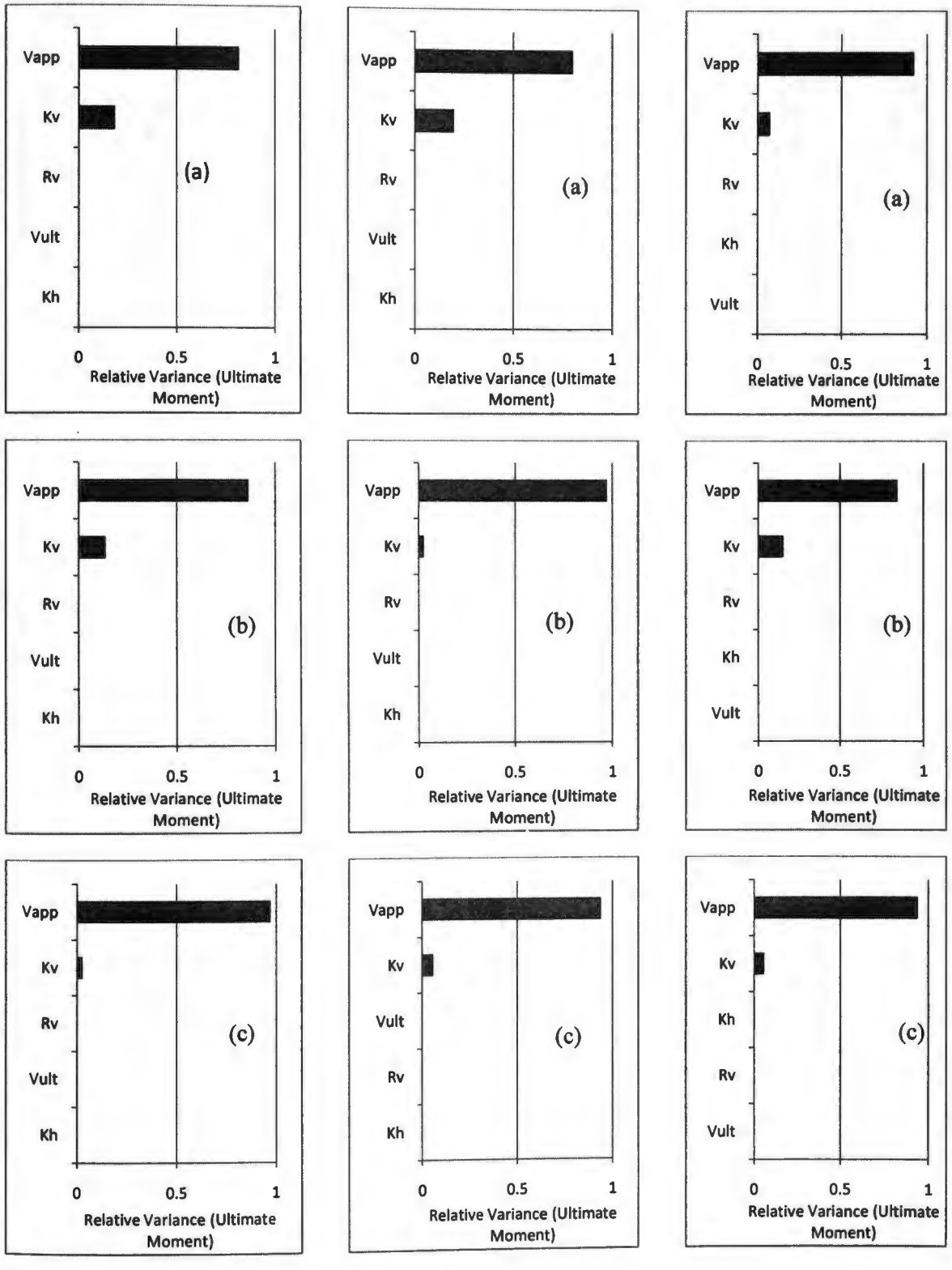

Stiff Clay Medium Stiff Clay Soft Clay

Fig. A.3. FOSM plots of ultimate moment capacity of soil-foundation system resting on clayey soils subjected to (a) 0.27 g (b) 0.55 g and (c) 0.98 g maximum ground shaking

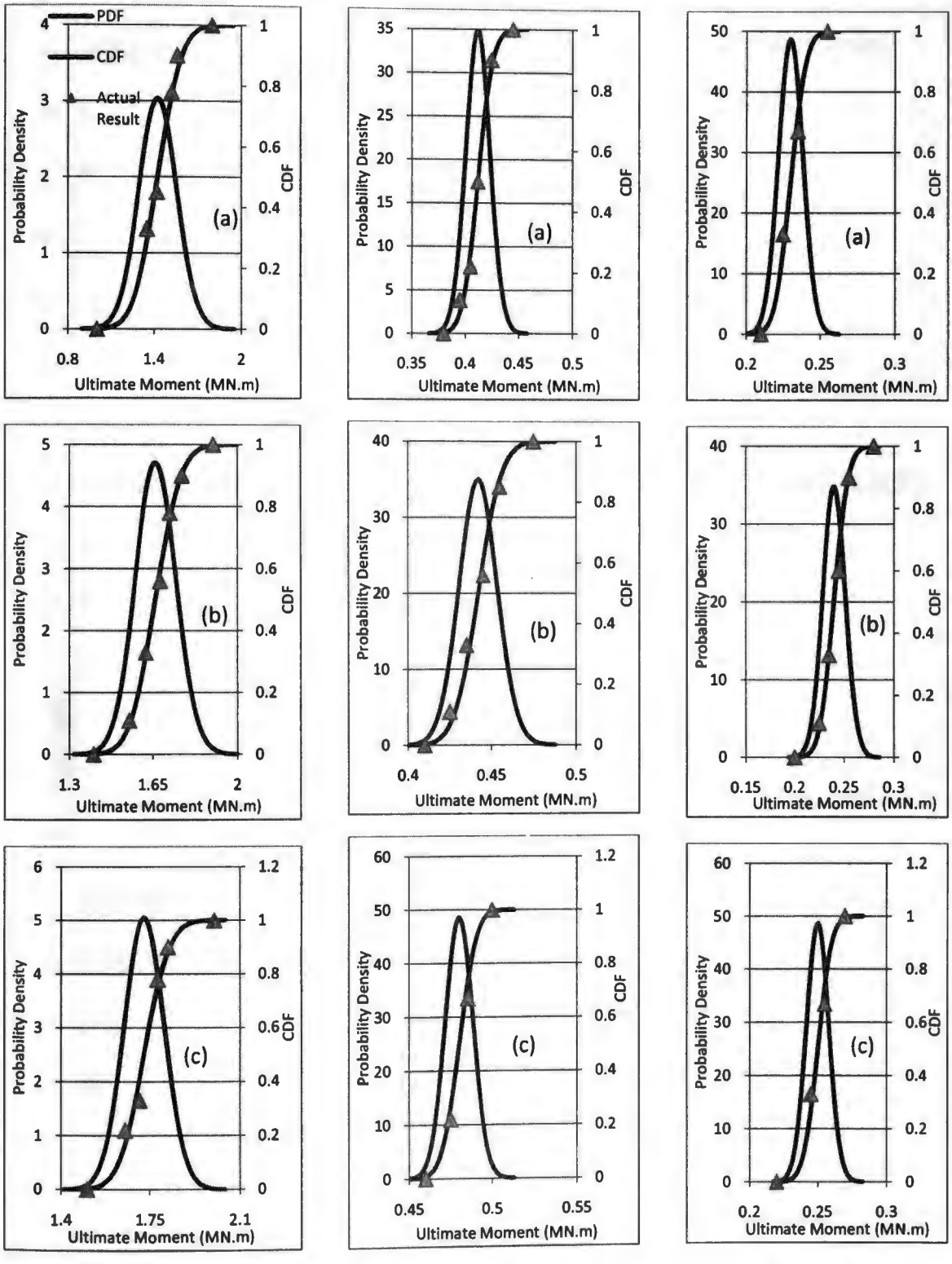

Dense Sand Medium Dense Sand Loose Sand

Fig. A.4. PDF and CDF plots of ultimate moment capacity of soil-foundation system resting on sandy soils subjected to (a) 0.27 g (b) 0.55 g and (c) 0.98 g maximum ground shaking

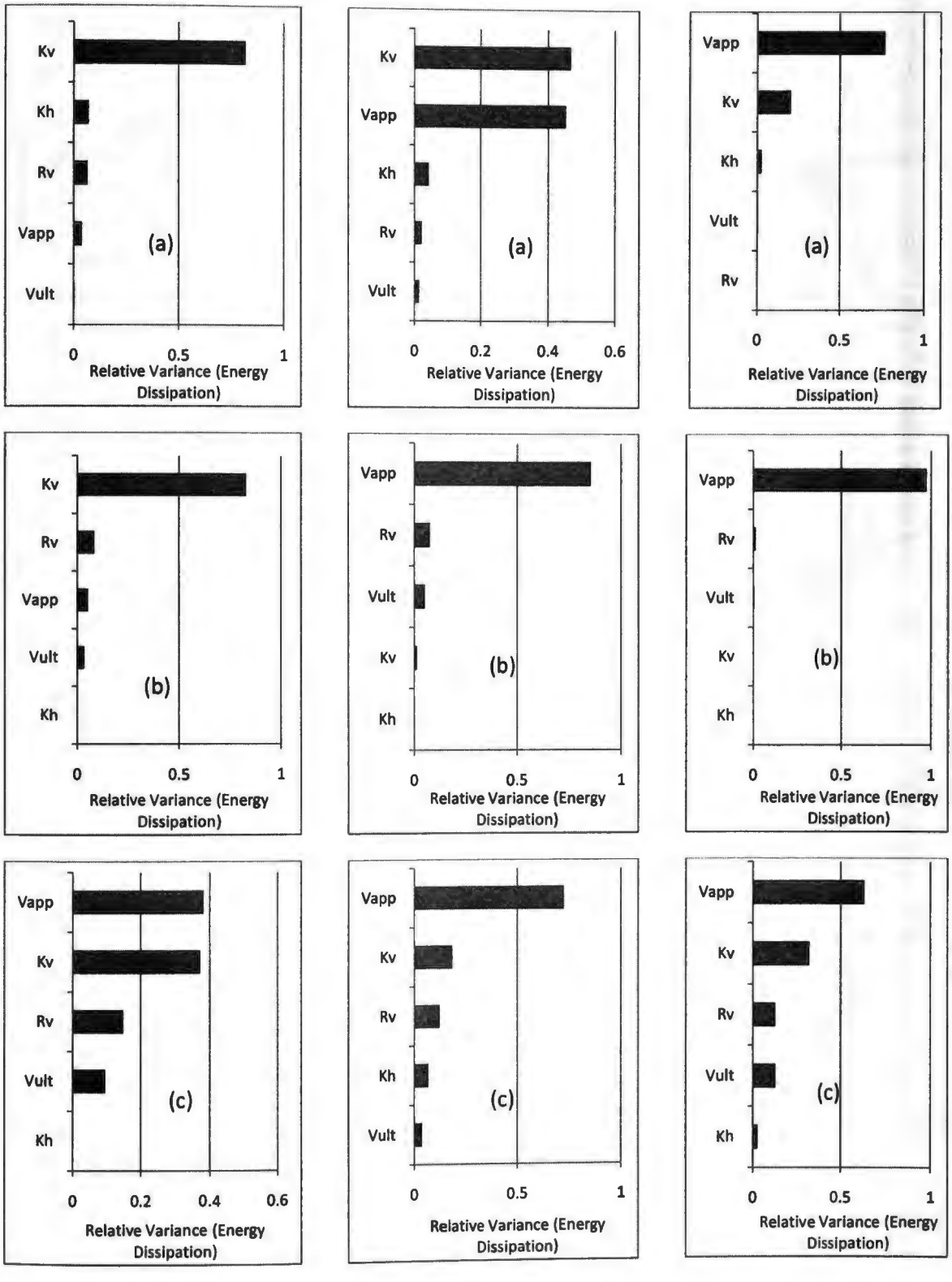

Dense Sand Medium Dense Sand Loose Sand

Fig. A.5. FOSM plots of energy dissipation of soil-foundation system resting on sandy soils subjected to (a) 0.27 g (b) 0.55 g and (c) 0.98 g maximum ground shaking

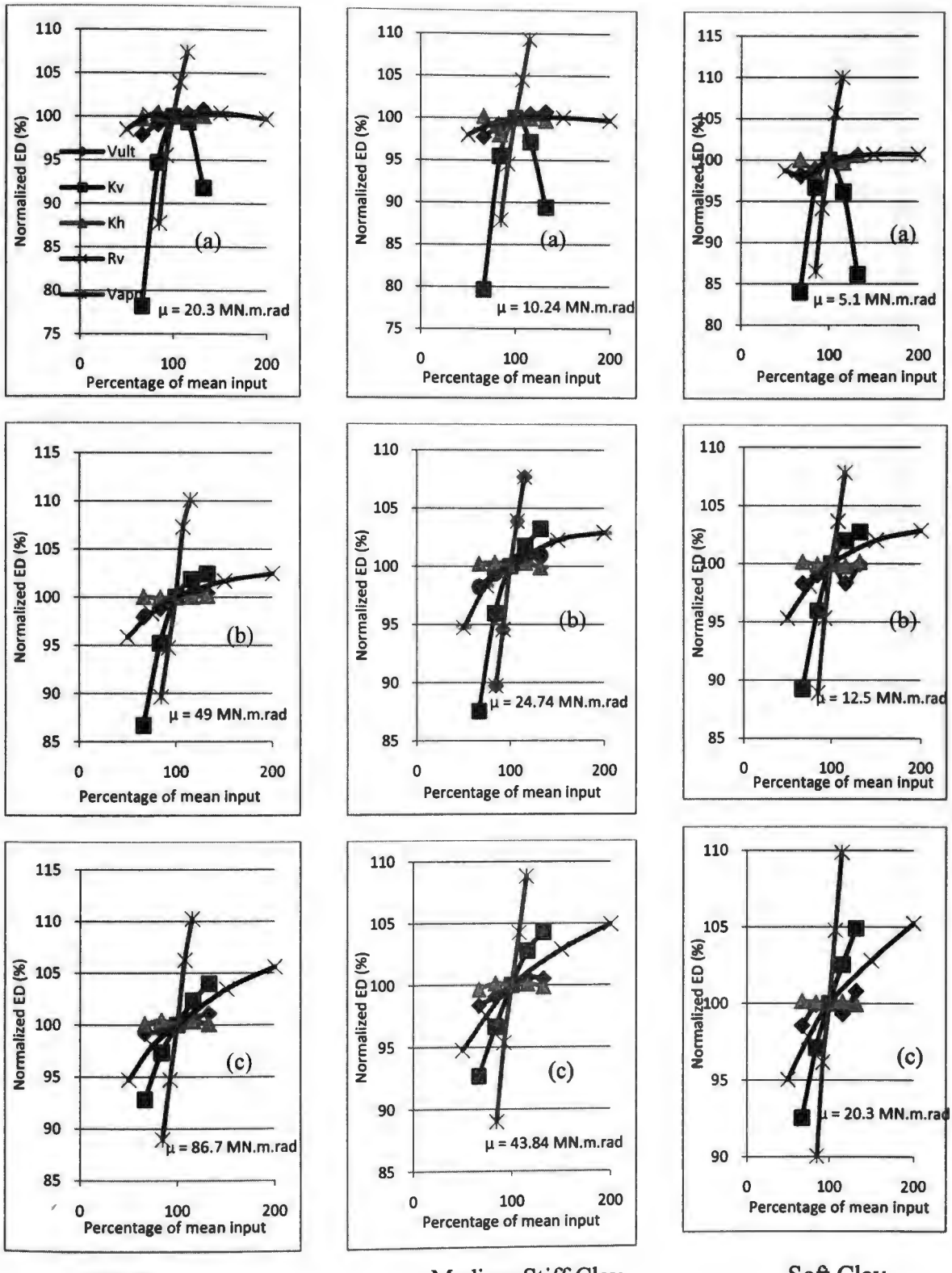

Fig. A.6. Spider plots of energy dissipation of soil-foundation system resting on clayey soils subjected to (a) 0.27 g (b) 0.55 g and (c) 0.98 g maximum ground shaking

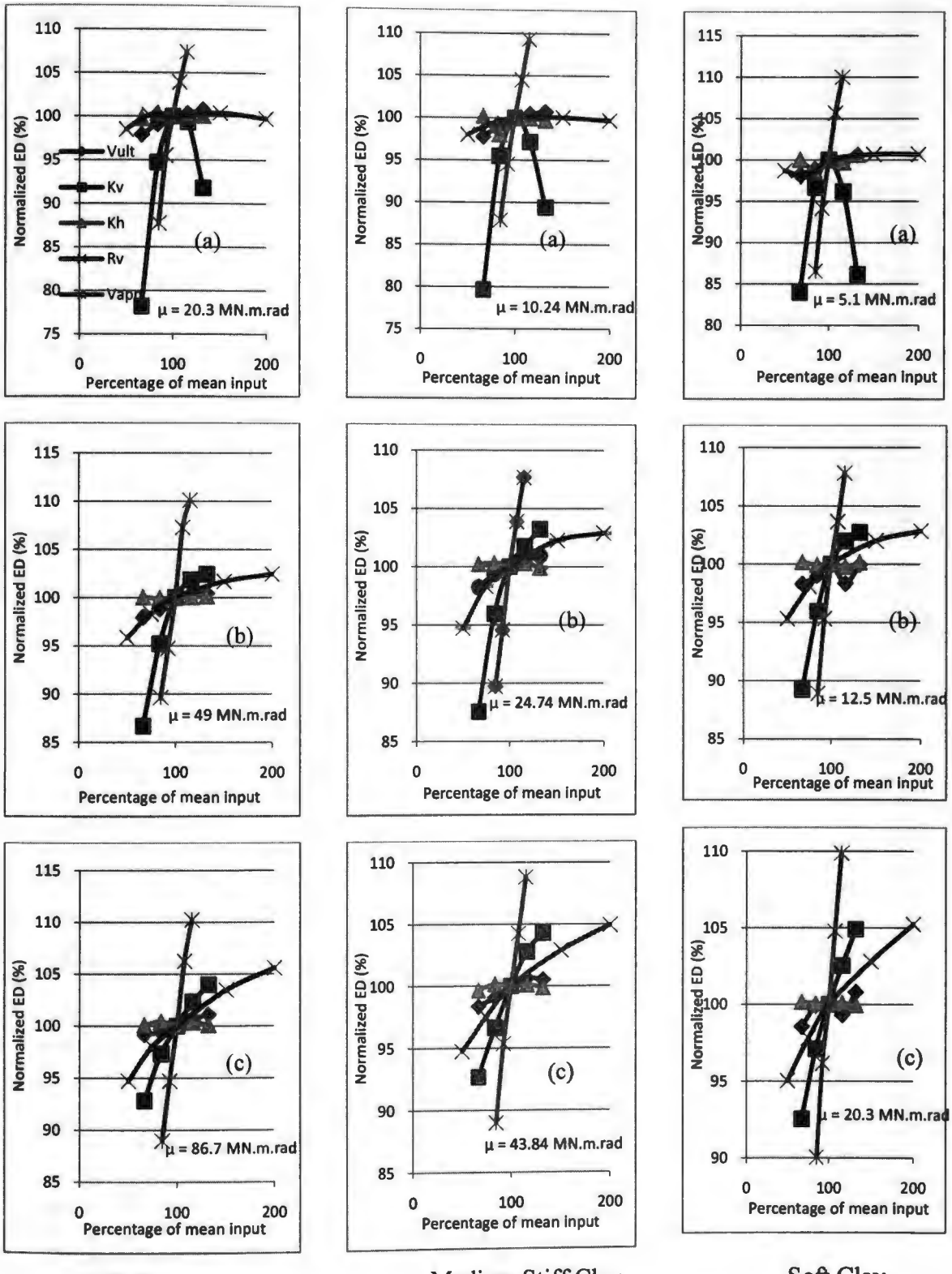

Stiff Clay Medium Stiff Clay Soft Clay

Fig. A.6. Spider plots of energy dissipation of soil-foundation system resting on clayey soils subjected to (a) 0.27 g (b) 0.55 g and (c) 0.98 g maximum ground shaking

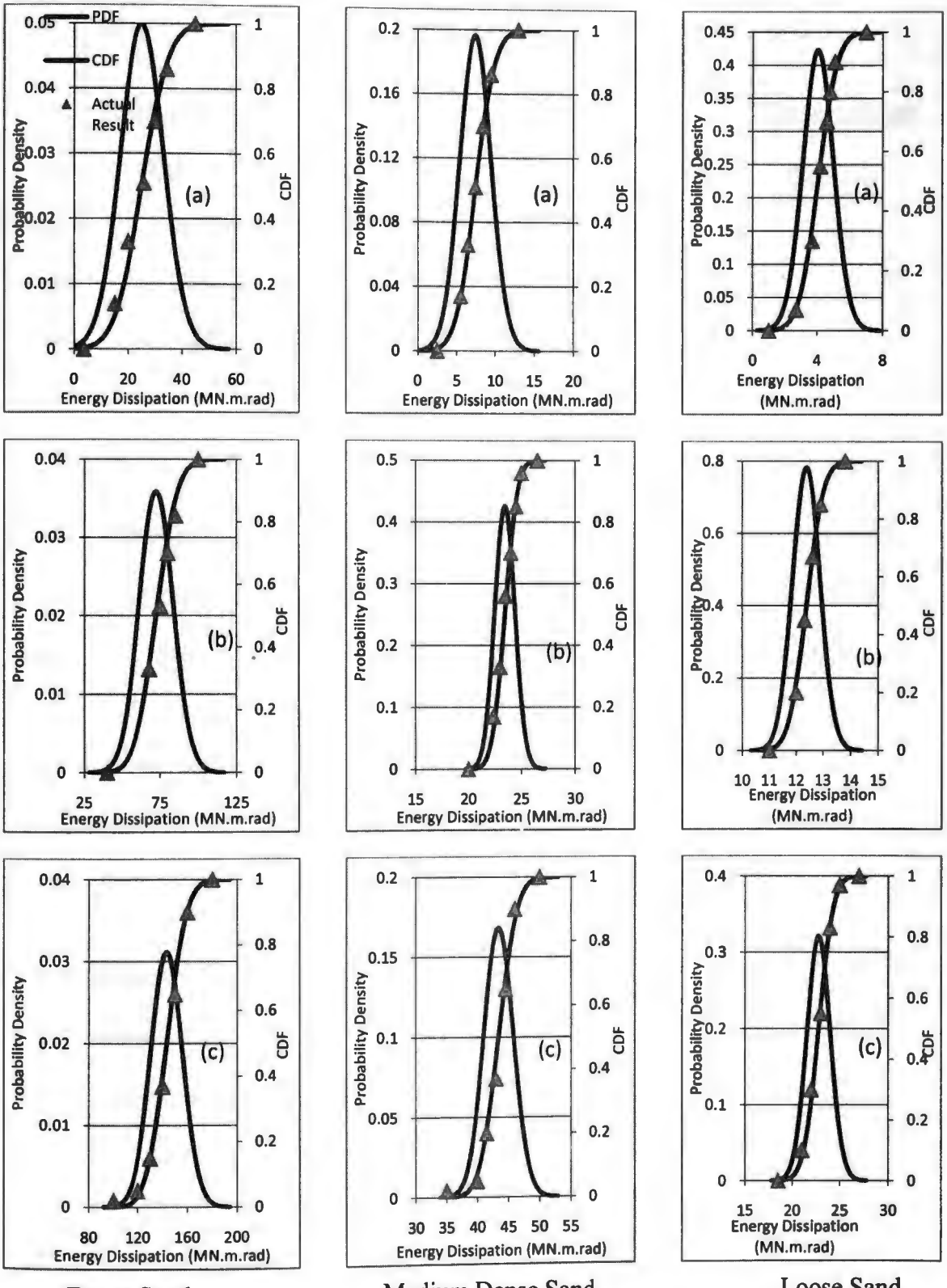

Fig. A.7. PDF and CDF plots of energy dissipation of soil-foundation system resting on sandy soils subjected to (a) 0.27 g (b) 0.55 g and (c) 0.98 g maximum ground shaking

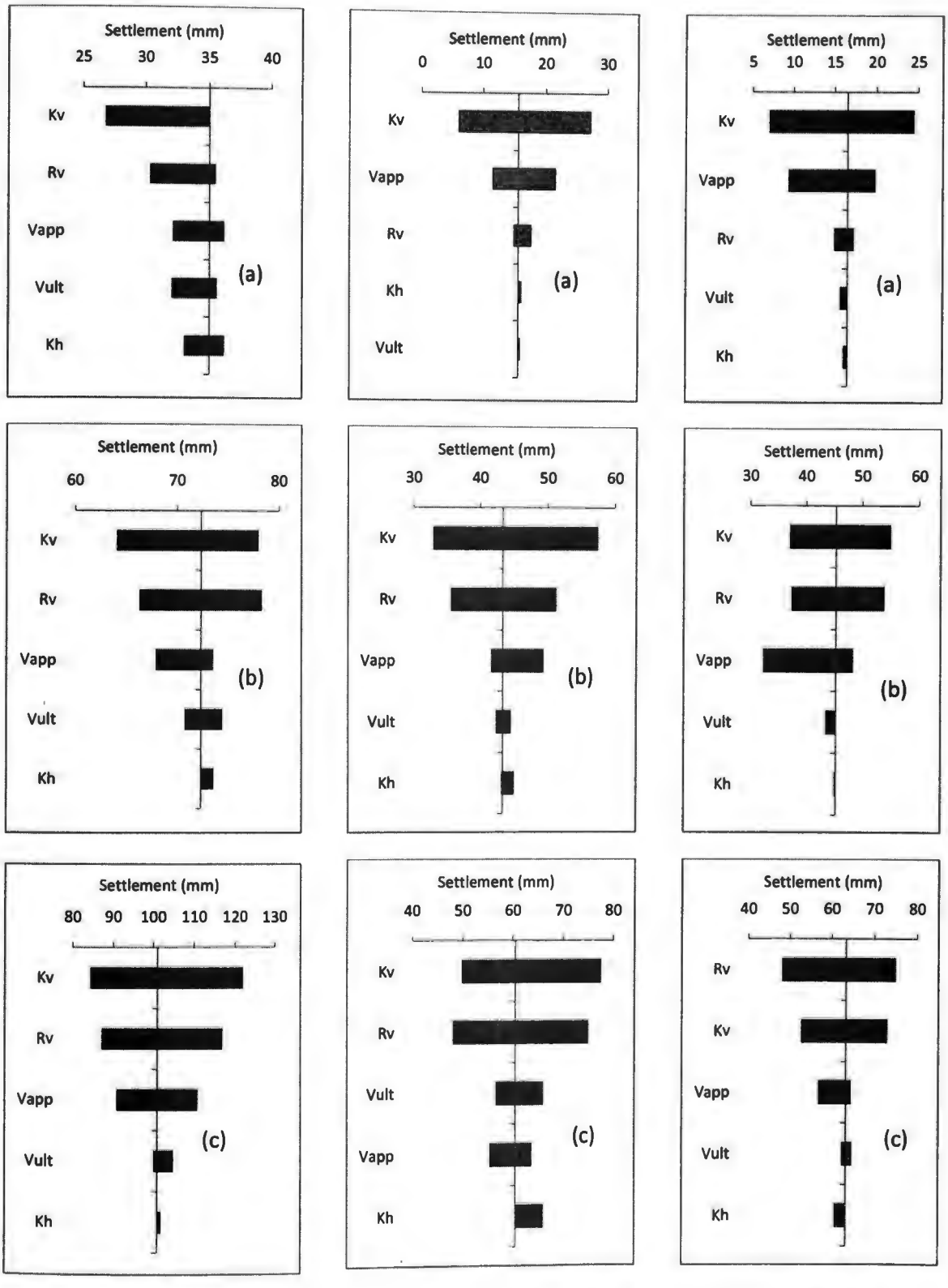

Dense Sand Medium Dense Sand Loose Sand

Fig. A.8. Tornado plots of settlement of soil-foundation system resting on sandy soils subjected to (a) 0.27 g (b) 0.55 g and (c) 0.98 g maximum ground shaking

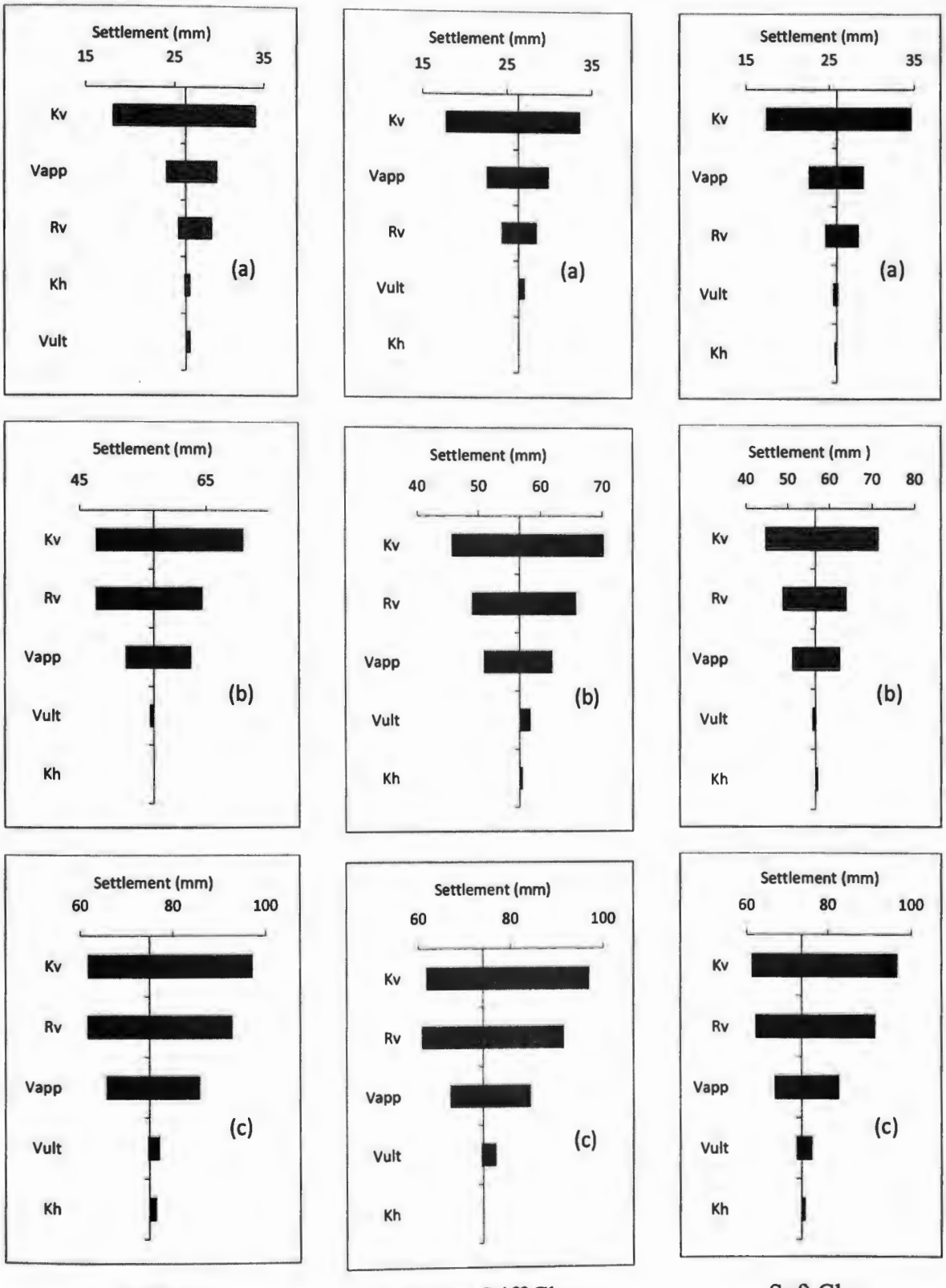

Stiff Clay Medium Stiff Clay Soft Clay

Fig. A.9. Tornado plots of settlement of soil-foundation system resting on clayey soils subjected to (a) 0.27 g (b) 0.55 g and (c) 0.98 g maximum ground shaking

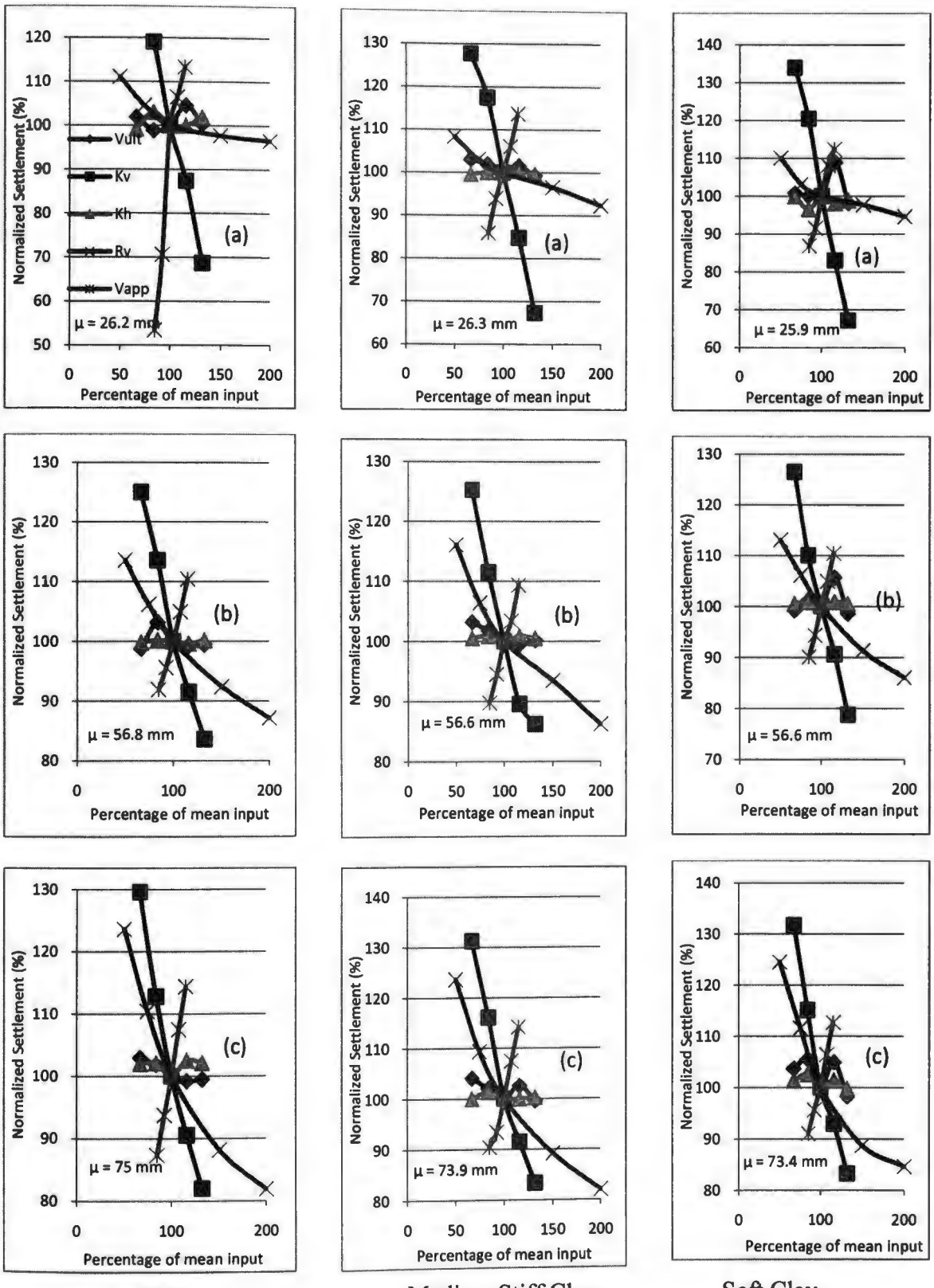

Stiff Clay Medium Stiff Clay Soft Clay

Fig. A.10. Spider plots of settlement of soil-foundation system resting on clayey soils subjected to (a) 0.27 g (b) 0.55 g and (c) 0.98 g maximum ground shaking

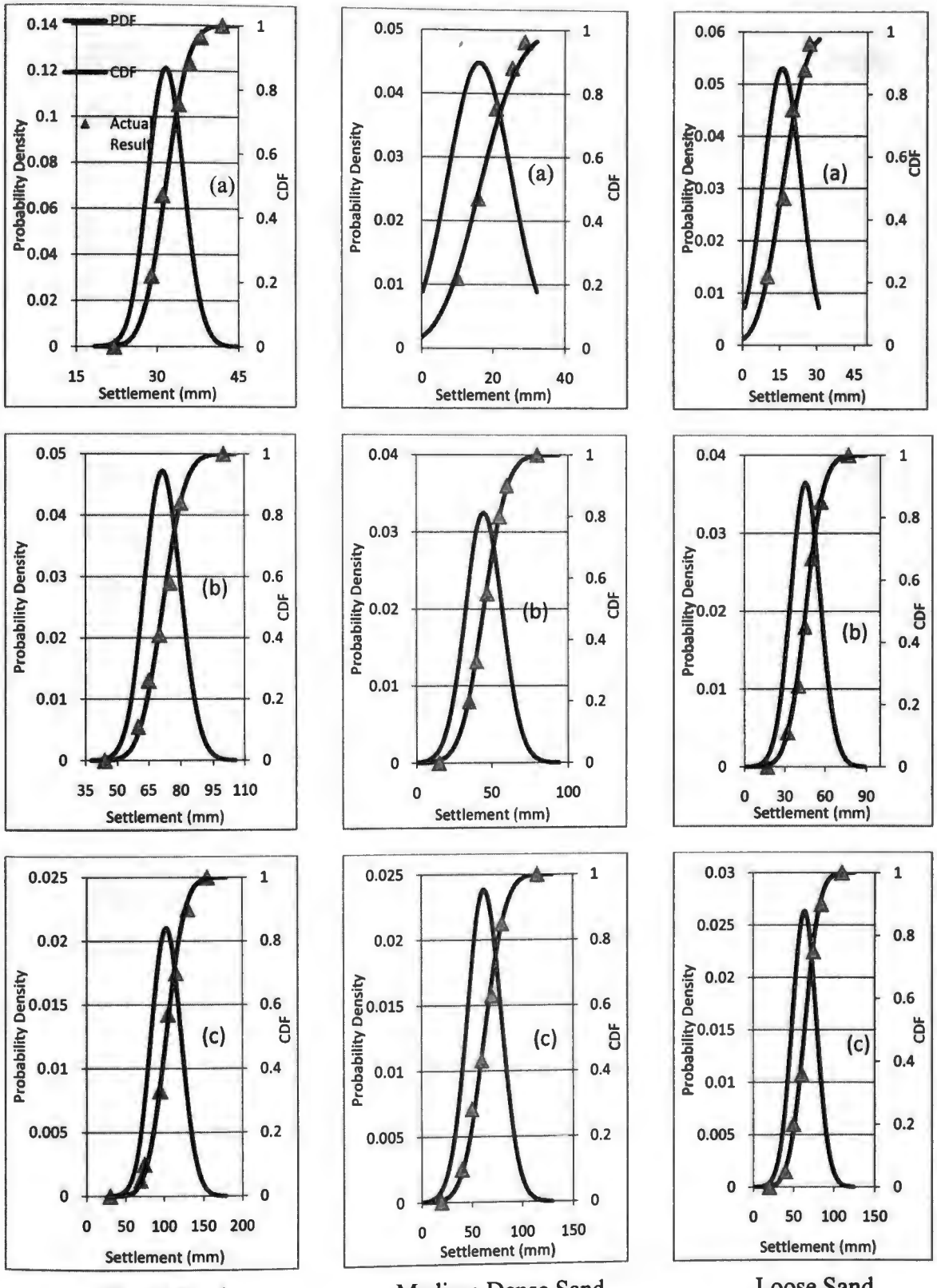

Fig. A.11. PDF and CDF plots of settlement of soil-foundation system resting on sandy soils subjected to (a) 0.27 g (b) 0.55 g and (c) 0.98 g maximum ground shaking

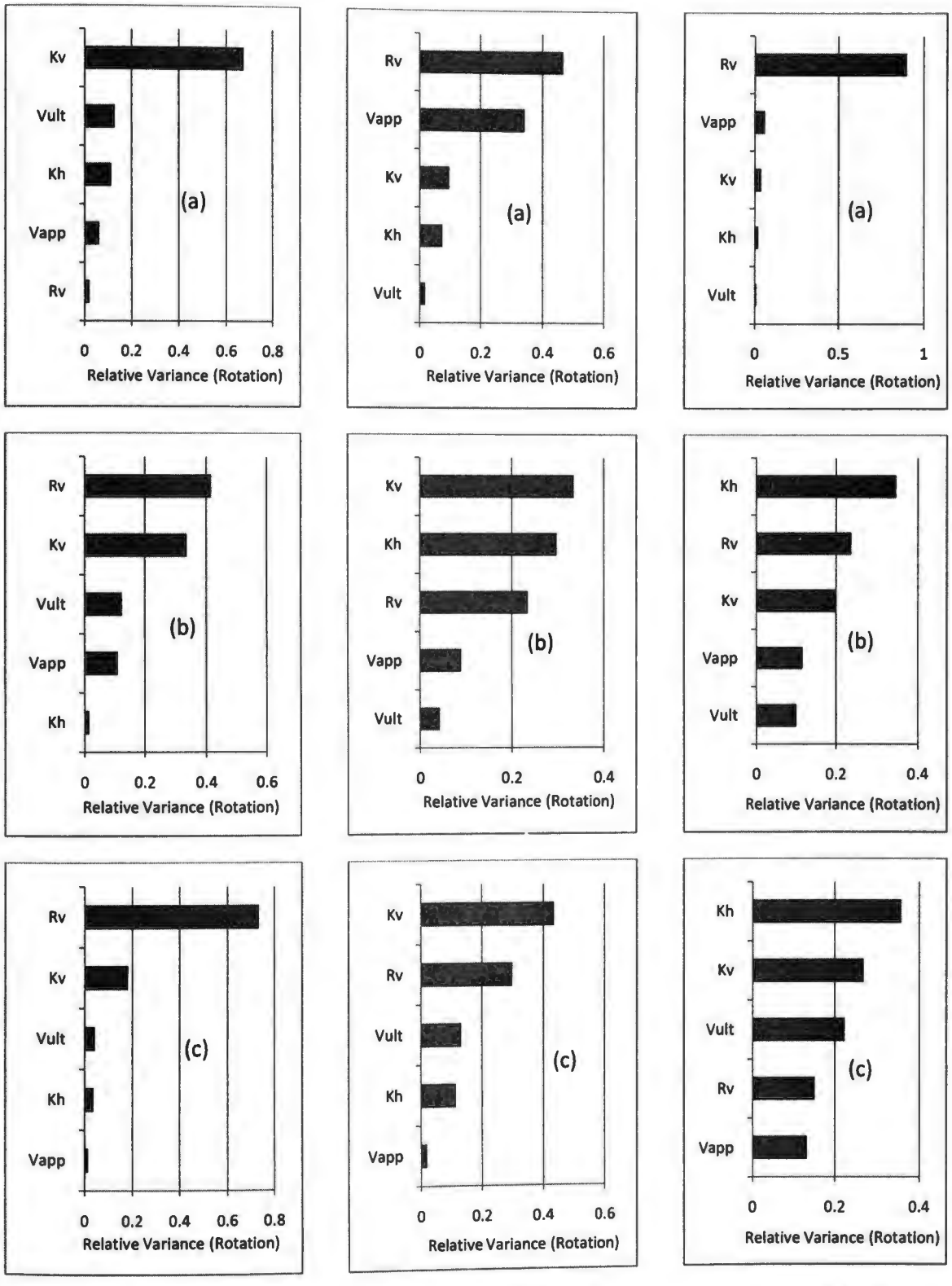

Fig. A.12. FOSM plots of rotation of soil-foundation system resting on sandy soils subjected to (a) 0.27 g (b) 0.55 g and (c) 0.98 g maximum ground shaking

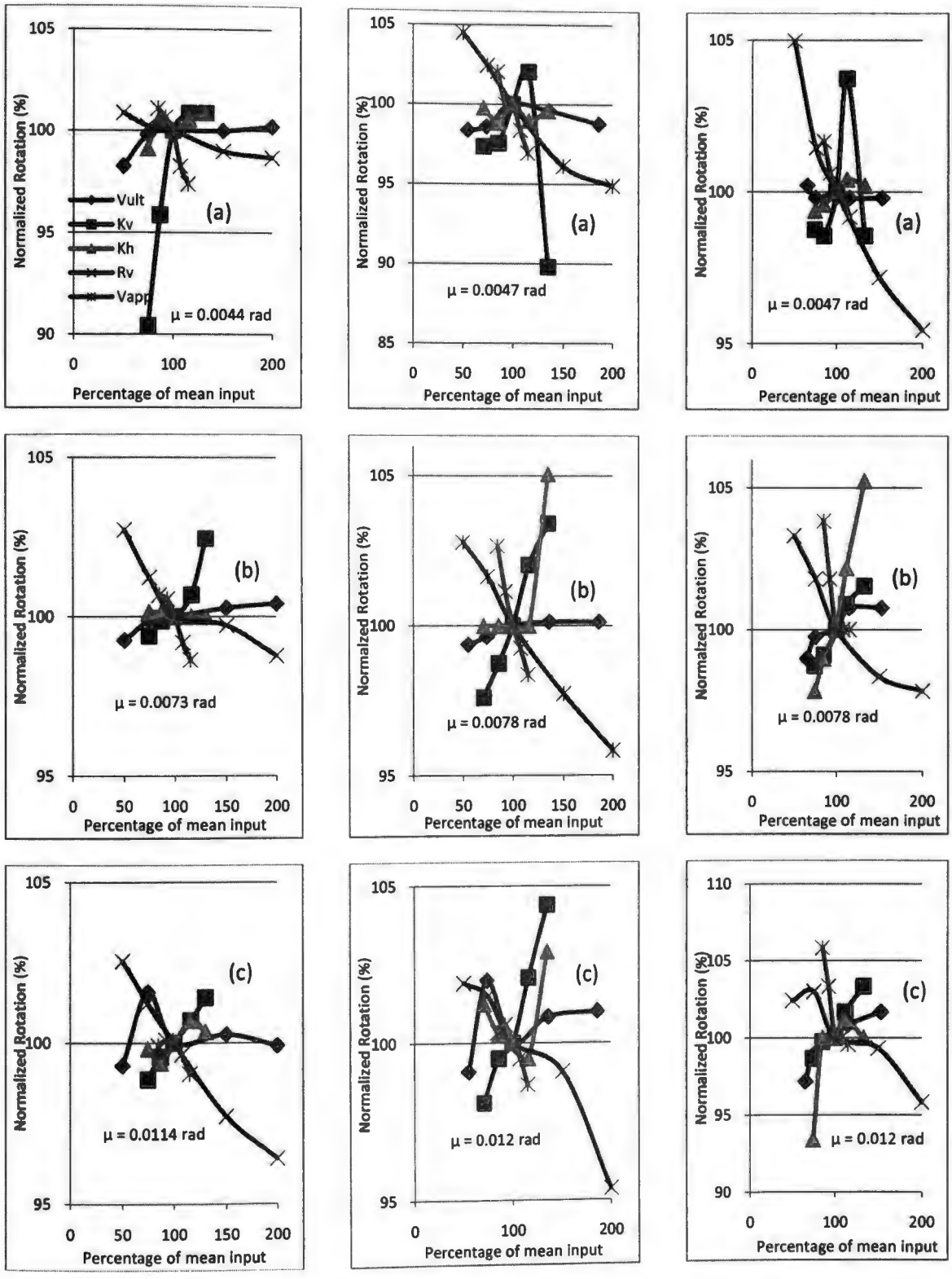

Fig. A.13. Spider plots of rotation of the soil-foundation system resting on sandy soils subjected to (a) 0.27 g (b) 0.55 g and (c) 0.98 g maximum ground shaking

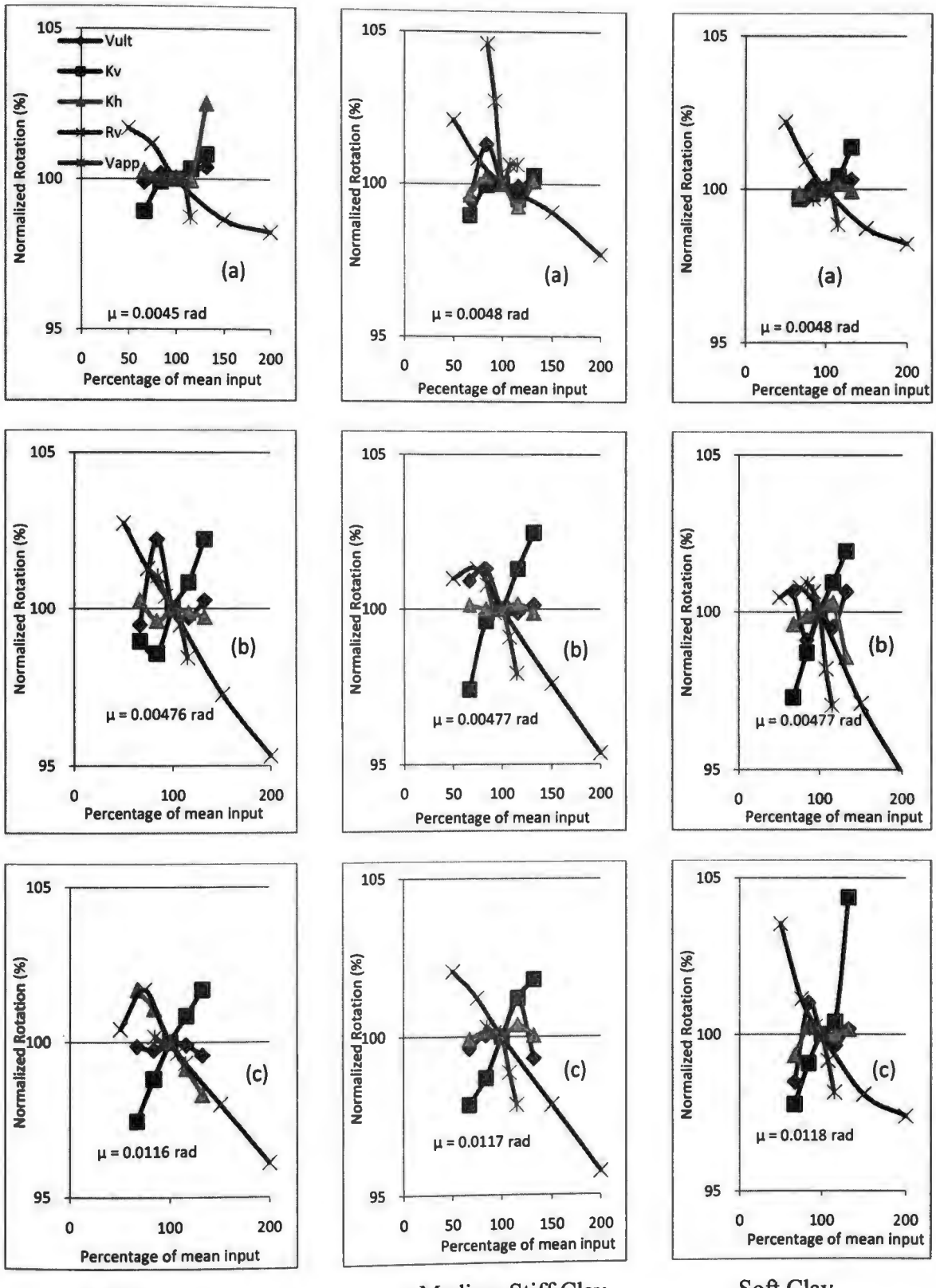

Stiff Clay Medium Stiff Clay Soft Clay

Fig. A.14. Spider plots of rotation of the soil-foundation system resting on clayey soils subjected to (a) 0.27 g (b) 0.55 g and (c) 0.98 g maximum ground shaking

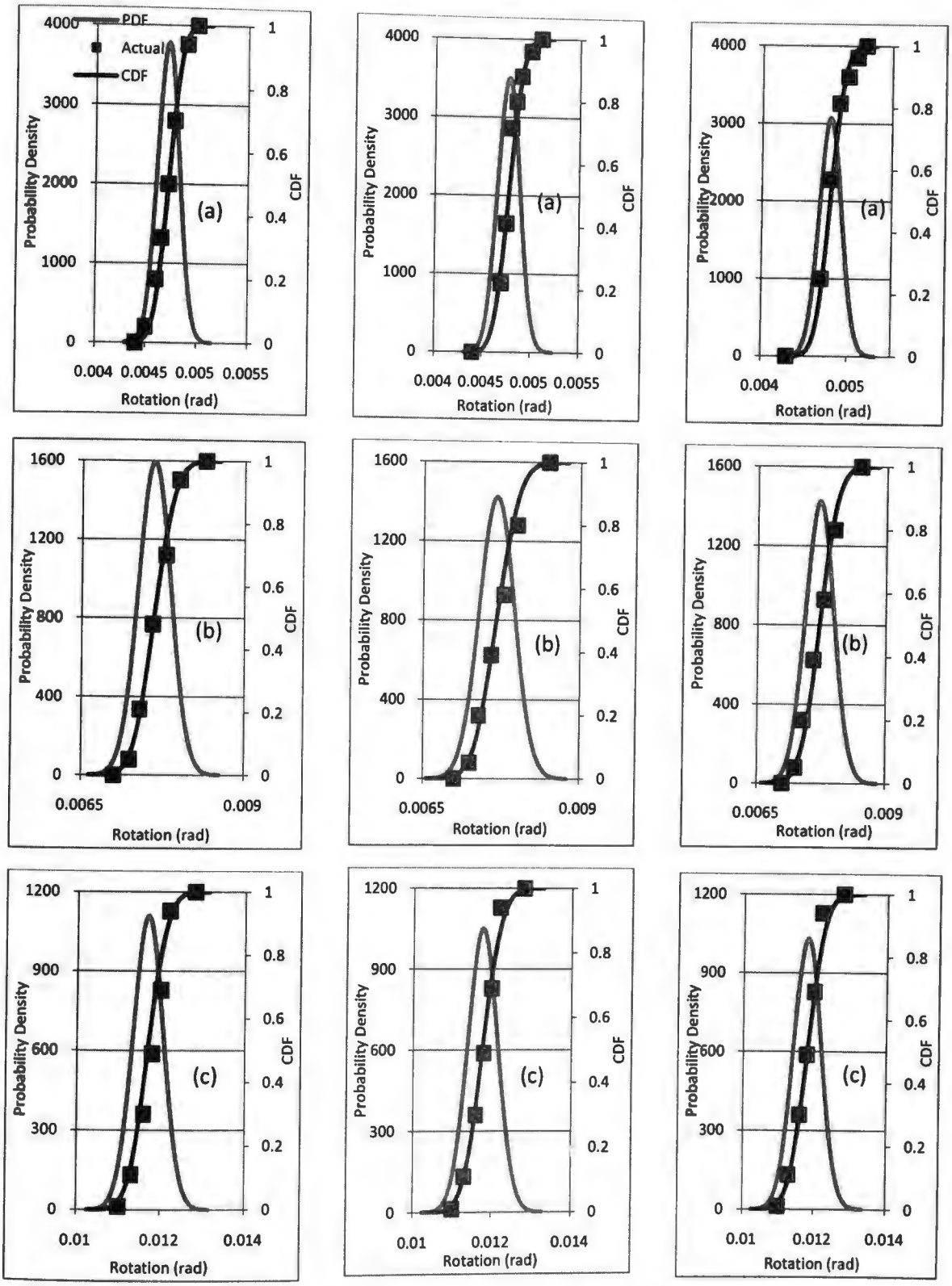

Fig. A.15. PDF and CDF plots of rotation of soil-foundation system resting on clayey soils subjected to (a) 0.27 g (b) 0.55 g and (c) 0.98 g maximum ground shaking

APPENDIX B. OPENSEES CODES

B.1. TCL Code for OpenSees Simulations of Shear Wall Structures Tested in Dynamic Shaking Using CIM. Shallow Foundation Resting on Dense Sand.

```
# Tcl file for shear wall structure on shallow foundation resting on dense sand
# units used: mass [Kg], length [m], time [s], and force [N]

# wipe out everything
wipe

# build a 2D model with 3 DOF
model BasicBuilder -ndm 2 -ndf 3

# define nodes
node 1 0 0
node 2 0 0
node 3 0 8

# linear coordinate transformation
geomTransf Linear 1

# define CIM – implemented as soilFootingSection2d in OpenSees
# section SFS2d matID Vult L Kv Kh Theta_Elastic Rv deltaL
section soilFootingSection2d 1 11e+6 4 10e+8 7.2e+8 0.001 0.1 0.01

# SFS2d material must be used with a zeroLengthSection (ZLS) element
# element ZLS eleID iNode jNode matID <orientation vectors>
element zeroLengthSection 1 1 2 1 -orient 0 -1 0 1 0 0

# define elasticBeamColumn element shear wall
# element elasticBeamColumn eleID iNode jNode A E I coord-trans
set E 2.0e+10

# shear wall element
element elasticBeamColumn 2 2 3 2.5 $E 1.33 1

# fix the base node in all three directions – the bottom end of CIM (SFS2d)
fix 1 1 1 1

# defining gravity loads – done in 10 increments
pattern Plain 1 Linear {
load 3 0 -0.113e+6 0
    }

# define analysis objects for gravity loading
```

```
test NormDispIncr 1e-12 10 1
algorithm Newton
system SparseGeneral
constraints Plain
numberer Plain
analysis Static

# define recorders
set name "node"
for {set n 1} {$n <= 3} {incr n 1} {
      set fileName [join [list $name $n] {}]
      recorder Node -file $fileName -node $n -dof 1 2 3 disp
}

set name "element"
for {set n 1} {$n <= 2} {incr n 1} {
      set fileName [join [list $name $n] {}]
      recorder Element -file $fileName -time -ele $n force
}

# apply gravity loads first
analyze 10

# set time back to zero again – before shaking
loadConst -time 0.0

puts "gravity loading done"

# wipe gravity analysis objects
wipeAnalysis

# define mass at node 3 in direction 1 (for seismic loading)
mass 3 0.115e+6 1e-9 0

# Eigen analysis
set PI 3.1415926
set lambdax [eigen 1]
set lambda [lindex $lambdax 0]
set omega [expr pow($lambda,0.5)]
set Tn [expr 2*$PI/$omega]
set fn [expr 1/$Tn]
puts "1st mode, Tn=$Tn sec, fn=$fn Hz"

# define analysis objects for seismic loading
test NormDispIncr 1e-12 10 1
```

```
algorithm Newton
system UmfPack
constraints Plain
numberer RCM

# define Newmark integrator with VariableTransient analysis method
integrator Newmark 0.6 0.32
analysis VariableTransient

# define Rayleigh damping for energy dissipation – in structure
rayleigh 0.01 0.01 0.01 0.01

# define ground motion characteristics
set dT 0.004882
set dTmin [expr $dT/10]
set dTmax $dT

# acceleration time history is read from an external file shakec.txt
set Series "Path -filePath shakec.txt -dt $dT -factor 9.81"

# acceleration is applied at the fixed base node in horizontal direction (1)
pattern UniformExcitation 2 1 -accel $Series

# apply shaking
set steps 4000
set itr 50

for {set i 1} {$i < $steps} {incr i 1} {
test NormDispIncr 1e-12 $itr 0
set ok [analyze 1 $dT $dTmin $dTmax $itr]

        if {$ok != 0} {
        test NormDispIncr 1e-10 $itr 0
        set ok [analyze 1 $dT $dTmin $dTmax $itr]
        }

        if {$ok != 0} {
        test NormDispIncr 1e-8 $itr 0
        set ok [analyze 1 $dT $dTmin $dTmax $itr]
        }

        if {$ok != 0} {
        test NormDispIncr 1e-6 $itr 0
        set ok [analyze 1 $dT $dTmin $dTmax $itr]
        }
```

```
}

# print out final node and element outputs on screen

for {set n 1} {$n <= 3} {incr n 1} {
     print node $n
}
print ele

# done - wipe out everything again
Wipe.
```

B.2. TCL Code for OpenSees Simulations of Shear Wall Structures Tested in Dynamic Shaking Using CIM. Shallow Foundation Resting on Medium Dense Sand.

```
# Tcl file for shear wall structure on shallow foundation resting on medium dense sand
# units used: mass [Kg], length [m], time [s], and force [N]

# wipe out everything
wipe

# build a 2D model with 3 DOF
model BasicBuilder -ndm 2 -ndf 3

# define nodes
node 1 0 0
node 2 0 0
node 3 0 8

# linear coordinate transformation
geomTransf Linear 1

# define CIM – implemented as soilFootingSection2d in OpenSees
# section SFS2d matID Vult L Kv Kh Theta_Elastic Rv deltaL
section soilFootingSection2d 1 3e+6 4 5.57e+8 4e+8 0.001 0.1 0.01

# SFS2d material must be used with a zeroLengthSection (ZLS) element
# element ZLS eleID iNode jNode matID <orientation vectors>
element zeroLengthSection 1 1 2 1 -orient 0 -1 0 1 0 0

# define elasticBeamColumn element shear wall
# element elasticBeamColumn eleID iNode jNode A E I coord-trans
set E 2.0e+10

# shear wall element
element elasticBeamColumn 2 2 3 2.5 $E 1.33 1
```

```
# fix the base node in all three directions – the bottom end of CIM (SFS2d)
fix 1 1 1 1

# defining gravity loads – done in 10 increments
pattern Plain 1 Linear {
load 3 0 -0.0283e+6 0
      }

# define analysis objects for gravity loading
test NormDispIncr 1e-12 10 1
algorithm Newton
system SparseGeneral
constraints Plain
numberer Plain
analysis Static

# define recorders
set name "node"
for {set n 1} {$n <= 3} {incr n 1} {
      set fileName [join [list $name $n] {}]
      recorder Node -file $fileName -node $n -dof 1 2 3 disp
}

set name "element"
for {set n 1} {$n <= 2} {incr n 1} {
      set fileName [join [list $name $n] {}]
      recorder Element -file $fileName -time -ele $n force
}

# apply gravity loads first
analyze 10

# set time back to zero again – before shaking
loadConst -time 0.0

puts "gravity loading done"

# wipe gravity analysis objects
wipeAnalysis

# define mass at node 3 in direction 1 (for seismic loading)
mass 3 0.0288e+6 1e-9 0

# Eigen analysis
set PI 3.1415926
```

```
set lambdax [eigen 1]
set lambda [lindex $lambdax 0]
set omega [expr pow($lambda,0.5)]
set Tn [expr 2*$PI/$omega]
set fn [expr 1/$Tn]
puts "1st mode, Tn=$Tn sec, fn=$fn Hz"

# define analysis objects for seismic loading
test NormDispIncr 1e-12 10 1
algorithm Newton
system UmfPack
constraints Plain
numberer RCM

# define Newmark integrator with VariableTransient analysis method
integrator Newmark 0.6 0.32
analysis VariableTransient

# define Rayleigh damping for energy dissipation – in structure
rayleigh 0.01 0.01 0.01 0.01

# define ground motion characteristics
set dT 0.004882
set dTmin [expr $dT/10]
set dTmax $dT

# acceleration time history is read from an external file shakec.txt
set Series "Path -filePath shakec.txt -dt $dT -factor 9.81"

# acceleration is applied at the fixed base node in horizontal direction (1)
pattern UniformExcitation 2 1 -accel $Series

# apply shaking
set steps 4000
set itr 50

for {set i 1} {$i < $steps} {incr i 1} {
test NormDispIncr 1e-12 $itr 0
set ok [analyze 1 $dT $dTmin $dTmax $itr]

        if {$ok != 0} {
        test NormDispIncr 1e-10 $itr 0
        set ok [analyze 1 $dT $dTmin $dTmax $itr]
        }
        if {$ok != 0} {
```

```
        test NormDispIncr 1e-8 $itr 0
        set ok [analyze 1 $dT $dTmin $dTmax $itr]
        }

        if {$ok != 0} {
        test NormDispIncr 1e-6 $itr 0
        set ok [analyze 1 $dT $dTmin $dTmax $itr]
        }
}

# print out final node and element outputs on screen

for {set n 1} {$n <= 3} {incr n 1} {
    print node $n
}
print ele

# done - wipe out everything again
Wipe
```

B.3. TCL Code for OpenSees Simulations of Shear Wall Structures Tested in Dynamic Shaking Using CIM. Shallow Foundation Resting on Loose Sand.

```
# Tcl file for shear wall structure on shallow foundation resting on loose sand
# units used: mass [Kg], length [m], time [s], and force [N]

# wipe out everything
wipe

# build a 2D model with 3 DOF
model BasicBuilder -ndm 2 -ndf 3

# define nodes
node 1 0 0
node 2 0 0
node 3 0 8

# linear coordinate transformation
geomTransf Linear 1

# define CIM – implemented as soilFootingSection2d in OpenSees
# section SFS2d matID Vult L Kv Kh Theta_Elastic Rv deltaL
section soilFootingSection2d 1 1.1e+6 4 3e+8 2.21e+8 0.001 0.1 0.01

# SFS2d material must be used with a zeroLengthSection (ZLS) element
# element ZLS eleID iNode jNode matID <orientation vectors>
```

```
element zeroLengthSection 1 1 2 1 -orient 0 -1 0 1 0 0

# define elasticBeamColumn element shear wall
# element elasticBeamColumn eleID iNode jNode A E I coord-trans
set E 2.0e+10

# shear wall element
element elasticBeamColumn 2 2 3 2.5 $E 1.33 1

# fix the base node in all three directions – the bottom end of CIM (SFS2d)
fix 1 1 1 1

# defining gravity loads – done in 10 increments
pattern Plain 1 Linear {
load 3 0 -0.0143e+6 0
    }

# define analysis objects for gravity loading
test NormDispIncr 1e-12 10 1
algorithm Newton
system SparseGeneral
constraints Plain
numberer Plain
analysis Static

# define recorders
set name "node"
for {set n 1} {$n <= 3} {incr n 1} {
    set fileName [join [list $name $n] {}]
    recorder Node -file $fileName -node $n -dof 1 2 3 disp
}

set name "element"
for {set n 1} {$n <= 2} {incr n 1} {
    set fileName [join [list $name $n] {}]
    recorder Element -file $fileName -time -ele $n force
}

# apply gravity loads first
analyze 10

# set time back to zero again – before shaking
loadConst -time 0.0
puts "gravity loading done"
# wipe gravity analysis objects
```

```
wipeAnalysis

# define mass at node 3 in direction 1 (for seismic loading)
mass 3 0.0146e+6 1e-9 0
# Eigen analysis
set PI 3.1415926
set lambdax [eigen 1]
set lambda [lindex $lambdax 0]
set omega [expr pow($lambda,0.5)]
set Tn [expr 2*$PI/$omega]
set fn [expr 1/$Tn]
puts "1st mode, Tn=$Tn sec, fn=$fn Hz"

# define analysis objects for seismic loading
test NormDispIncr 1e-12 10 1
algorithm Newton
system UmfPack
constraints Plain
numberer RCM

# define Newmark integrator with VariableTransient analysis method
integrator Newmark 0.6 0.32
analysis VariableTransient

# define Rayleigh damping for energy dissipation – in structure
rayleigh 0.01 0.01 0.01 0.01

# define ground motion characteristics
set dT 0.004882
set dTmin [expr $dT/10]
set dTmax $dT

# acceleration time history is read from an external file shakec.txt
set Series "Path -filePath shakec.txt -dt $dT -factor 9.81"

# acceleration is applied at the fixed base node in horizontal direction (1)
pattern UniformExcitation 2 1 -accel $Series

# apply shaking
set steps 4000
set itr 50

for {set i 1} {$i < $steps} {incr i 1} {
test NormDispIncr 1e-12 $itr 0
set ok [analyze 1 $dT $dTmin $dTmax $itr]
```

```
        if {$ok != 0} {
        test NormDispIncr 1e-10 $itr 0
        set ok [analyze 1 $dT $dTmin $dTmax $itr]
        }

        if {$ok != 0} {
        test NormDispIncr 1e-8 $itr 0
        set ok [analyze 1 $dT $dTmin $dTmax $itr]
        }

        if {$ok != 0} {
        test NormDispIncr 1e-6 $itr 0
        set ok [analyze 1 $dT $dTmin $dTmax $itr]
        }
}

# print out final node and element outputs on screen

for {set n 1} {$n <= 3} {incr n 1} {
    print node $n
}
print ele

# done - wipe out everything again
wipe
```

B.4. TCL Code for OpenSees Simulations of Shear Wall Structures Tested in Dynamic Shaking Using CIM. Shallow Foundation Resting on Stiff Clay.

```
# Tcl file for shear wall structure on shallow foundation resting on stiff clay
# units used: mass [Kg], length [m], time [s], and force [N]

# wipe out everything
wipe

# build a 2D model with 3 DOF
model BasicBuilder -ndm 2 -ndf 3

# define nodes
node 1 0 0
node 2 0 0
node 3 0 8

# linear coordinate transformation
geomTransf Linear 1
```

```
# define CIM – implemented as soilFootingSection2d in OpenSees
# section SFS2d matID Vult L Kv Kh Theta_Elastic Rv deltaL
section soilFootingSection2d 1 6.8e+6 4 8.35e+8 6e+8 0.001 0.1 0.01

# SFS2d material must be used with a zeroLengthSection (ZLS) element
# element ZLS eleID iNode jNode matID <orientation vectors>
element zeroLengthSection 1 1 2 1 -orient 0 -1 0 1 0 0

# define elasticBeamColumn element shear wall
# element elasticBeamColumn eleID iNode jNode A E I coord-trans
set E 2.0e+10

# shear wall element
element elasticBeamColumn 2 2 3 2.5 $E 1.33 1

# fix the base node in all three directions – the bottom end of CIM (SFS2d)
fix 1 1 1 1

# defining gravity loads – done in 10 increments
pattern Plain 1 Linear {
load 3 0 -0.06e+6 0
    }

# define analysis objects for gravity loading
test NormDispIncr 1e-12 10 1
algorithm Newton
system SparseGeneral
constraints Plain
numberer Plain
analysis Static

# define recorders
set name "node"
for {set n 1} {$n <= 3} {incr n 1} {
    set fileName [join [list $name $n] {}]
    recorder Node -file $fileName -node $n -dof 1 2 3 disp
}

set name "element"
for {set n 1} {$n <= 2} {incr n 1} {
    set fileName [join [list $name $n] {}]
    recorder Element -file $fileName -time -ele $n force
}

# apply gravity loads first
```

```
analyze 10

# set time back to zero again – before shaking
loadConst -time 0.0

puts "gravity loading done"

# wipe gravity analysis objects
wipeAnalysis

# define mass at node 3 in direction 1 (for seismic loading)
mass 3 0.061e+6 1e-9 0

# Eigen analysis
set PI 3.1415926
set lambdax [eigen 1]
set lambda [lindex $lambdax 0]
set omega [expr pow($lambda,0.5)]
set Tn [expr 2*$PI/$omega]
set fn [expr 1/$Tn]
puts "1st mode, Tn=$Tn sec, fn=$fn Hz"

# define analysis objects for seismic loading
test NormDispIncr 1e-12 10 1
algorithm Newton
system UmfPack
constraints Plain
numberer RCM

# define Newmark integrator with VariableTransient analysis method
integrator Newmark 0.6 0.32
analysis VariableTransient

# define Rayleigh damping for energy dissipation – in structure
rayleigh 0.01 0.01 0.01 0.01

# define ground motion characteristics
set dT 0.004882
set dTmin [expr $dT/10]
set dTmax $dT

# acceleration time history is read from an external file shakec.txt
set Series "Path -filePath shakec.txt -dt $dT -factor 9.81"

# acceleration is applied at the fixed base node in horizontal direction (1)
```

```
pattern UniformExcitation 2 1 -accel $Series

# apply shaking
set steps 4000
set itr 50

for {set i 1} {$i < $steps} {incr i 1} {
test NormDispIncr 1e-12 $itr 0
set ok [analyze 1 $dT $dTmin $dTmax $itr]

        if {$ok != 0} {
        test NormDispIncr 1e-10 $itr 0
        set ok [analyze 1 $dT $dTmin $dTmax $itr]
        }

        if {$ok != 0} {
        test NormDispIncr 1e-8 $itr 0
        set ok [analyze 1 $dT $dTmin $dTmax $itr]
        }

        if {$ok != 0} {
        test NormDispIncr 1e-6 $itr 0
        set ok [analyze 1 $dT $dTmin $dTmax $itr]
        }
}

# print out final node and element outputs on screen
for {set n 1} {$n <= 3} {incr n 1} {
    print node $n
}
print ele

# done - wipe out everything again
wipe
```

B.5. TCL Code for OpenSees Simulations of Shear Wall Structures Tested in Dynamic Shaking Using CIM. Shallow Foundation Resting on Medium Stiff Clay.

```
# Tcl file for shear wall structure on shallow foundation resting on medium stiff clay
# units used: mass [Kg], length [m], time [s], and force [N]

# wipe out everything
wipe

# build a 2D model with 3 DOF
model BasicBuilder -ndm 2 -ndf 3
```

```
# define nodes
node 1 0 0
node 2 0 0
node 3 0 8

# linear coordinate transformation
geomTransf Linear 1

# define CIM – implemented as soilFootingSection2d in OpenSees
# section SFS2d matID Vult L Kv Kh Theta_Elastic Rv deltaL
section soilFootingSection2d 1 3.384e+6 4 4.26e+8 3.06e+8 0.001 0.1 0.01

# SFS2d material must be used with a zeroLengthSection (ZLS) element
# element ZLS eleID iNode jNode matID <orientation vectors>
element zeroLengthSection 1 1 2 1 -orient 0 -1 0 1 0 0

# define elasticBeamColumn element shear wall
# element elasticBeamColumn eleID iNode jNode A E I coord-trans
set E 2.0e+10

# shear wall element
element elasticBeamColumn 2 2 3 2.5 $E 1.33 1

# fix the base node in all three directions – the bottom end of CIM (SFS2d)
fix 1 1 1 1

# defining gravity loads – done in 10 increments
pattern Plain 1 Linear {
load 3 0 -0.03e+6 0
      }

# define analysis objects for gravity loading
test NormDispIncr 1e-12 10 1
algorithm Newton
system SparseGeneral
constraints Plain
numberer Plain
analysis Static

# define recorders
set name "node"
for {set n 1} {$n <= 3} {incr n 1} {
      set fileName [join [list $name $n] {}]
      recorder Node -file $fileName -node $n -dof 1 2 3 disp
```

```
}

set name "element"
for {set n 1} {$n <= 2} {incr n 1} {
      set fileName [join [list $name $n] {}]
      recorder Element -file $fileName -time -ele $n force
}

# apply gravity loads first
analyze 10

# set time back to zero again – before shaking
loadConst -time 0.0

puts "gravity loading done"

# wipe gravity analysis objects
wipeAnalysis

# define mass at node 3 in direction 1 (for seismic loading)
mass 3 0.0306e+6 1e-9 0

# Eigen analysis
set PI 3.1415926
set lambdax [eigen 1]
set lambda [lindex $lambdax 0]
set omega [expr pow($lambda,0.5)]
set Tn [expr 2*$PI/$omega]
set fn [expr 1/$Tn]
puts "1st mode, Tn=$Tn sec, fn=$fn Hz"

# define analysis objects for seismic loading
test NormDispIncr 1e-12 10 1
algorithm Newton
system UmfPack
constraints Plain
numberer RCM

# define Newmark integrator with VariableTransient analysis method
integrator Newmark 0.6 0.32
analysis VariableTransient

# define Rayleigh damping for energy dissipation – in structure
rayleigh 0.01 0.01 0.01 0.01
```

```
# define ground motion characteristics
set dT 0.004882
set dTmin [expr $dT/10]
set dTmax $dT
# acceleration time history is read from an external file shakec.txt
set Series "Path -filePath shakec.txt -dt $dT -factor 9.81"

# acceleration is applied at the fixed base node in horizontal direction (1)
pattern UniformExcitation 2 1 -accel $Series

# apply shaking
set steps 4000
set itr 50

for {set i 1} {$i < $steps} {incr i 1} {
test NormDispIncr 1e-12 $itr 0
set ok [analyze 1 $dT $dTmin $dTmax $itr]

        if {$ok != 0} {
        test NormDispIncr 1e-10 $itr 0
        set ok [analyze 1 $dT $dTmin $dTmax $itr]
        }

        if {$ok != 0} {
        test NormDispIncr 1e-8 $itr 0
        set ok [analyze 1 $dT $dTmin $dTmax $itr]
        }

        if {$ok != 0} {
        test NormDispIncr 1e-6 $itr 0
        set ok [analyze 1 $dT $dTmin $dTmax $itr]
        }
}

# print out final node and element outputs on screen
for {set n 1} {$n <= 3} {incr n 1} {
    print node $n
}
print ele

# done - wipe out everything again
wipe
```

B.6. TCL Code for OpenSees Simulations of Shear Wall Structures Tested in Dynamic Shaking Using CIM. Shallow Foundation Resting on Soft Clay.

```
# Tcl file for shear wall structure on shallow foundation resting on soft clay
# units used: mass [Kg], length [m], time [s], and force [N]

# wipe out everything
wipe

# build a 2D model with 3 DOF
model BasicBuilder -ndm 2 -ndf 3

# define nodes
node 1 0 0
node 2 0 0
node 3 0 8

# linear coordinate transformation
geomTransf Linear 1

# define CIM – implemented as soilFootingSection2d in OpenSees
# section SFS2d matID Vult L Kv Kh Theta_Elastic Rv deltaL
section soilFootingSection2d 1 1.7e+6 4 2.17e+8 1.56e+8 0.001 0.1 0.01

# SFS2d material must be used with a zeroLengthSection (ZLS) element
# element ZLS eleID iNode jNode matID <orientation vectors>
element zeroLengthSection 1 1 2 1 -orient 0 -1 0 1 0 0

# define elasticBeamColumn element shear wall
# element elasticBeamColumn eleID iNode jNode A E I coord-trans
set E 2.0e+10

# shear wall element
element elasticBeamColumn 2 2 3 2.5 $E 1.33 1

# fix the base node in all three directions – the bottom end of CIM (SFS2d)
fix 1 1 1 1

# defining gravity loads – done in 10 increments
pattern Plain 1 Linear {
load 3 0 -0.015e+6 0
    }

# define analysis objects for gravity loading
test NormDispIncr 1e-12 10 1
algorithm Newton
system SparseGeneral
constraints Plain
```

```
numberer Plain
analysis Static
# define recorders
set name "node"
for {set n 1} {$n <= 3} {incr n 1} {
      set fileName [join [list $name $n] {}]
      recorder Node -file $fileName -node $n -dof 1 2 3 disp
}

set name "element"
for {set n 1} {$n <= 2} {incr n 1} {
      set fileName [join [list $name $n] {}]
      recorder Element -file $fileName -time -ele $n force
}

# apply gravity loads first
analyze 10

# set time back to zero again -- before shaking
loadConst -time 0.0

puts "gravity loading done"

# wipe gravity analysis objects
wipeAnalysis

# define mass at node 3 in direction 1 (for seismic loading)
mass 3 0.0153e+6 1e-9 0

# Eigen analysis
set PI 3.1415926
set lambdax [eigen 1]
set lambda [lindex $lambdax 0]
set omega [expr pow($lambda,0.5)]
set Tn [expr 2*$PI/$omega]
set fn [expr 1/$Tn]
puts "1st mode, Tn=$Tn sec, fn=$fn Hz"

# define analysis objects for seismic loading
test NormDispIncr 1e-12 10 1
algorithm Newton
system UmfPack
constraints Plain
numberer RCM
```

```
# define Newmark integrator with VariableTransient analysis method
integrator Newmark 0.6 0.32
analysis VariableTransient

# define Rayleigh damping for energy dissipation – in structure
rayleigh 0.01 0.01 0.01 0.01

# define ground motion characteristics
set dT 0.004882
set dTmin [expr $dT/10]
set dTmax $dT

# acceleration time history is read from an external file shakec.txt
set Series "Path -filePath shakec.txt -dt $dT -factor 9.81"
# acceleration is applied at the fixed base node in horizontal direction (1)
pattern UniformExcitation 2 1 -accel $Series

# apply shaking
set steps 4000
set itr 50

for {set i 1} {$i < $steps} {incr i 1} {
test NormDispIncr 1e-12 $itr 0
set ok [analyze 1 $dT $dTmin $dTmax $itr]

        if {$ok != 0} {
        test NormDispIncr 1e-10 $itr 0
        set ok [analyze 1 $dT $dTmin $dTmax $itr]
        }

        if {$ok != 0} {
        test NormDispIncr 1e-8 $itr 0
        set ok [analyze 1 $dT $dTmin $dTmax $itr]
        }

        if {$ok != 0} {
        test NormDispIncr 1e-6 $itr 0
        set ok [analyze 1 $dT $dTmin $dTmax $itr]
        }
}

# print out final node and element outputs on screen

for {set n 1} {$n <= 3} {incr n 1} {
     print node $n
```

```
}
print ele

# done - wipe out everything again
Wipe
```

APPENDIX C. COEFFICIENT OF CORRELATION CALCULATION

Table C.1. Correlation Coefficient calculation between initial horizontal stiffness and initial vertical stiffness of shallow foundation resting on sandy soils

No.	Kh (MN/m)	Kv (MN/m)	Kh - Kh'	Kv - Kv'	$(Kh - Kh')^2$	$(Kv - Kv')^2$	(Kh - Kh') × (Kv - Kv')
1.	956	1329	487	677	237169	458329	329699
2.	719	1000	250	348	62500	121104	87000
3.	539	750	70	98	4900	9604	6860
4.	400	557	-69	-95	4761	9025	6555
5.	286	397	-183	-255	33489	65025	46665
6.	221	307	-248	-345	61504	119025	85560
7.	163	227	-306	-425	93636	180625	130050
Mean	Kh' = 469	Kv' = 652		Sum (∑)	497959	962737	692389

$$\text{Coefficient of correlation} = \frac{\sum\{(K_h - K_h')\times(K_v - K_v')\}}{\sqrt{\{\sum(K_h - K_h')^2\}\times\{\sum(K_v - K_v')^2\}}}$$

$$= \frac{692389}{\sqrt{497959 \times 962737}}$$

$$\approx 1.0$$

Table C.2. Correlation Coefficient calculation between initial horizontal stiffness and initial vertical stiffness of shallow foundation resting on clayey soils

No.	Kh (MN/m)	Kv (MN/m)	Kh - Kh'	Kv - Kv'	$(Kh - Kh')^2$	$(Kv - Kv')^2$	(Kh - Kh') × (Kv - Kv')
1.	106	147	-123	-167	15129	27889	20541
2.	156	217	-73	-97	5329	9409	7081
3.	207	287	-22	-27	484	729	594
4.	306	426	77	112	5929	12544	8624
5.	405	563	176	249	30976	62001	43824
6.	600	835	371	521	137641	271441	193291
7.	795	1105	566	791	320356	625681	447706
Mean	Kh' = 368	Kv' = 511		Sum (∑)	515844	1009694	721661

$$\text{Coefficient of correlation} = \frac{\sum\{(K_h - K_h')\times(K_v - K_v')\}}{\sqrt{\{\sum(K_h - K_h')^2\}\times\{\sum(K_v - K_v')^2\}}}$$

$$= \frac{721661}{\sqrt{515844 \times 1009694}}$$

$$\approx 1.0$$